

10/10/80

*A STUDY OF THE TRANSPORT PROPERTIES
OF SOME BINARY GAS MIXTURES*

by

PAWITTAR SINGH ARORA, M.Sc. (Hons.)

*A THESIS SUBMITTED FOR THE DEGREE OF
DOCTOR OF PHILOSOPHY
AT THE UNIVERSITY OF ADELAIDE,
NOVEMBER, 1979*

DEPARTMENT OF PHYSICAL AND INORGANIC CHEMISTRY

Awarded 13th June 1980

SUMMARY

Binary diffusion coefficients, D_{12} , for the systems He-N₂, He-O₂, He-Ar, He-CO₂ and N₂-Ar have been measured at 300K as a function of concentration with a two bulb cell (A₁) using connecting tubes of different diameters. For comparison, the same binary systems were studied with a Loschmidt cell (A₃). The data obtained from these two cells mentioned above shows that the Wirz relation to calculate the end correction, which is usually applied to the connecting tubes of two bulb cells, is not precise enough for the present accuracy (i.e. 0.1%) and suggests that it would be better to calibrate two bulb cells with the most accurate data available in literature rather than to use the Wirz relation.

An entirely different, small two bulb cell (A₂) was constructed and calibrated with the data obtained from a Loschmidt cell (A₃). This cell (A₂) was then used to study the concentration and temperature dependences of D_{12} for several binary gas mixtures.

A study of the concentration dependence of diffusion coefficients for the system He-Ar has also been done in the Loschmidt cell (A₃) at 277.00K and 323.15K to measure the change in concentration dependence of D_{12} with temperature.

For the sake of comparison, the binary diffusion coefficients for all the systems under study were predicted

using Kihara's second approximation to the Chapman-Enskog theory. The results show a reasonably good agreement with the experimental values.

Measurements of D_{12} were made as a function of temperature between 275 - 325K for all the noble gas systems except Kr-Xe and for the systems He-N₂, He-O₂, He-CO, Ar-N₂, Ar-O₂, Ar-CO, Kr-CH₄ and CF₄-CH₄ with a small two bulb cell (A₂) and a Loschmidt cell (A₃). These results together with some excellent second virial coefficient data were used to calculate potential parameters which predicted, within the experimental errors, almost all the transport data available in the literature. The potential parameters for like interactions were also calculated by combining the viscosity and the second virial coefficient data from the literature. These parameters (ϵ_{11} and σ_{11}) were then used to calculate the self diffusion coefficients which show a fairly good agreement with the results in the literature.

The temperature dependence of binary diffusion coefficients for the almost Lorentzian gas mixtures He-Ar, He-Kr, H₂-Ar and D₂-Ar were also studied using a Loschmidt cell (A₃) at one atmosphere pressure and over the temperature range 275 - 325K. Thermal diffusion coefficients for the Lorentzian gas mixtures (mentioned above) were calculated with the help of a method suggested by Mason and discussed with reference to the data available in the literature.

Finally, the Loschmidt cell (A₃) was modified to study the pressure dependence of mutual diffusion coefficients

for the systems He-Ar, He-O₂, He-N₂ and He-CO₂ up to approximately 25 - 30 atmospheres. But due to lack of precision (i.e. 0.1%) at high pressures, success was only achieved up to 20 atmospheres. The experimental results thus obtained were compared and discussed in terms of the Thorne-Enskog theory of moderately dense gases.

DECLARATION

I certify that this thesis does not incorporate, without acknowledgement, any material previously submitted for a degree or diploma in an university, and that to the best of my knowledge and belief it does not contain any material previously published or written by another person, except where due reference is made in the text.

Pawittar S. Arora.

ACKNOWLEDGEMENTS

It gives me great pleasure to express my deep sense of gratitude to Dr. Peter J. Dunlop for his keen interest, technical guidance, active supervision, vital encouragement, constructive criticism and valuable suggestions throughout the course of my investigations which led to the successful completion of this piece of work. I am equally grateful to Dr. M.L. Martin for his help in the absence of Dr. Dunlop.

I would like to express my thanks to my colleagues (Michael, Graham, Ian and Robert) and Professor T.N. Bell for their interest and cooperation during my stay in this Department. Grateful thanks are expressed to Dr. S.P.S. Badwal for his suggestions and criticism of the draft of this thesis. I am equally grateful to Paul for his helpful suggestions and for providing me with the necessary facilities for making the diagrams.

The technical staff of the Engineering and Electronic Workshops are acknowledged for their efforts in the construction and maintenance of the apparatus used in this work. Thanks are also due to Helen for providing me with most of the raw data from cell A_2 .

Special thanks go to Pat who not only has encouraged and helped me in many ways throughout this period, but also patiently endured many weekends and evenings to make it possible to complete this research work.

I owe my thanks to Mrs. Angela McKay for her ever available help of typing this manuscript in a most expert and efficient manner.

Throughout the period of this project I was supported by a U.R.G. scholarship.

TABLE OF CONTENTS

	<u>Page</u>
<i>SUMMARY</i>	(i)
<i>DECLARATION</i>	(iv)
<i>ACKNOWLEDGEMENTS</i>	(v)
<i>TABLE OF CONTENTS</i>	(vi)
<i>LIST OF TABLES</i>	(ix)
<i>LIST OF FIGURES</i>	(xii)
<i>CHAPTER 1: GENERAL INTRODUCTION</i>	1
<i>REFERENCES</i>	8
<i>CHAPTER 2: THEORETICAL ASPECTS OF TRANSPORT AND EQUILIBRIUM PROPERTIES IN GASES</i>	
2.1 Introduction	14
2.2 Chapman-Enskog Theory for Dilute Gases	14
2.3 Extension of Chapman-Enskog Theory for Moderately Dense Gases	24
2.4 Diffusion Coefficient Equations at Low Pressures	27
2.5 [m,6,8] Intermolecular Potential Function	29
2.6 Collision Integrals and Reduced Second Virial Coefficients	31
<i>REFERENCES</i>	33
<i>CHAPTER 3: METHODS AND MATERIALS</i>	
3.1 Introduction	37
3.2 Theory of the Two Bulb Apparatus	37
3.3 Construction of the Two Bulb Cells	42
3.4 Calculations for the End Correction	43
3.5 Calculations for the Cell Constants	47
3.6 Advantages of the Cell A_2	48
3.7 Common Features of Cells A_1 and A_2	48
3.8 Experimental Procedure for Two Bulb Cells	49

Continued.....

	<u>Page</u>
3.9 Theory of Loschmidt Cell	49
3.10 Construction of the Loschmidt Cell	53
3.11 Common Features of the Cells A_1 , A_2 and A_3	54
3.12 Experimental Procedure for the Loschmidt Cell	55
3.13 Pressure Measurements	56
3.14 Temperature Control	58
3.15 Determination of Diffusion Coefficients	60
<i>REFERENCES</i>	64

CHAPTER 4: THE CONCENTRATION DEPENDENCE OF DIFFUSION

4.1 Introduction	66
4.2 Results and Discussion of the Cells A_1 and A_3	66
4.3 Results from the Small Two Bulb Cell (A_2)	83
4.4 Theoretical Predictions for Concentration Dependence of D_{12}	85
4.5 Concentration Dependence of Diffusion Coefficient for He-Ar at 277K and 323.15K	93
<i>REFERENCES</i>	98

CHAPTER 5A: THE TEMPERATURE DEPENDENCE OF DIFFUSION

5A.1 Introduction	101
5A.2 Experimental and Results	104
5A.3 Calculations of the Potential Parameters for Unlike Interactions	105
5A.4 Calculations of Viscosities	115
5A.5 Calculations for Diffusion Coefficients at Very High and Low Temperatures	120
5A.6 Calculations of Thermal Diffusion Coefficients	123
5A.7 Calculations of the Potential Parameters for Like Interactions	125
5A.8 Calculations of Self Diffusion Coefficients	129
<i>REFERENCES</i>	134

*CHAPTER 5B: THE TEMPERATURE DEPENDENCE OF DIFFUSION IN
ALMOST LORENTZIAN GAS MIXTURES*

5B.1 Introduction	139
5B.2 Experimental and Results	142
5B.3 Calculations for Exact Lorentzian Thermal Diffusion Factors (α_L)	144
<i>REFERENCES</i>	148

Continued...

	<u>Page</u>
<i>CHAPTER 6: THE PRESSURE DEPENDENCE OF DIFFUSION</i>	
6.1 Introduction	150
6.2 Experimental and Results	151
6.3 Comparison with Enskog-Thorne Theory	160
REFERENCES	163
<i>APPENDIX 1: EQUATIONS TO CALCULATE P's AND Q's FOR CHAPMAN-ENSKOG THEORY</i>	165
<i>APPENDIX 2: NON-IDEALITY TERM USED IN SECTION 2.3.</i>	167
<i>APPENDIX 3: EXPERIMENTAL DATA FOR THE TEMPERATURE DEPENDENCE OF DIFFUSION</i>	169
<i>PUBLICATIONS FROM THE THESIS</i>	175

LIST OF TABLES

	<u>Page</u>	
3.1	Cell and Tube Dimensions	42
3.2	Effective Lengths and End Corrections for Various Tubes	45
3.3	Measurements of the Diffusional Columns	53
3.4	Least-square Constants for Bourdon Capsules	58
4.1	Concentration Dependence Results of the Diffusion Coefficients for He/O ₂ System at 300K with Two Bulb Cell (A ₁)	69
4.2	Concentration Dependence Results of the Diffusion Coefficients for He/N ₂ System at 300K with Two Bulb Cell (A ₁)	71
4.3	Concentration Dependence Results of the Diffusion Coefficients for He/Ar System at 300K with Two Bulb Cell (A ₁)	73
4.4	Concentration Dependence Results of the Diffusion Coefficients for He/CO ₂ System at 300K with Two Bulb Cell (A ₁)	75
4.5	Concentration Dependence Results of the Diffusion Coefficients for N ₂ /Ar System at 300K with Two Bulb Cell (A ₁)	77
4.6	Concentration Dependence Results of the Diffusion Coefficients for He/Ne System at 300K with Two Bulb Cell (A ₁)	79
4.7	Least-square Data for Eq. 4.1 at 300K	81
4.8	Deviations Between the Data Obtained by the Two Bulb Cell (A ₁) and Loschmidt Cell (A ₃)	83
4.9	Least-square Parameters of Equation 4.1 for the Systems Performed in Small Two Bulb Cell (A ₂) at 300K	84
4.10	Predicted Diffusion Coefficients for the Rare Gas Mixtures at 300K using Kihara's second approximation	86
4.11	Predicted Diffusion Coefficients for Some Other Binary Gas Mixtures at 300K using Kihara's second approximation	87
4.12	Comparison of Experimental and Predicted Values of $(P\mathcal{D}_{12})_{x_2=1} / (P\mathcal{D}_{12})_{x_2=0}$	92
4.13	Experimental and Predicted Values of the Diffusion Coefficients for He-Ar System at 277.00K	94
4.14	Experimental and Predicted Values of the Diffusion Coefficients for He-Ar System at 323.15K	95
4.15	Least-square Parameters of Equation 4.1 for the System He-Ar at 277.00K and 323.15K	97

Continued...

4.16	Comparison of the Experimental and Predicted Values of $(PD_{12})_{x_2=1}/(PD_{12})_{x_2=0}$ for He-Ar System at 277.00K and 323K	97
5A.1	Least-square Coefficients for Equation 5A.1	106
5A.2	Tests of [m,6,8] Potentials for Noble Gas Mixtures	109, 110
5A.3	Tests of [m,6,8] Potentials for Some Other Binary Gas Mixtures	111
5A.4	Differences $(B_{12}^{calc}-B_{12}^{exp})$ for the data of Brewer (Noble Gas Mixtures)	113
5A.5	Differences $(B_{12}^{calc}-B_{12}^{exp})$ for Some Other Binary Gas Mixtures	114
5A.6	Percentage Deviations $[(\eta_{mix}^{calc}-\eta_{mix}^{exp})/\eta_{mix}^{exp}] \times 100$ for the Binary Viscosity Data of Kestin and co-workers (Noble Gas Mixtures)	116
5A.7	Percentage Deviations $[(\eta_{mix}^{calc}-\eta_{mix}^{exp})/\eta_{mix}^{exp}] \times 100$ for Some Other Binary Gas Mixtures	117
5A.8	Percentage Deviations $[(\eta_{mix}^{calc}-\eta_{mix}^{exp})/\eta_{mix}^{exp}] \times 100$ for the Ternary Gas Mixtures	118
5A.9	Percentage Deviations $[(D_{12}^{calc}-D_{12}^{exp})/D_{12}^{exp}] \times 100$ for the Noble Gas Mixtures - van Heijnin et al.	121
5A.10	Percentage Deviations $[(D_{12}^{calc}-D_{12}^{exp})/D_{12}^{exp}] \times 100$ for the Noble Gas Mixtures - Hogervorst	122
5A.11	Comparison of Experimental and Predicted Thermal Diffusion Factors at 306K	124
5A.12	Tests of [m,6,8] Potentials for Some Pure Gases	126
5A.13	Differences $(B_{11}^{calc}-B_{11}^{exp})$ of Pure Gases for the Data of Brewer	127
5A.14	Differences $(B_{11}^{calc}-B_{11}^{exp})$ of Pure Gases for the Compilation of Dymond and Smith	128
5A.15	Percentage Deviations $[(D)_1^{calc}-(D)_1^{exp}]/(D)_1^{exp} \times 100$ for the Data of Winn	130
5A.16	Percentage Deviations $[(D)_1^{calc}-(D)_1^{exp}]/(D)_1^{exp} \times 100$ for the Data Published in the Literature	131
5A.17	Differences $(B_{12}^{calc}-B_{12}^{exp})$ Obtained by Assuming an (11,6,8, $\gamma=3$) Potential Derived from Our Diffusion Data Alone	132
5B.1	Experimental Results for the Temperature Dependence of the Diffusion Coefficients in Almost Lorentzian Gas Mixtures	143
5B.2	Least-square Coefficients for Eq.5B.8	144
5B.3	Least-square Coefficients for Eq.5B.9	145

Continued.....

	<u>Page</u>
5B.4 Predicted Values of the Ratios $(\partial \ln D_{12} / \partial \ln T)_p$ for the systems He-Ar and He-Kr using Chapman-Enskog Theory	146
5B.5 Comparison Between the Calculated and the Literature Values of α_L at 300K	146
6.1 Pressure Dependence Results at Two Temperatures for the Systems He-Ar, He-N ₂ , He-O ₂ and He-CO ₂	152
6.2 Least-square Parameters for Eqs. 6.1 and 6.4 and Diffusion "Virial Coefficients"	154
6.3 Second Virial Coefficients and Effective Distance Parameters	155
A3.1 Experimental Results for the Temperature Dependence of Diffusion	170 - 174

LIST OF FIGURES

	<u>Page</u>
3.1 A Schematic Diagram of the Small Two Bulb Cell (A ₂)	46
3.2 The Wheatstone Bridge Circuit	62
4.1 Concentration Dependence of the Diffusion Coefficient for the system He/O ₂ at 300K	70
4.2 Concentration Dependence of the Diffusion Coefficient for the system He/N ₂ at 300K	72
4.3 Concentration Dependence of the Diffusion Coefficient for the system He/Ar at 300K	74
4.4 Concentration Dependence of the Diffusion Coefficient for the system He/CO ₂ at 300K	76
4.5 Concentration Dependence of the Diffusion Coefficient for the system N ₂ /Ar at 300K	78
4.6 Concentration Dependence of the Diffusion Coefficient for the system He/Ne at 300K	80
4.7 Concentration Dependence of the Diffusion Coefficient for the systems He-Kr and He-Xe at 300K	88
4.8 Concentration Dependence of the Diffusion Coefficient for the systems Ne-Ar, Ne-Kr and Ne-Xe at 300K	89
4.9 Concentration Dependence of the Diffusion Coefficient for the systems Ar-Kr and Ar-Xe at 300K	90
4.10 Concentration Dependence of the Diffusion Coefficient for the systems Ar-O ₂ and CH ₄ -Kr at 300K	91
4.11 Concentration Dependence of Diffusion Coefficient for the system He-Ar at 323.15K and 277.00K	96
5A.1 A Typical Fit of the Temperature Dependence Data for Ar-Kr system	108
5A.2 Deviations, $(\Delta\phi/\epsilon)$, of Several Potentials from the the (11,6,8, $\gamma=3$) as a Function of the Reduced Separation (r/σ)	133
6.1 Density Dependence of the Diffusion Coefficient (n vs. nD_{12}) for the system He-Ar	156
6.2 Density Dependence of the Diffusion Coefficient (n vs. nD_{12}) for the system He-N ₂	157
6.3 Density Dependence of the Diffusion Coefficient (n vs. nD_{12}) for the system He-O ₂	158
6.4 Density Dependence of the Diffusion Coefficient (n vs. nD_{12}) for the system He-CO ₂	159

CHAPTER 1GENERAL INTRODUCTION

Recently, considerable attention has been paid to the study of the transport properties of gases, since these can furnish valuable information regarding the nature of the forces existing between atoms and molecules. Among these properties diffusion is of great interest because, to the first approximation, it depends only upon the interactions between the unlike molecules while all other properties (e.g. viscosity, thermal conductivity, thermal diffusion) depend upon both like and unlike forces between the atoms or molecules.

Two types of cells are in common use to study diffusion in gases:

1. The two bulb cell designed by Ney and Armistead¹.
2. The shearing cell of Loschmidt design².

Several workers³⁻¹⁹, after some modifications, made practical use of these cells to determine the tracer, mutual and thermal diffusion coefficients using a mass spectrometer^{3,7}, a differential thermal conductivity analyser⁴⁻⁶, an interferometer¹⁶, electrodes¹⁰, thermistors^{8,9} etc. to measure concentrations. The results obtained before the early 1970's have been reviewed by Marrero and Mason²⁰. This compilation also indicates that a lot of work has been done on diffusion as a function of temperature whereas the inform-

ation about the concentration and pressure dependence of diffusion is meagre.

To aid this scarcity, Van Heijningen *et al.*^{8,9} (in the late 1960's) constructed a two bulb apparatus and studied the concentration and temperature dependence of diffusion coefficients for binary mixtures of noble gases using thermistors to measure the rate of change in concentration. The reproducibility of the results given by them is 1 - 2%.

Some attempts were made^{8,9} to examine the Chapman-Cowling and Kihara expressions²¹, but due to the lack of accurate and precise experimental data, the workers failed to notice the finer details of these theories.

The necessity of the reliable and accurate data for diffusion to study the finer details of the expressions belonging to various transport properties forms the fundamental basis of this thesis.

Dunlop and co-workers²²⁻²⁵ improved the experimental techniques and obtained very precise data ($\approx \pm 0.1\%$) which was not accurate enough because of the improper use of the thermistor bridge. Later Yabsley and Dunlop²⁶ modified the Wheatstone bridge circuit and collected a considerable amount of data (accurate and precise) for some binary gas systems. In 1976, these authors constructed a two bulb cell and reported²⁷ the concentration dependence of binary diffusion coefficients for He-Ar and He-O₂ systems at 300K using two connecting tubes of different diameters and gave an equation, similar to the one given by Wirz²⁸, to calculate the end correction.

The first project of this thesis was to continue the above study with the aims:

- i. to give accurate and precise binary diffusion coefficients for several gas mixtures;
- ii. to investigate the details of Wirz relation²⁸;
- iii. to test the agreement between Kihara's second approximation to the Chapman-Enskog theory and the experimental data;
- iv. to measure the variation in concentration dependence of D_{12} with temperature (over $\approx 46K$).

All these aspects have been discussed in Chapter 4.

As stated earlier, the information about the forces between the atoms or molecules can be obtained from the study of the transport properties as a function of temperature. Many workers^{5,6, 8-10, 29-45} tried to obtain potential parameters (ϵ, σ) with the help of these physical properties.

Mason *et al.*¹⁰ predicted the potential parameters from the temperature dependence study of thermal diffusion coefficients and calculated D_{12} for the same systems to test their parameters.

Kestin and co-workers³³⁻³⁸ measured the viscosity coefficients for several gases and their mixtures, calculated the force parameters with the application of their theory of corresponding states^{37,38} and predicted the diffusion coefficients and thermal conductivities over a wide range of temperatures.

Smith *et al.*^{39,40} proposed a method to calculate the interaction energy parameter (η_{12}), which in turn depends upon the potential parameters, from the temperature dependence

of viscosities and obtained this parameter (η_{12}) for the mixtures of He-Ar, Ar-Kr and CH₄-CF₄.

Many authors^{5, 6, 8, 9, 29-32, 44, 45} measured binary diffusion coefficients as a function of temperature and calculated the potential parameters using Lennard Jones [12,6] and exp-6 potential models. The values reported by Van Heijningen^{8, 9} and Hogervorst²⁹⁻³² for these parameters are noteworthy since these authors measured the diffusion coefficients for almost all the noble gas mixtures over a wide range of temperature with a reproducibility of 1 - 2%.

It was noticed that the potential parameters obtained from one of the transport or equilibrium properties can reproduce the same data or the data for the same property at low and high temperatures, but unable to generate the data for another transport or equilibrium property within the experimental errors (e.g. the potential parameters obtained from viscosities have not predicted virial coefficients, (see Chapter 5A) because of the:

- i. less availability of the precise experimental data;
- ii. less flexibility of the intermolecular potential models.

Klein *et al.*⁴¹⁻⁴³ modified a three variable [m,6] potential model to a four variable [m,6,8] potential model. They calculated the force constants for many gases with the application of their [m,6,8] potential function and suggested⁴² that the gases Ar, Kr, Xe follow the corresponding states law since the potential that applies to them differ only in the two parameters σ and ϵ/k .

The aims of the second project (discussed in Chapter 5A) were:

- i. to see if potential parameters obtained from very precise experimental diffusion coefficients measured over a small temperature range ($\approx 46\text{K}$) can reproduce all the literature data or not;
- ii. to see if noble gas mixtures are conformal with any of the *assumed* [m,6,8] group of potentials.

It was considered desirable to calculate the potential parameters for the mixtures with diatomic or polyatomic molecules to see the changes produced by the internal energies of the molecules in predicting the literature data. The potential parameters for like interactions obtained by combining the viscosity and second virial coefficient data are also discussed in Chapter 5A.

The purpose of the next project was to verify the relation, given by Mason⁴⁸, between the thermal diffusion and the temperature derivatives of the diffusion coefficients.

Los and co-workers⁴⁴⁻⁴⁷ measured the binary diffusion coefficients for some Lorentzian gas mixtures as a function of temperature and calculated the Lorentzian thermal diffusion coefficients, α_L , at various temperatures for the same mixtures.

For further investigation of the Mason's equations⁴⁸, the temperature dependence of binary diffusion coefficients for almost Lorentzian gas mixtures He-Ar, He-Kr, H₂-Ar and D₂-Ar were measured and listed in Chapter 5B. The Lorentzian thermal diffusion coefficients were also calculated and discussed in the same chapter in terms of the limited data available in the literature.

The final project for this thesis was to study the effect of pressure on diffusion coefficients.

Because of the difficulties in handling the gases at high pressures, there is little data available in the literature^{15,49-58}. Some attempts⁵²⁻⁵⁸ were also made to study the tracer diffusion coefficients as a function of pressure, but the results obtained by these workers^{15,49-58} are not very good (reproducibility is not better than 5%).

Recently Staker *et al.*⁵⁹ constructed a Loschmidt cell and measured the binary diffusion coefficients for the mixtures He-Ne, He-Ar, He-Kr, He-Xe, He-N₂ and He-CO₂ at 300K and up to only 9 atmospheres. Bell *et al.*⁶⁰ used the same cell under similar conditions and added the data for ten more binary systems containing helium as the major component.

The purpose of this project was to perform the experiments at moderately high pressures up to 25 - 30 atmospheres and at different temperatures. It was done by modifying the cell used by the previous workers^{59,60} and the results obtained have been discussed (Chapter 6) with reference to the Thorne-Enskog theory⁶¹.

In addition to the above, Chapter 2 contains some theoretical aspects of the Chapman-Enskog theory and its extension by Enskog and Thorne for binary diffusion coefficients at moderately high pressure. This chapter also gives some information about the diffusion at low pressures and the use of the four variable [m,6,8] intermolecular potential function.

1.

In Chapter 3 very brief descriptions of the three cells used to measure D_{12} together with experimental procedures are given. A method to determine the diffusion coefficients from the raw experimental data is also discussed at the end of this chapter.

REFERENCES

1. Ney, E.P. and Armistead, F.C., *Phys. Rev.* 71
(1947) 14.
2. Loschmidt, J., *Akad. Wiss. Wien* 61 (1870) 367.
3. Winn, E.B., *Phys. Rev.* 80 (1950) 1024.
4. Mathur, B.P. and Saxena, S.C., *Appl. Sci. Res.* 18
(1968) 325.
5. Srivastava, B.N. and Srivastava, K.P., *J. Chem. Phys.* 30 (1959) 984.
6. Paul, R. and Srivastava, I.B., *J. Chem. Phys.* 35 (1961) 1621.
7. Malinauskas, A.P., *J. Chem. Phys.* 42 (1965) 156.
8. Van Heijningen, R.J.J., Feberwee, A., Van Oosten, A.
and Beenakker, J.J.M., *Physica* 32 (1966) 1649.
9. Van Heijningen, R.J.J., Harpe, J.P. and Beenakker,
J.J.M., *Physica* 38 (1968) 1.
10. Lonsdale, H.K. and Mason, E.A., *J. Phys. Chem.* 61 (1957) 1544.
11. McCarthy, K.P. and Mason, E.A., *Phys. Fluids* 3
(1960) 908.
12. Strehlow, R.A., *J. Chem. Phys.* 21 (1953) 2101.

13. Boardman, L.E. and Wild, N.E., *Proc. Roy. Soc. (London)* A162 (1937) 511.
14. Amdur, I., Irvine, J.W., Mason, E.A. and Ross, J., *J. Chem. Phys.* 20 (1952) 436.
15. Berry, V.J. and Koller, R.C., *Amer. Inst. Chem. Eng. J.* 6 (1960) 274.
16. Boyd, C.A., Stein, N., Steingrimsson, V. and Rumpel, W.F., *J. Chem. Phys.* 19 (1951) 548.
17. Ivakin, B.A. and Suetin, P.E., *Zh. Tekh. Fiz.* 34 (1964) 1155; [*Sov. Phys.-Tech. Phys.*, 9 866].
18. Ljunggren, S., *Ark. Kemi.*, 24 (1965) 1.
19. Walker, R.E. and Westenberg, A.A., *J. Chem. Phys.* 29 (1958) 1139.
20. Marrero, T.F. and Mason, E.A., *J. Chem. Phys. Ref. Data* 1 (1972) 3.
21. Hirschfelder, J.O., Curtiss, C.F. and Bird, R.B., *Molecular Theory of Gases and Liquids* (4th printing) Wiley (1964).
22. Carson, P.J., Dunlop, P.J. and Bell, T.N., *J. Chem. Phys.* 56 (1972) 531.
23. Yabsley, M.A., Carson, P.J. and Dunlop, P.J., *J. Phys. Chem.* 77 (1973) 703.

24. Staker, G.R., Yabsley, M.A., Symons, J.M. and Dunlop, P.J., *Chem. Soc. Faraday Trans. I* 70 (1974) 825.
25. Staker, G.R., Dunlop, P.J., Harris, K.R. and Bell, T.N., *Chem. Phys. Lett.* 32 (1975) 561.
26. Yabsley, M.A. and Dunlop, P.J., *J. Phys.* E8, (1975) 834.
27. Yabsley, M.A. and Dunlop, P.J., *Physica* 85A (1976) 160.
28. Wirz, P., *Helv. Phys. Acta* 20 (1947) 3.
29. Hogervorst, W. and Freudenthal, J., *Physica* 37 (1967) 97.
30. Hogervorst, W., *Physica* 51 (1971) 59.
31. Hogervorst, W., *Physica* 51 (1971) 77.
32. Hogervorst, W., *Physica* 51 (1971) 90.
33. Kestin, J., Ro, S.T. and Wakeham, W.A., *J. Chem. Phys.* 56 (1972) 5837.
34. Kestin, J., Ro, S.T. and Wakeham, W.A., *J. Chem. Phys.* 56 (1972) 4086.
35. Kestin, J., Khalifa, H.E. and Wakeham, W.A., *J. Chem. Phys.* 67 (1977) 4254.
36. Kestin, J., Khalifa, H.E., Ro, S.T. and Wakeham, W.A., *Physica* 88A (1977) 242.

37. Kestin, J., Ro, S.T. and Wakeham, W.A., *Physica*
58 (1972) 165.
38. Kestin, J., Khalifa, H.E. and Wakeham, W.A.,
Physica 90A (1978) 215.
39. Maitland, G.C. and Smith, E.B., *J. Chem. Soc.*
Faraday Trans. I 70 (1974) 1191.
40. Gough, D.W., Matthews, G.P. and Smith, E.B.,
J. Chem. Soc. Faraday Trans. I 72 (1976) 645.
41. Klein, M. and Hanley, H.J.M., *J. Chem. Phys.* 53
(1970) 4722.
42. Hanley, H.J.M. and Klein, M., *J. Phys. Chem.* 76
(1972) 1743.
43. Klein, M., Hanley, H.J.M., Smith, F.J. and
Holland, P., *Tables of Collision Integrals
and Second Virial Coefficients for the [m,6,8]
Intermolecular Potential Function*, U.S. National
Bureau of Standards Circular, NSRD-NBS47 (1974).
44. Vugts, H.F., Boerboom, A.J.H. and Los, J., *Physica*
44 (1969) 219.
45. Wahby, A.S.M., Boerboom, A.J.H. and Los, J.,
Physica 75 (1974) 573.
46. Van de Ree, J., and Los, J., *Physica* 75 (1974) 548.
47. Wahby, A.S.M., Boerboom, A.J.H. and Los, J.,
Physica 75 (1974) 560.

48. Mason, E.A., *J. Chem. Phys.* 27 (1957) 782.
49. Reamer, H.H. and Sage, B.H., *J. Chem. Eng. Data*
8 (1963) 34.
50. Islam, M. and Stryland, J.C., *Physica* 45 (1969) 115.
51. De Paz, M., Tantalo, F. and Varni, G., *J. Chem. Phys.* 61 (1974) 3875.
52. Jefferies, Q.R. and Drickamer, H.G., *J. Chem. Phys.*
22 (1954) 436.
53. Becker, E., Vogell, W. and Zigan, F., *Z. Naturforsch*
8a (1953) 686.
54. Durbin, L. and Kobayashi, R., *J. Chem. Phys.* 37
(1962) 1643.
55. Trappeniers, N.J. and Michels, J.P.J., *Chem. Phys. Letters* 18 (1972) 1.
56. Chou, C. and Martin, J.J., *Ind. Eng. Chem.* 49
(1957) 758.
57. Balenovic, Z., Myers, M.N. and Giddings, J.C.,
J. Chem. Phys. 52 (1970) 915.
58. Codastefano, P., Ricci, M.A. and Zanza, V.,
Physica 92A (1978) 315.
59. Staker, G.R. and Dunlop, P.J., *Chem. Phys. Letters*
42 (1976) 419.

60. Bell, T.N., Shankland, I.R. and Dunlop, P.J.,
Chem. Phys. Letters 45 (1977) 445.
61. Chapman, S. and Cowling, T.G., *The Mathematical
Theory of Non-Uniform Gases*, Cambridge
University Press, 3rd edition (1970).

CHAPTER 2THEORETICAL ASPECTS OF TRANSPORT AND
EQUILIBRIUM PROPERTIES IN GASES*2.1 Introduction*

The transport properties of gases depend upon the forces between atoms or molecules and their general changes in composition, temperature and pressure. Chapman and Enskog¹ (1910-1917), independently, developed a theory for monoatomic gases and their mixtures which includes these intermolecular interactions. In the beginning of this chapter, the kinetic approach of Chapman and Enskog¹ to transport properties for dilute gases is described. Extension of this theory by Enskog², applicable to moderately dense gases for single components, and Thorne's² generalisation for their binary mixtures are also discussed here. The equations for diffusional flow at very low pressures (Knudsen diffusion) and the ones to calculate the collision integrals and reduced second virial coefficients for the [m,6,8] intermolecular potentials are given at the end of the chapter.

2.2 Chapman-Enskog Theory for Dilute Gases

Since the theory is quite long and cumbersome, a detailed study has been avoided and only a summary of its basic fundamentals, assumptions and the results of the derivations for transport coefficients are given here.

Assumptions of Chapman-Enskog Theory

i. The Chapman-Enskog theory¹ takes into account only binary collisions and therefore restricts its application to the gases or gas mixtures at low densities which means the results obtained from this theory are not applicable at sufficiently high pressures where ternary and high order collisions occur.

ii. The first approximation of the Chapman-Enskog theory obtained from the distribution function is applicable when gradients in physical quantities (e.g. concentration, temperature, density, molecular velocities, etc.) are slightly different from equilibrium. For larger gradients, the higher terms of the series approximation of the distribution function must be considered.

iii. The pressure of the gas should be high enough for the mean free path to be negligible as compared with the dimensions of the container, thus the gas behaves as a *continuum* (collisions of the gas molecules with the container can be neglected). The theory does not apply to systems at very low pressures because the gas molecules collide frequently with the walls of the container which makes the equilibrium hard to establish within the gas itself. The Knudsen gas behaviour is an extreme case where gas-wall collisions predominate^{3,4}.

iv. The Chapman-Enskog theory is applicable only to mono-atomic gases or gas mixtures with no internal degrees of freedom. Strictly the theory is limited to spherical molecules, however this can be relaxed to apply to the molecules which are not too non-spherical^{4,5} or polar⁶ because some of the transport properties of gases (e.g. diffusion and viscosity) are little affected by the internal degrees of freedom.

v. The molecular size should be negligible as compared to the mean free path so that the distribution function of the colliding species can be evaluated at the same point, r , in space at the moment of contact.

vi. The distance between the two colliding molecules should be large enough to ignore the molecular interactions so that the second order distribution function can be expressed as the product of the two first order functions.

vii. At very low temperature ($< 200\text{K}$) quantum mechanical diffraction effects, similar to those diffraction effects in optics, are significant for lighter gases such as helium, hydrogen and their isotopes. These effects have been shown^{7,8} in evaluating the quantum-corrected collision integrals for the Lennard-Jones [12,6] potential where phase shifts are more important than the angle of deflection. Chapman and Enskog used *Classical-mechanics* which exclude these quantum effects thereby imposing further restrictions on its use.

The Chapman-Enskog theory is based upon the knowledge of the first order distribution function $f_i(r, v_i, t)$ which is defined as $f_i(r, v_i, t) dr, dv_i$ and is the probable number of molecules of the i th species to be found at a particular time t in the spatial range (dr about r) and in the velocity range (dv_i about v_i). At equilibrium, when there is no gradient in the concentration, velocity and temperature, this function reduces to Maxwell distribution

$$f_i^0 = n_i (m_i / 2\pi kT)^3 \exp(-m_i v_i^2 / 2kT) \quad \dots \quad 2.1$$

where n_i and m_i are the number density and molecular weight of the species i at temperature T , and k is a Boltzmann's constant.

When the system is not at equilibrium, the distribution function may be given by Boltzmann integro-differential equation⁹, which describes the variation of f_i due to molecular interactions and can be solved by a perturbation method developed by Chapman and Enskog. Since the equation is derived for the properties of gases which are under conditions only slightly different from equilibrium, the distribution function term decays to zero as the system approaches to equilibrium, thus giving a linearised integro-differential equation. In this way, f_i can be written as

$$f_i = f_i^0 + f_i^0 \psi_i \quad \dots \quad 2.2$$

where f_i^0 is a Maxwell distribution function given by equation 2.1 and ψ_i is the perturbation function which is proportional to the relevant transport gradient and can be calculated from the molecular velocities using a variation technique¹⁰ or by the solution of an infinite set of linear equations¹.

Generally, the transport coefficients can be determined in principle from the ratio of two infinite determinants¹ which can not be solved exactly. However, these coefficients may be approximated by systematically truncating the determinants. Two separate truncation schemes were used by Chapman and Cowling¹ and by Kihara¹¹.

The final equations derived by Chapman and Enskog to predict the transport coefficients of gases and their mixtures (used in Chapters 4, 5 and 6) are given here.

a. *Diffusion Coefficient for Binary Mixtures*

The diffusion coefficient of a binary mixture, to the first approximation, for both the schemes can be written as

$$[D_{12}]_1 = \frac{3}{8\sqrt{\pi}} \left[\frac{k^3 T^3 (M_1 + M_2)}{2M_1 M_2} \right]^{1/2} \frac{1}{P \sigma_{12}^2 \Omega_{12}^{(1,1)*} (T^*)} \dots \quad 2.3$$

where D_{12} is the diffusion coefficient, T is the temperature, P is the pressure, M_1 and M_2 are the molecular weights of the species 1 and 2, σ_{12} is the distance between the molecules when interaction energy is zero, $\Omega_{12}^{(1,1)*}$ is the reduced collision integral which depends upon the reduced temperature, $T^* = kT/\epsilon_{12}$, ϵ_{12} is the depth of the potential energy well and k is Boltzmann's constant.

As can be seen in the first approximation equation 2.3, the diffusion coefficients of binary mixtures depend only upon the interactions between the unlike molecules which means that the temperature dependence of the diffusion coefficients gives an excellent method* to calculate the force constants for dissimilar pairs of molecules. The same equation 2.3 also shows that $[D_{12}]_1$ is independent of composition but inversely proportional to the pressure, thus predicting that the quantity $P[D_{12}]_1$ should be constant at constant temperature.

The higher approximations of D_{12} for both the methods are given by:

$$[D_{12}]_k = [D_{12}]_1 f_{D_{12}}^{(k)} \dots \quad 2.4$$

where $f_{D_{12}}^k$ is the higher approximation factor which depends upon the molefractions, molecular weights, molecular sizes and collision integrals.

* The exact method to calculate the potential parameters from the temperature dependence of the diffusion coefficient has been described in Chapter 5.

Kihara's second approximation for D_{12} may be written as

$$[D_{12}]_2 = [D_{12}]_1 [1 + \delta_{12}] , \quad \dots \quad 2.5$$

whereas the Chapman-Cowling equation is expressed in the form of

$$[D_{12}]_2 = [D_{12}]_1 \left[\frac{1}{1 - \delta_{12}} \right] , \quad \dots \quad 2.6$$

The factor δ_{12} can be calculated by the following expression

$$\delta_{12} = \frac{(6C_{12}^* - 5)^2}{10} \left\{ \frac{x_1^2 P_1 + x_2^2 P_2 + x_1 x_2 P_{12}}{x_1^2 Q_1 + x_2^2 Q_2 + x_1 x_2 Q_{12}} \right\} . \quad \dots \quad 2.7$$

where x_1 and x_2 are the molefractions of the components 1 and 2 respectively, C_{12}^* is a ratio of the collision integrals given by equation 2.15 and P's and Q's are the complicated expressions* presented in Appendix 1. The tangled equations for much higher approximations can be found elsewhere^{12,13}.

b. Self Diffusion Coefficient.

The coefficient of self diffusion $[D]_1$ to a first approximation can be given by the following relation

$$[D]_1 = \frac{3}{8\sqrt{\pi}} [MkT]^{1/2} \frac{1}{P\sigma^2 \Omega^{(1,1)*} (T^*)} , \quad \dots \quad 2.8$$

where all symbols have their usual meanings.

The higher approximations for $[D]_1$ can be written as

$$[D]_k = [D]_1 f_D^{(k)} \quad \dots \quad 2.9$$

where k is the degree of higher approximation.

* Both Kihara and Chapman-Cowling gave the same expressions to calculate the values of P's whereas they differ in those of Q's .

The second approximation for self diffusion coefficient, for both the schemes, is similar to that given for binary mixture except that δ is only a function of reduced temperature T^* and the equations can be written as

$$[D]_2 = [D]_1 [1+\delta] \quad \dots \quad \text{Kihara's second approximation} \quad \dots \quad 2.10$$

$$[D]_2 = [D]_1 \left[\frac{1}{1-\delta} \right] \quad \dots \quad \text{Chapman-Cowling second approximation} \quad \dots \quad 2.11$$

where δ can be calculated as

$$\delta = \frac{(6C_{12}^* - 5)^2}{(55 - 12B^* + 16A^*)} \quad , \quad \dots \quad 2.12$$

and

$$A^* = \Omega^{(2,2)^*} / \Omega^{(1,1)^*} \quad \dots \quad 2.13$$

$$B^* = \{5\Omega^{(1,2)^*} - 4\Omega^{(1,3)^*}\} / \Omega^{(1,1)^*} \quad \dots \quad 2.14$$

$$C^* = \Omega^{(1,2)^*} / \Omega^{(1,1)^*} \quad \dots \quad 2.15$$

The values of these ratios of collision integrals (A^* , B^* and C^*) are very close to unity.

c. The Coefficient of Viscosity for a Pure Gas.

The coefficient of viscosity for a pure gas to its first approximation is given by the Chapman-Enskog theory

$$[\eta]_1 = \frac{5}{16\sqrt{\pi}} [MkT]^{1/2} \frac{1}{\sigma^2 \Omega^{(2,2)^*} (T^*)} \quad \dots \quad 2.16$$

For higher approximations $[\eta]_1$ can be expressed as

$$[\eta]_k = [\eta]_1 f_{\eta}^{(k)} \quad \dots \quad 2.17$$

where η represents the coefficient of viscosity of a gas. The quantity $f_{\eta}^{(k)}$ (higher approximation term) is a function of T^* and differs only slightly from unity. The coefficient of viscosity (equation 2.16) depends only upon the interactions of like molecules, the temperature dependence study of which makes an important tool (see Chapter 5) to calculate the potential parameters for pure gases.

d. *The Coefficient of Viscosity for Binary Mixtures.*

The coefficient of viscosity for binary gas mixtures can be calculated by the use of the following relations.

$$\frac{1}{[\eta_{\text{mix}}]_1} = \frac{X_{\eta} + Y_{\eta}}{1 + Z_{\eta}} = X_{\eta} \left[\frac{1 + (Y_{\eta}/X_{\eta})}{1 + Z_{\eta}} \right], \quad \dots \quad 2.18$$

$$X_{\eta} = \frac{x_1^2}{[\eta_1]_1} + \frac{2x_1 x_2}{[\eta_{12}]_1} + \frac{x_2^2}{[\eta_2]_1}, \quad \dots \quad 2.19$$

$$Y_{\eta} = \frac{3}{5} A^* \left\{ \frac{x_1}{[\eta_1]_1} \left(\frac{M_1}{M_2} \right) + \frac{2x_1 x_2}{[\eta_{12}]_1} \left(\frac{(M_1 + M_2)^2}{4M_1 M_2} \right) \right. \\ \left. \left(\frac{[\eta_{12}]_1^2}{[\eta_1]_1 [\eta_2]_1} \right) + \frac{x_2^2}{[\eta_2]_1} \left(\frac{M_2}{M_1} \right) \right\}, \quad \dots \quad 2.20$$

$$Z_{\eta} = \frac{3}{5} A^* \left[x_1^2 \left(\frac{M_1}{M_2} \right) + 2x_1 x_2 \left\{ \left(\frac{M_1 + M_2}{4M_1 M_2} \right)^2 \left(\frac{[\eta_{12}]_1}{[\eta_1]_1} \right) \right. \right. \\ \left. \left. + \frac{[\eta_{12}]_1}{[\eta_2]_1} \right\} - 1 \right] + x_2^2 \left(\frac{M_2}{M_1} \right) \quad \dots \quad 2.21$$

$$[\eta_{12}]_1 = \frac{5}{16\sqrt{\pi}} \left[\frac{2M_1 M_2 kT}{(M_1 + M_2)} \right]^{1/2} \frac{1}{\sigma_{12}^2 \Omega_{12}^{(2,2)*}(T^*)}, \quad \dots \quad 2.22$$

where $[\eta_{\text{mix}}]_1$ is the coefficient of viscosity for a binary

gas mixture to the first approximation and $[\eta_1]_1$ and $[\eta_2]_1$ are the viscosities of pure components 1 and 2 respectively. $[\eta_{12}]_1$ is a hypothetical viscosity coefficient for a substance whose molecular weight is $2M_1M_2/(M_1+M_2)$ with potential parameters ϵ_{12} and σ_{12} .

The quantity $|1+(Y_\eta/X_\eta)/(1+Z_\eta)|$ (equation 2.18) is quite large and may contribute as much as 50% to the final values, but becomes very small if $M_1 \approx M_2$ and the interaction between the like and the unlike pairs are nearly the same.

e. *The Coefficient of Viscosity for Ternary Mixtures.*

The coefficient of viscosity for ternary mixtures is given by equation 2.23 in the form of a ratio of determinants which can be computed by solving the defined quantities H_{ij} 's.

$$[\eta_{\text{mix}}]_1 = - \frac{\begin{vmatrix} H_{11} & H_{12} & H_{13} & x_1 \\ H_{12} & H_{22} & H_{23} & x_2 \\ H_{13} & H_{23} & H_{33} & x_3 \\ x_1 & x_2 & x_3 & 0 \end{vmatrix}}{\begin{vmatrix} H_{11} & H_{12} & H_{13} \\ H_{12} & H_{22} & H_{23} \\ H_{13} & H_{23} & H_{33} \end{vmatrix}} \dots 2.23$$

The factors H_{ii} and H_{ij} can be calculated in terms of $[\eta_{ij}]_1$ as follows

$$H_{11} = \frac{x_1^2}{[\eta_1]_1} + \left[\frac{2x_1x_2}{[\eta_{12}]_1} \cdot \frac{M_1M_2}{(M_1+M_2)^2} \left(\frac{5}{3A_{12}^*} + \frac{M_2}{M_1} \right) \right] \\ + \left[\frac{2x_1x_3}{[\eta_{13}]_1} \cdot \frac{M_1M_3}{(M_1+M_3)^2} \left(\frac{5}{3A_{13}^*} + \frac{M_3}{M_1} \right) \right] \dots 2.24$$

$$H_{22} = \frac{x_2^2}{[\eta_2]_1} + \left[\frac{2x_1 x_2}{[\eta_{12}]_1} \cdot \frac{M_1 M_2}{(M_1 + M_2)^2} \left(\frac{5}{3A_{12}^*} + \frac{M_1}{M_2} \right) \right] \\ + \left[\frac{2x_2 x_3}{[\eta_{23}]_1} \cdot \frac{M_2 M_3}{(M_2 + M_3)^2} \left(\frac{5}{3A_{23}^*} + \frac{M_3}{M_2} \right) \right], \quad \dots \quad 2.25$$

$$H_{33} = \frac{x_3^2}{[\eta_3]_1} + \left[\frac{2x_1 x_3}{[\eta_{13}]_1} \cdot \frac{M_1 M_3}{(M_1 + M_3)^2} \left(\frac{5}{3A_{13}^*} + \frac{M_1}{M_3} \right) \right] \\ + \left[\frac{2x_2 x_3}{[\eta_{23}]_1} \cdot \frac{M_2 M_3}{(M_2 + M_3)^2} \left(\frac{5}{3A_{23}^*} + \frac{M_2}{M_3} \right) \right], \quad \dots \quad 2.26$$

$$H_{12} = - \frac{2x_1 x_2}{[\eta_{12}]_1} \cdot \frac{M_1 M_2}{(M_1 + M_2)^2} \left(\frac{5}{3A_{12}^*} - 1 \right), \quad \dots \quad 2.27$$

$$H_{13} = - \frac{2x_1 x_3}{[\eta_{13}]_1} \cdot \frac{M_1 M_3}{(M_1 + M_3)^2} \left(\frac{5}{3A_{13}^*} - 1 \right), \quad \dots \quad 2.28$$

$$H_{23} = - \frac{2x_2 x_3}{[\eta_{23}]_1} \cdot \frac{M_2 M_3}{(M_2 + M_3)^2} \left(\frac{5}{3A_{23}^*} - 1 \right), \quad \dots \quad 2.29$$

where all symbols have their usual significance.

f. Calculations for Thermal Diffusion Coefficient.

Both Chapman and Kihara gave a similar expression to calculate the thermal diffusion factor $[\alpha_T]_1$ to a first approximation, which is written as

$$[\alpha_T]_1 = (6C_{12}^* - 5) \frac{x_2 S_2 - x_1 S_1}{x_1^2 Q_1 + x_2^2 Q_2 + x_1 x_2 Q_{12}}, \quad \dots \quad 2.30$$

where subscript 1 is used for light component

$$S_1 = \frac{M_1}{M_2} \left(\frac{2M_2}{M_1 + M_2} \right)^{1/2} \left[\frac{\Omega_{11}^{(2,2)*}}{\Omega_{11}^{(1,1)*}} \right] \left(\frac{\sigma_{11}}{\sigma_{22}} \right)^2 \\ - \frac{4M_1 M_2 A_{12}^*}{(M_1 + M_2)^2} - \frac{15M_2 (M_2 - M_1)}{2(M_1 + M_2)^2}, \quad \dots \quad 2.31$$

The relation for S_2 can be obtained from that of S_1 by the interchange of subscripts and the expressions for Q 's to calculate $[\alpha_T]_1$ are given in Appendix 1. In order to differentiate between Kihara's expression from that of Chapman and Cowling, the letters in the former are marked with a bar while those in the latter are left unbarred. The thermal diffusion coefficient to a second approximation $[\alpha_T]_2$ for Kihara's approach can be given as

$$[\bar{\alpha}_T]_2 = [\alpha_T]_1 (1 + \bar{K}_1) + \bar{K}_2, \quad \dots \quad 2.32$$

$$\bar{K}_1 = h_3 h_5 + h_4 h_{-6} + h_{-3} h_{-5} + h_{-4} h_6, \quad \dots \quad 2.33$$

$$\begin{aligned} \bar{K}_2 = & \frac{5}{2x_2} \left(\frac{M_1 + M_2}{2M_1} \right)^{1/2} (h_{-1} h_{-5} + h_1 h_6 - h_2 h_4 + h_2 h_{-3}) \\ & - \frac{5}{2x_1} \left(\frac{M_1 + M_2}{2M_2} \right)^{1/2} (h_1 h_6 + h_{-1} h_{-6} - h_{-2} h_{-4} + h_2 h_3), \end{aligned} \quad \dots \quad 2.34$$

where h_k 's are the quantities consisting of the combinations of C_{ij} values which are the remains of the corresponding elements a_{ij} after discarding the derivatives of their collision integrals.

A brief method to obtain h_k 's according to Kihara's extended scheme is given elsewhere¹².

2.3 *Extension of Chapman-Enskog Theory for Moderately Dense Gases*

The experimental results differ from the Chapman-Enskog approach (Section 2.2), according to which the product of the number density and the diffusion coefficient is independent of

number density or pressure. This theory of dilute gases was first modified by Enskog¹ to study the real nature of fluids for pure components. The modified kinetic theory, of rigid spherical molecules, for dense gases is based on the fact that the molecules have finite size and only binary collisions occur. The three body, or higher order collisions^{1,14}, are neglected. At high pressures, as the gases are compressed, there is (i) transport of energy and momentum from the centre of one molecule to the centre of the other; (ii) probability of increasing the collisions due to the increased excluded volume, and (iii) probability of decreasing the collisions due to the shielding effect of the molecules. Thus a factor Y (dependent on the number density) is introduced to compensate the frequency of the collisions for a gas made up of point particles and is related to the equation of state

$$P = nkT(1 + \frac{2}{3} n\pi\sigma^3 Y) \quad \dots \quad 2.35$$

Enskog solved a modified integro-differential equation for the distribution function in a dense gas which yields the following equation for the self diffusion

$$nD = (nD)_0 / Y \quad \dots \quad 2.36$$

where $(nD)_0$ is a product of the number density and the diffusion coefficient for a dilute gas. The factor Y is calculated by

$$Y = 1 + \frac{5}{12} n\pi\sigma^3 + \dots \quad \dots \quad 2.37$$

Thorne¹ generalised the Enskog theory for binary gas

mixtures whereas Tham and Gubbins¹⁵ extended the same for multi-component mixtures.

Thorne's equation for the mutual diffusion coefficient of dense gases is written as

$$nD_{12} = \frac{(nD_{12})_0}{Y_{12}}, \quad \dots \quad 2.38$$

where

$$Y_{12} = 1 + \frac{2}{3} \pi n \left[x_1 \sigma_{11}^3 \left(\frac{\sigma_{11} + 4\sigma_{22}}{4\sigma_{11} + 4\sigma_{22}} \right) + x_2 \sigma_{22}^3 \left(\frac{4\sigma_{11} + \sigma_{22}}{4\sigma_{11} + 4\sigma_{22}} \right) \right] + \dots \quad \dots \quad 2.39$$

Thorne's diffusion coefficient, D_{12} , can be related to the experimental diffusion coefficient, \mathcal{D}_{12} , by a relation¹⁵

$$\frac{(n\mathcal{D}_{12})}{(nD_{12})} = \left(\frac{\partial \ln a_1}{\partial \ln x_1} \right)_{T,P} \quad \dots \quad 2.40$$

where a_1 is activity of component 1 and $(\partial \ln a_1 / \partial \ln x_1)_{T,P}$ is a non-ideality thermodynamic factor.

For binary mixtures¹⁶, this factor can be written as

$$\left(\frac{\partial \ln a_1}{\partial \ln x_1} \right)_{T,P} = 1 - 4x_1 x_2 B^E P, \quad \dots \quad 2.41$$

which is also given^{15,17} by

$$\left(\frac{\partial \ln a_1}{\partial \ln x_1} \right)_{T,P} = [1 + n\pi x_1 x_2 (\sigma_{22} - \sigma_{11})^2 (\sigma_{22} + \sigma_{11})]. \quad \dots \quad 2.42$$

This relation has been derived in Appendix 2.

By combining equations 2.38 and 2.40

$$\frac{(n\mathcal{D}_{12})}{(nD_{12})_0} = \left(\frac{\partial \ln a_1}{\partial \ln x_1} \right)_{T,P} Y_{12}^{-1} \quad \dots \quad 2.43$$

By substituting the value of the non-ideality factor (from equation 2.42) into equation 2.43

$$\frac{(nD_{12})}{(nD_{12})_0} = [1 + n\pi x_1 x_2 (\sigma_{22} - \sigma_{11})^2 (\sigma_{22} + \sigma_{11})] Y_{12}^{-1} \dots 2.44$$

The above expression can be rearranged to give a linear equation

$$\frac{(nD_{12})}{(nD_{12})_0} = (1 + B_D^{RS} n) \dots 2.45$$

where

$$B_D^{RS} = x_1 x_2 \pi (\sigma_{22} - \sigma_{11})^2 (\sigma_{22} + \sigma_{11}) - (Y_{12} - 1)/n \dots 2.46$$

Thorne's generalisation as visualised recently¹⁸⁻²² is consistent with the phenomenological theory to a first order number density terms and is inconsistent with the irreversible thermodynamics. Van Beijeren and Ernst²² modified this theory in terms of the local-equilibrium radial distribution function which includes the second and higher order terms in the number density. This modified theory^{21,22} seems to be consistent with the irreversible thermodynamics.

2.4 Diffusion Coefficient Equations at Low Pressures

The Chapman-Enskog solution¹ to Boltzmann's equation assumed that the molecules have small mean free path which means that the collisions with the walls are ~~significant~~ ^{insignificant}, but at very low pressures (≈ 3 torr) where the mean free paths become large enough so that collisions with the walls are significant, the experimental binary diffusion coefficient, D_{12} , will differ from the Chapman-Enskog binary diffusion

coefficient, \mathcal{D}_{12} , where the above effects (Knudsen effects) are absent.

The relation used to convert D_{12} into \mathcal{D}_{12} (in Chapter 4 for two bulb apparatus) was obtained from the work of Mason *et al.*²³ who studied the gas transport phenomena through porous media with a "dusty-gas" model. The work of these authors²³ was based on the flow equations of Zhdanov, Kagan and Sazykin²⁴ which were derived in terms of composition, pressure and temperature gradients using Grad's 13-moment approximation. The final expression (to convert D_{12} into \mathcal{D}_{12}) can be written in the form

$$PD_{12} = (P\mathcal{D}_{12}) [1+A(\text{Pr})^{-1}] [1+(A+B)(\text{Pr})^{-1}+C(\text{Pr})^{-2}]^{-1}, \quad \dots \quad 2.47$$

where

$$A = (16/3)\tilde{v}_2 \eta b, \quad \dots \quad 2.47a$$

$$B = (P\mathcal{D}_{12})b/(2/3\tilde{v}_1), \quad \dots \quad 2.47b$$

$$C = 8\eta b(P\mathcal{D}_{12})(1 - \beta_1), \quad \dots \quad 2.47c$$

$$b = (1 - x_1 \beta_1)^{-1}, \quad \dots \quad 2.47d$$

$$\tilde{v}_i = (8kT/\pi m_i)^{1/2}, \quad i = 1, 2, \quad \dots \quad 2.47e$$

$$\beta_1 = [1 - (m_1/m_2)^{1/2}], \quad \dots \quad 2.47f$$

and all the symbols have their usual significance. Equation 2.47 can be solved by using the average value for x_1, x_2, η and P and adjusting the value for $(P\mathcal{D}_{12})$ to get a minimum difference between the experimental and the predicted values.

For the small values of $(\text{Pr})^{-1}$, the above equation can be approximated to

$$(PD_{12}) = (P\mathcal{D}_{12}) [1 - B(\text{Pr})^{-1}], \quad \dots \quad 2.48$$

which shows that a typical plot between $(Pr)^{-1}$ and (PD_{12}) should be a straight line with (PD_{12}) as an intercept and $-B(PD_{12})$ as a limiting slope which deviates from equation 2.47 by $\approx .2\%$ when $(Pr)^{-1} = 3500 \text{ atm}^{-1} \text{ cm}^{-1}$ and by $\approx 1\%$ when $(Pr)^{-1} = 6800 \text{ atm}^{-1} \text{ cm}^{-1}$.

The above equation 2.48 can be rearranged to a form

$$(PD_{12}) = (PD_{12}) (1 + B'(PD_{12})(Pr)^{-1} + 2(B'(PD_{12})(Pr)^{-1})^2 + \dots) \quad \dots \quad 2.49$$

where

$$B' = b/(2/3\tilde{v}_1) \quad \dots \quad 2.49a$$

The reproducibility of the results by this expression was much better when the value of the slip factor, introduced by Mason²³, was used as one (limiting value) rather than any other value (< 1) from the literature.

2.5 [m,6,8] Intermolecular Potential Function

In the present study [m,6,8] intermolecular potential^{25,26} is of common use because it has more flexibility over the exp-6, [m,6] potential functions²⁷⁻²⁹ and the law of corresponding states³⁰. The limitations of the latter potential functions are;

- (i) a set of potential parameters obtained from them over a certain temperature range is unable to correlate the experimental data at different (low and high) temperatures;

- (ii) a set of potential parameters calculated from three variable potential functions²⁸ can only predict one type of property (e.g. ϵ_{12} and σ_{12} calculated from viscosity data (non-equilibrium property) can not predict the second virial coefficients (equilibrium property));
- (iii) a set of potential parameters calculated from them is unable to predict the data from scattering experiments.

To overcome these limitations Klein *et al.*^{25,26} introduced an additional variable, C/r^8 , in [m,6] potential to make it a four parameter potential function. This semi-theoretical [m,6,8] potential can be written as

$$\phi(r) = \frac{A}{r^m} - \frac{B}{r^6} - \frac{C}{r^8}, \quad \dots \quad 2.50$$

where A is the coefficient of repulsion and B and C are the coefficients of attraction, m represents the extent of repulsion and exponents six and eight are the indices of attraction based on fundamental quantum mechanical ideas².

In reduced form, equation 2.50 can be written as

$$\phi^*(r^*) = \frac{1}{m-6} [6+2\gamma] \left(\frac{1}{r^*}\right)^m - \frac{1}{m-6} [m-\gamma(m-8)] \left(\frac{1}{r^*}\right) - \frac{\gamma}{(r^*)^8}, \quad \dots \quad 2.51$$

where $\phi^* = \phi/\epsilon$, $r^* = r/r_m$, $\gamma = C/r_m^8$ measures the strength of the inverse eighth power attraction, ϵ is the depth of the potential well and r_m is the intermolecular separation at which $\phi^* = -\epsilon$.

Generally r is denoted by σ when $\phi = 0$ and if d is the ratio of these lengths (i.e. $d = \frac{r}{\sigma}$), equation 2.51 can be represented as

$$\begin{aligned} \phi^*(r^*) &= \frac{d^m}{m-6} [6+2\gamma] \left(\frac{1}{r^*}\right)^m \\ &- \frac{d^6}{m-6} [m-\gamma(m-8)] \left(\frac{1}{r^*}\right)^6 - \frac{\gamma d^8}{(r^*)^8} \dots \quad 2.52 \end{aligned}$$

where $r^* = r/r_m$ if $d = 1$ and $r^* = r/\sigma$ if the actual value of d is used. Therefore an appropriate value of r^* should be used to compute the quantities dependent on it.

2.6 Collision Integrals and Reduced Second Virial Coefficients

The collision integrals $\Omega^{(\ell, s)*}(T^*)$ used to predict the transport properties (see Chapters 4 and 5) can be related to this reduced potential function through the following relations

$$\Omega^{(\ell, s)*}(T^*) = \frac{2}{(s-1)! T^{*(s-2)}} \int_0^\infty \exp\left[-\frac{g^{*2}}{T^*}\right] g^{*(2s+3)} Q^{(\ell)*}(g^*) dg^*, \quad \dots \quad 2.53$$

where $Q^{(\ell)*}(g^*)$ is a cross section and a function of the reduced energy of the collision. This factor can be written as

$$Q^{(\ell)*}(g^*) = \frac{2}{1-\frac{1}{2}\left[\frac{1+(-1)^\ell}{1+\ell}\right]} \int_0^\infty (1-\cos^\ell \chi) b^* db^*. \quad \dots \quad 2.54$$

$\chi(g^*, b^*)$ is a scattering angle and is given by

$$\chi(g^*, b^*) = \pi - 2b^* \int_0^\infty \frac{dr^*/r^*}{\sqrt{1-(b^*)^2/(r^*)^2 - \phi^*(r^*)/g^{*2}}}, \quad \dots \quad 2.55$$

where r_m^* in this case is the reduced distance between a pair of molecules at the time of closest approach and b^* is the reduced impact parameter.

The reduced second virial coefficients, $B^*(T^*)$, used in equation 5A.5 can be related to [m,6,8] intermolecular potential function by:

$$B^*(T^*) = 3 \int_0^{\infty} [1 - \exp(-\phi^*(r^*)/T^*)] r^{*2} dr^* \dots 2.56$$

On partial integration, the above expression can be written as

$$B^*(T^*) = - \frac{1}{T^*} \int_0^{\infty} \frac{d\phi^*(r^*)}{dr^*} \exp(-\phi^*(r^*)/T^*) r^{*3} dr^* \dots 2.57$$

where all the symbols have their usual meanings.

The numerical values of the collision integrals and the reduced second virial coefficients for the [m,6,8] potential are tabulated elsewhere²⁶. These tables²⁶ present more accurate numerical values than the tables published by other workers^{27,31-34}.

REFERENCES

1. Chapman, S., and Cowling, T.G., *The Mathematical Theory of Non-uniform Gases*, 3rd edition, Cambridge University Press, New York (1970).
2. Hirschfelder, J.O., Curtiss, C.F. and Bird, R.B., *Molecular Theory of Gases and Liquids*, 4th printing, Wiley (1967).
3. Van Heijningen, R.J.J., Harpe, J.P. and Beenakker, J.J.M., *Physica* 38 (1968) 1.
4. Van Heijningen, R.J.J., Feberwee, A., Van Oosten, A., and Beenakker, J.J.M., *Physica* 32 (1966) 1649.
5. Kestin, J. and Yata, J., *J. Chem. Phys.* 49 (1968) 4780.
6. Yabsley, M.A., Carson, P.J. and Dunlop, P.J., *J. Phys. Chem.* 77 (1973) 703.
7. Munn, R.J., Smith, F.J., Mason, E.A. and Monchick, L., *J. Chem. Phys.* 42 (1965) 537.
8. Imam-Rahajoe, S., Curtiss, C.F. and Bernstein Jr., R.B., *J. Chem. Phys.* 42 (1965) 531.
9. Boltzmann, L., *Wein Sitz.* 66 (1872) 275.
10. Curtiss, C.F. and Hirschfelder, J.O., *J. Chem Phys.* 17 (1949) 550.

11. Kihara, T., *Revs. Modern Phys.* 25 (1953) 831.
12. Mason, E.A., *J. Chem. Phys.* 27 (1957) 75.
13. Mason, E.A., *J. Chem. Phys.* 27 (1957) 782.
14. Reed, T.M. and Gubbins, K.E., *Applied Statistical Mechanics*, McGraw-Hill (1973).
15. Tham, M.K. and Gubbins, K.E., *J. Chem. Phys.* 55 (1971) 268.
16. Guggenheim, E.A., *Thermodynamics* (North-Holland, Amsterdam) (1957) p.218.
17. Douglass, D.C. and Frisch, H.L., *J. Phys. Chem.* 73 (1969) 3039.
18. García-Colín, L.S., Barajas, L. and Piña, E., *Phys. Lett.* 37A (1971) 395.
19. Barajas, L., Garcia-Colin, L.S. and Piña, E., *J. Stat. Phys.* 7 (1973) 161.
20. Van Beijeren, H. and Ernst, M.H., *Physica* 68 (1973) 437.
21. Piña, E., *J. Stat. Phys.* 11 (1974) 433.
22. Van Beijeren, H. and Ernst, M.H., *Physica* 70 (1973) 225.
23. Mason, E.A., Malinauskas, A.P. and Evans, R.B., *J. Chem. Phys.* 46 (1967) 3199.

24. Zhadanov, V., Kagan, Yu. and Sazykin, A., *Soviet Phys. JETP* 15 (1962) 596. [*Zh. Eksperim. i Teor. Fiz.* 42 (1962) 857.]
25. Klein, M. and Hanley, H.J.M., *J. Chem. Phys.* 53 (1970) 4722.
26. Klein, M., Hanley, H.J.M., Smith, F.J. and Holland, P., *Tables of Collision Integrals and Second Virial Coefficients for the [m,6,8] Intermolecular Potential Function*, U.S. National Bureau of Standards Circular, NSRDS-NBS 47 (1974).
27. Hanley, H.J.M. and Klein, M., *J. Chem. Phys.* 50 (1969) 4765.
28. A three-parameter potential function is a model potential with a distance, an energy and, usually, a repulsive parameter (such as α for the exp-6 or m for the $m-6$ functions).
29. Klein, M. and Smith, F.J., *J. Res. Nat. Bur. Stand. (U.S.)* 72A (Phys. and Chem.), No. 4 (July-Aug. 1968) 359-423.
30. Kestin, J., Ro, S.T. and Wakeham, W.A., *Physica* 58 (1972) 165.
31. Monchick, L. and Mason, E.A., *J. Chem. Phys.* 35 (1961) 1676.
32. O'Connell, J.P. and Prausnitz, J.M., *Advances in Thermophysical Properties at Extreme Pressures*, pp. 19 - 31, ASME, New York (1965).

33. Lin, S.T. and Hsu, H.W., *J. Chem. Eng. Data* 14
(1969) 328.
34. Krieger, F.A., Report RM-646, The Rand Corporation,
Santa Monica, California.

CHAPTER 3

METHODS AND MATERIALS

3.1 *Introduction*

Three different cells have been described in this chapter. The first two, A_1 and A_2 , are of the two bulb apparatus type developed by Ney and Armistead¹ and the third one, A_3 , is a shearing cell of Loschmidt² design. The theory, construction and experimental procedures for these three cells have been compared and discussed here. Pressure measurement, temperature control and the determination of the diffusion coefficients are also described at the end of this chapter.

Cell A_1 was used to study the end correction equation given by Dunlop and Yabsley³. The cell A_2 was designed and calibrated against the Loschmidt cell, A_3 . Both the cells were used to study the concentration and temperature dependence of diffusion. Later, the shearing cell, A_3 , was modified to measure the effect of pressure on the diffusion coefficients.

3.2 *Theory of the Two Bulb Apparatus*

The following assumptions were made in the development of the theory:

- (i) The concentration gradient in the connecting tube is linear. Thus for a given point at time t ,

$$J = - D_{12} \frac{dC}{dx} = \text{Constant} \quad \dots \quad 3.1$$

- (ii) The volume of the connecting tube is negligible compared to the volume of the bulbs.
- (iii) The concentration gradient lies not only along the length of the tube but also a distance beyond each end. More precisely, the effective length of the tube is equal to its actual length plus an end correction factor analogous to that in the theory appertaining to sound⁴.
- (iv) The diffusion coefficient is independent of concentration. Isothermal diffusion is an irreversible process, which may be described by Fick's first law:

$$J = - D_{12} \frac{\partial C}{\partial x} \quad \dots \quad 3.2$$

where J is the flux,

D_{12} is the diffusion coefficient
and $\frac{\partial C}{\partial x}$ is the concentration gradient.

This is a first order partial differential equation and was solved by Barnes⁵, Gordon⁶ and Stokes⁷ for a diaphragm cell.

The two bulb apparatus is very similar to the diaphragm cell except that the diaphragm (a group of many fine capillaries held together) is replaced by a single tube. Mason *et al.*⁸ proved that both the diaphragm and the tube are functionally equivalent in their respective cells.

If V_l and V_u are the volumes of the lower and upper bulbs respectively, the change in concentration with time can be given by

$$\frac{dC_l}{dt} = - J(t) \frac{A}{V_l} , \quad \dots \quad 3.3$$

$$\frac{dC_u}{dt} = J(t) \frac{A}{V_u} , \quad \dots \quad 3.4$$

where C_l and C_u are the initial concentrations in lower and upper bulbs respectively, A is the effective cross section of the connecting tube, and $J(t)$ is the diffusional flow as a function of time. On subtracting 3.4 from 3.3:

$$\frac{d(\Delta C)}{dt} = - J(t) A \left(\frac{1}{V_l} + \frac{1}{V_u} \right) , \quad \dots \quad 3.5$$

where

$$\Delta C = C_l - C_u . \quad \dots \quad 3.6$$

The average value of the time dependent differential diffusion coefficient, D_{12} , over the concentration range C_l to C_u can be represented by the following equation:

$$D_{12}(t) \equiv \frac{1}{\Delta C} \int_{C_u}^{C_l} D \, dC , \quad \dots \quad 3.7$$

$$= - \frac{1}{\Delta C} \int_{x=0}^{L_{\text{eff}}} D \left(\frac{\partial C}{\partial x} \right) dx , \quad \dots \quad 3.8$$

$$= \frac{L_{\text{eff}} J(t)}{\Delta C} , \quad \dots \quad 3.9$$

where L_{eff} is the effective length of the connecting tube and x is the co-ordinate whose value is positive in the upward direction.

Combining equations 3.5 and 3.9

$$\frac{d \ln \Delta C}{dt} = \frac{D_{12} A}{L_{\text{eff}}} \left[\frac{1}{V_{\ell}} + \frac{1}{V_u} \right] \quad \dots \quad 3.10$$

On integrating

$$\Delta C(t) = \Delta C(t=0) \exp(t/\tau) \quad \dots \quad 3.11$$

Equation 3.11 can be rewritten as

$$C_{\ell}(t) - C_u(t) = (C_{\ell}^0 - C_u^0) \exp(t/\tau), \quad \dots \quad 3.12$$

where τ is the relaxation time and is given by

$$\tau = \left[\frac{D_{12} A}{L_{\text{eff}}} \left(\frac{1}{V_{\ell}} + \frac{1}{V_u} \right) \right]^{-1} \quad \dots \quad 3.13$$

This equation was derived by Ney and Armistead¹ assuming that quasi-stationary state exists in the connecting tube. However, in practise, a quasi-stationary state does not exist except when an extremely narrow tube joins two bulbs of infinite volumes.

Fick's second law is represented by the second order partial differential equation:

$$\frac{\partial C}{\partial t} = D_{12} \frac{\partial^2 C}{\partial x^2} \quad \dots \quad 3.14$$

On applying the initial condition

$$C_c(x, 0) = C_{\ell}(t=0); \quad 0 \leq x \leq L_{\text{eff}} \quad \dots \quad 3.15$$

and the boundary conditions

$$C_c(0, t) = C_{\ell}(t), \quad \dots \quad 3.16$$

$$C_c(L_{\text{eff}}, t) = C_u(t), \quad \dots \quad 3.17$$

$$\frac{\partial C_{\ell}}{\partial t} = - \frac{D_{12} A}{V_{\ell}} \left(\frac{\partial C_c}{\partial x} \right)_{x=L} \quad \dots \quad 3.18$$

and

$$\frac{\partial C_u}{\partial t} = \frac{D_{12} A}{V_u} \left(\frac{\partial C_c}{\partial x} \right)_{x=0} \quad \dots \quad 3.19$$

C_c is the concentration in the connecting tube.

If both the bulbs have the same volume (i.e. $V_\ell = V_u$) then the solution is given by:

$$C_\ell(t) - C_u(t) = [C_\ell(t=0) - C_u(t=0)] \exp(-t/\tau) \quad \dots \quad 3.20$$

$$\tau = \left[\left(1 - \frac{V_c}{6V_\ell} \right) \frac{D_{12} A}{L_{\text{eff}}} \left(\frac{1}{V_\ell} + \frac{1}{V_u} \right) \right]^{-1} \quad \dots \quad 3.21$$

where V_c is the volume of the connecting tube.

This equation differs from that of Ney and Armistead¹ by a factor of $\left(1 - \frac{V_c}{6V_\ell} \right)$ which, in fact, is the correction factor for non-attainment of the quasi-stationary state.

The difference arose because these authors ignored the volume of the connecting tube.

Paul⁹ derived an expression similar to equation 3.21, but with a factor of $\left(1 - \frac{V_c}{4V_\ell} \right)$ instead of $\left(1 - \frac{V_c}{6V_\ell} \right)$.

For a situation when the two bulbs have different volumes ($V_\ell \neq V_u$), Equation 3.21 can be written by replacing V_c/V_ℓ by $2V_c/(V_\ell + V_u)$. Thus

$$\tau = \left[\left(1 - \frac{V_c}{3(V_\ell + V_u)} \right) \frac{A D_{12}}{L_{\text{eff}}} \left(\frac{1}{V_\ell} + \frac{1}{V_u} \right) \right]^{-1} \quad \dots \quad 3.22$$

Annis *et al.*¹⁰ found the solution of Fick's second law independently and gave the following expression for the quasi-stationary state correction factor:

$$K = 1 + \frac{1}{3} \frac{V_c}{V_u} \left(\frac{1-\beta-\beta^2}{1+\beta} \right) \quad \dots \quad 3.23$$

where β is the ratio of the bulb volume

$$\beta = \frac{V_u}{V_l} \quad \dots \quad 3.24$$

If $V_u = V_l$ and on putting the value of β in Equation (3.23)

$$K = \left(1 + \frac{V_c}{6V_u}\right) \quad \dots \quad 3.25$$

This expression is identical to the one derived by Barnes⁵.

3.3 Construction of Two Bulb Cells

Two cells of this kind have been explained below.

a. Cell A₁.

Exact details of this cell together with a diagram have been described elsewhere³.

The cell consisted of two stainless steel (type 316) bulbs which were linked together with an interchangeable, precision bore, brass connecting tube using swagelok fittings.

The cell and tube dimensions, together with their percentage errors, are listed in Table 3.1.

Table 3.1

Cell and Tube Dimensions

Volume of the upper bulb : 5879.4 cm³ ± 0.03%

Volume of the lower bulb : 5824.2 cm³ ± 0.03%

Tube No.	L(cm)	radius (cm)
1	18.052±0.01%	0.2763±0.05%
2	68.186±0.003%	0.5353±0.03%
3	35.603±0.01%	0.3842±0.07%
4	17.971±0.01%	0.9208±0.03%

The results from Tubes 1 and 2 were discussed by Yabsley *et al.*³.

Some portion of the connecting tube was generally protruded into the bulbs, thus decreasing their volumes. The effective volumes of the two bulbs were calculated, for accurate measurement of D_{12} , and are listed below.

Length of the tube protruded into each bulb:	5.40 cm
Outer diameter of the tube	: 2.22 cm
Effective volume of the upper bulb	: 5858.6 cm ³
Effective volume of the lower bulb	: 5803.4 cm ³ .

A silicone oil manometer, which is discussed later in this chapter, was connected to one side of the upper bulb to measure the pressure inside the cell. This manometer was used to measure the pressures for all the experiments performed with tubes 1, 2, 3 whereas a Bourdon Gauge was employed for tube 4.

3.4 *Calculations for the End Correction*

As stated previously, the concentration gradient in the tube in reality does not actually terminate at the ends of the tube but continues a little further, so a proper correction should be made to the length of the tube. As mentioned earlier¹¹ the ends of the tube were advanced into each bulb to maintain its outer diameter. Rayleigh⁴ considered two extremes of the annulus flange and showed that for an infinitely thick annulus flange⁴, this correction is $0.82r$, whereas for an infinitely thin annulus flange^{4,12} (no flange) it is $0.58r$, where r is the radius of the connecting tube. Therefore, the end correction should lie between these limits.

Wirz¹³, while measuring the velocity of sound, studied the variation of the end correction using pipes of different dimensions and concluded that

$$\alpha = 0.60 + 0.22 \exp(-kr/\omega) \quad \dots \quad 3.26$$

where α is the end correction for a pipe;

k is the dimensionless constant whose value

is given by $0.129 < k < 0.136$;

and ω is the flange width of the pipe.

Yabsley *et al.*³ supported the Wirz relationship by obtaining similar parameters after least squares analysis of their data. The following equation was given by them.

$$\alpha = 0.596 + 0.219 \exp(-0.125r/\omega) \quad \dots \quad 3.27$$

The agreement between equations 3.26 and 3.27 is excellent. The effective length of the connecting tube can thus be calculated from the following relation,

$$L_{\text{eff}} = L + 2\alpha r \quad \dots \quad 3.28$$

The effective lengths and the end corrections calculated for various tubes are given in Table 3.2.

The results obtained from Tubes 1 and 2 were discussed earlier by Yabsley *et al.*³, whereas the results obtained from Tubes 3 and 4 were used for further investigation of Wirz's relation. From these results it was concluded that his relation might be valid in form but is not good enough for the present purpose, which requires an accuracy of 0.1% (see section 4.2).

Table 3.2

Effective Lengths and End Corrections for Various Tubes

Tube No.	External Diameter (cm)	ω (cm)	End Correction	L_{eff}
1	2.22	0.5692	0.81	18.500
2	2.22	0.8282	0.79	69.032
3	2.22	0.7258	0.80	36.217
4	2.22	0.1892	0.71	19.285

b. Cell A₂.

A schematic diagram of the diffusion cell is shown in Figure 3.1. This cell was similar to A₁ but machined from a stainless steel cylindrical block (1) and was designed so that precision bore (9) brass connecting tubes (5) of different dimensions could be inserted.

The ends of the cell (1) were covered with stainless plates (2), screwed into a flange (3) thus leaving the upper and the lower compartments (bulbs). To make the cell vacuum tight, viton O-rings (4) were placed in the annular grooves (8) cut into each end plate (2). A similar technique was used to seal the other metal-metal interfaces.

The dimensions of the cell are given below:

Length of the cell	:	10.65 cm
Outer diameter of the cell	:	7.60 cm
Inner diameter of the cell at the ends	:	3.50 cm
Length of the connecting tube	:	4.25 cm

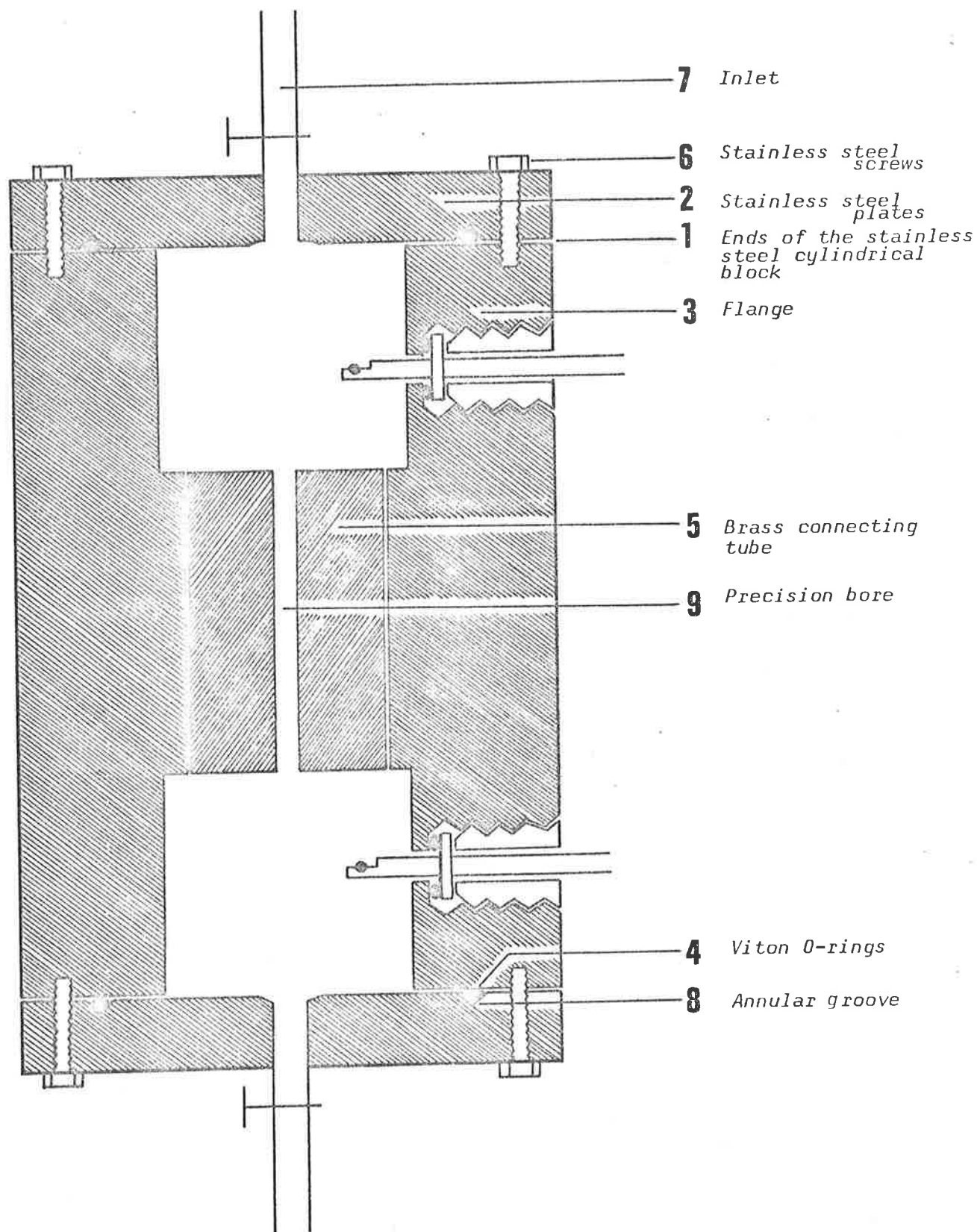


Figure 3.1: A Schematic Diagram of the Small Two Bulb Cell (A₂).

Outer diameter of the connecting tube : 2.55 cm
 Inner diameter of the connecting tube : 0.40 cm
 Depth of the bulbs : 3.20 cm

A correction was applied to the bulb volumes due to the space lying within the gas inlets and the end plates. The value of this correction factor was calculated to be + 0.6 cm³.

Pressure measurements were made by the Bourdon Gauge described later in this chapter.

3.5 Calculations for the Cell Constant

The cell constant was calculated by calibrating this cell against the Loschmidt cell.

The relaxation time for the two bulb apparatus was given by equation 3.21 as

$$\tau = \left[\left(1 - \frac{V_c}{6V_\ell} \right) \frac{D_{12} A}{L_{\text{eff}}} \left(\frac{1}{V_\ell} + \frac{1}{V_u} \right) \right]^{-1}$$

and that of the Loschmidt cell is given by

$$\tau = L^2 / \pi^2 D_{12} \quad \dots \quad 3.29$$

where L is a cell constant which can also be written in the form of

$$L = \pi \sqrt{\tau D_{12}} \quad \dots \quad 3.30$$

On rearranging equation 3.21 and multiplying both sides by π^2 , it becomes

$$\pi^2 \tau D_{12} = \frac{L_{\text{eff}}}{A} \left[\left(1 - \frac{V_c}{6V_\ell} \right) \left(\frac{1}{V_\ell} + \frac{1}{V_u} \right) \right]^{-1} \pi^2 \quad \dots \quad 3.31$$

$$\text{or} \quad \pi \sqrt{\tau D_{12}} = \pi \left[\frac{L_{\text{eff}}}{A} \left(\left(1 - \frac{V_c}{6V_\ell} \right) \left(\frac{1}{V_\ell} + \frac{1}{V_u} \right) \right)^{-1} \right]^{1/2} \quad \dots \quad 3.32$$

From equations 3.30 and 3.32

$$L = \pi \left[\frac{L_{\text{eff}}}{A} \left(\left(1 - \frac{V_c}{6V_\ell} \right) \left(\frac{1}{V_\ell} + \frac{1}{V_u} \right) \right)^{-1} \right]^{1/2} \quad \dots \quad 3.33$$

For present computation purposes, the value of the cell constant was calculated to be 70.48 cm(Atm*)^{1/2}.

3.6 Advantages of the Cell A₂

- (i) There is no need for the accurate measurement of the cell dimensions as the cell was calibrated against a shearing cell.
- (ii) Due to its small size, expensive gas mixtures can be studied.
- (iii) The diffusion coefficients of all types of binary gas pairs (heavy or light) can be measured by selecting their respective pressures and the radius of the connecting tube.

3.7 Common Features of Cells A₁ and A₂

In both the cells, a similar pair of matched thermistors (one in each bulb) were mounted to monitor the concentration changes with time. These thermistors were connected to a Wheatstone bridge by two-core shielded cables. Full details of the thermistors and of the bridge circuit will be given at the end of this chapter.

* 1 Atm. = 101.325 K Pascals.

3.8 *Experimental Procedure for Two Bulb Cells*

After complete evacuation, one of the two gases of the system under study was admitted into the entire diffusion cell. This cell was then sealed and left for few minutes to achieve thermal equilibrium. The pressure inside the cell was recorded. The manifold was evacuated to a sufficient low pressure ($\approx 10^{-5}$ mm Hg) and then filled with the second gas to a pressure greater than that within the cell. The gas was allowed to establish temperature equilibrium and then let into the cell slowly through either the top or bottom valve, depending upon the density of the gas. The final pressure in the cell was recorded. Molefractions of the gas components were calculated from their partial pressures.

3.9 *Theory of the Loschmidt Cell*

The following assumptions were made by Loschmidt:

- (i) There should be uniform cross-sectional area over the entire length of the cell.
- (ii) The diffusion coefficient should be independent of concentration.
- (iii) The two halves of the cell are symmetrical about the central plates.

Relaxation time, τ , for the shearing cell may be obtained by solving the diffusional flow equation under the experimental conditions. The binary diffusion process is governed by Fick's second law, which for the one-dimensional case is given by

$$\frac{\partial C_i}{\partial t} = D_{12} \frac{\partial^2 C_i}{\partial x^2} \quad \dots \quad 3.34$$

where $i = 1, 2$.

$C_i(x, t)$ is the concentration of the i th component of the mixture at position x along the axis of diffusion, at time t , at constant pressure and temperature in the cell.

The restricted diffusion occurs inside this cell for which the boundary conditions are given below

$$\left. \frac{\partial C_i}{\partial x} \right|_{x=0} = 0 \quad \text{for all } t, \quad \dots \quad 3.35(a)$$

$$\left. \frac{\partial C_i}{\partial x} \right|_{x=L} = 0 \quad \text{for all } t, \quad \dots \quad 3.35(b)$$

where $x = 0$ is the lower end of the cell and $x = L$ is the upper end of the cell.

Under these conditions, the solution¹⁸ of equation 3.34 for a binary system is:

$$C_i(x, t) = A_0 + \sum_{j=1}^{\infty} A_j \exp\left(-\frac{j^2 \pi^2 D_{12} t}{L^2}\right) \cdot \cos\left(\frac{\pi j x}{L}\right) \dots \quad 3.36$$

where A_0 and A_j are the Fourier coefficients and can be obtained from predetermined initial conditions (i.e. at $t = 0$) of the experiment. The initial concentration of the i th component may be approximated by a step function. Hence

$$C_i(0, 0) \mu_{-1}(x) + [C_i(L, 0) - C_i(0, 0)] \mu_{-1}(x-a), \quad \dots \quad 3.37(a)$$

where

$$\mu_{-1}(z) = \begin{cases} 0 & z \leq 0 \\ 1 & z > 0. \end{cases} \quad \dots \quad 3.37(b)$$

From equation 3.36 the concentration of the i th component may be written (at $t = 0$) as

$$C_i(x, 0) = A_0 + \sum_{J=1}^{\infty} A_J \cos\left(\frac{\pi x J}{L}\right) . \quad \dots \quad 3.38$$

The Fourier coefficients may be written as

$$A_0 = \frac{1}{L} \int_0^L C_i(x, 0) dx \quad , \quad \dots \quad 3.39(a)$$

$$A_J = \frac{2}{L} \int_0^L C_i(x, 0) \cos\left(\frac{\pi x J}{L}\right) dx \quad , \quad \dots \quad 3.39(b)$$

substituting the value of $C(x, 0)$ from equation 3.37

$$A_0 = \frac{1}{L} \int_0^a C_i(0, 0) dx + \frac{1}{L} \int_a^L C_i(L, 0) dx \quad \dots \quad 3.40(a)$$

$$A_J = \frac{2}{L} \int_0^a C_i(0, 0) \cos\left(\frac{\pi x J}{L}\right) dx + \frac{2}{L} \int_a^L C_i(L, 0) \cos\left(\frac{\pi x J}{L}\right) dx \quad \dots \quad 3.40(b)$$

$$A_0 = \frac{a}{L} C_i(0, 0) + \left(\frac{L-a}{L}\right) C_i(L, 0) \quad \dots \quad 3.41(a)$$

$$= \bar{C}_i(0) .$$

$$\text{and } A_J = -\frac{2}{J\pi} \sin\left(\frac{\pi J a}{L}\right) [C_i(0, 0) - C_i(L, 0)] \quad \dots \quad 3.41(b)$$

$$= -\frac{2}{J\pi} \sin\left(\frac{\pi J a}{L}\right) \Delta C_i(0) ,$$

where $\bar{C}_i(0)$ is the mean concentration of the i th component at the beginning and $\Delta C_i(t)$ is the difference in concentration of the upper and lower halves of the cell at the beginning of the experiment.

The symmetry properties of the Fourier series in equation 3.36 may be utilized as first suggested by Onsager¹⁴ if the cell is designed so that *differences* in concentration are measured at two planes at right angles to the direction of

diffusion and at a distance of $(L/2 - x)$ from the cell centre, for then all the even terms vanish to give

$$\begin{aligned} \Delta C_i(t) = & 2A_1 \exp\left(-\frac{\pi^2 D_{12} t}{L^2}\right) \cos\left(\frac{\pi x_1}{L}\right) \\ & + 2A_3 \exp\left(-\frac{9\pi^2 D_{12} t}{L^2}\right) \cos\left(\frac{3\pi x_1}{L}\right) \\ & + 2A_5 \exp\left(-\frac{25\pi^2 D_{12} t}{L^2}\right) \cos\left(\frac{5\pi x_1}{L}\right) + \dots \\ & \dots \quad 3.42 \end{aligned}$$

Onsager further indicated that if x_1 was chosen to be $L/6$, then the second term in equation 3.42 vanished to give

$$\begin{aligned} \left[C_i\left(\frac{5L}{6}\right) - C_i\left(\frac{L}{6}\right) \right]_t = & A'_1 \exp\left(-\frac{\pi^2 D_{12} t}{L^2}\right) + A'_5 \exp\left(-\frac{25\pi^2 D_{12} t}{L^2}\right) + \dots \\ & \text{higher order terms} \\ & \dots \quad 3.43 \end{aligned}$$

For large values of t , the higher order terms may be neglected and D_{12} can be obtained from the following relation by determining the variation with time of the difference function $F(C_i)$ (i.e. concentration of i th component).

$$F(C_i) \equiv \ln\left[C_i\left(\frac{5L}{6}\right) - C_i\left(\frac{L}{6}\right) \right]_t = A \exp(-t/\tau) \quad \dots \quad 3.44$$

where τ is the relaxation time and is equal to

$$\tau = L^2 / D_{12} \pi^2 \quad \dots \quad 3.45$$

3.10 Construction of the Loschmidt Cell

The basic Loschmidt cell consisted of a vertical tube of uniform cross section, separated into two equal parts by a stopcock with a bore equal to the diameter of the tube. In more recent designs of the apparatus, the stopcock is not used. Instead a shear technique is employed in which the cell is closed by sliding one half of the cell over the other.

Cell A₃

Details of this cell, together with a figure, have been described elsewhere¹⁵. In short, the cell was constructed by machining two identical brass blocks (diameter 18.5 cm). Two diffusional channels in each block were honed out, parallel to the axis of the block which was lying 180° apart. The mating surfaces of the adjacent halves were made optically flat by grinding against each other. Thus there were four separate compartments in this cell which, when lined up, formed two independent diffusion columns. The lengths and the internal diameters of these columns are given in Table 3.3.

Table 3.3

Measurements of the Columns

	Diffusional Columns	
	1	2
Length (cm)	40.049	40.049
Int. diam. (cm)	3.81	2.54

The two halves of the cell were held together with a stainless steel rod, 1.9 cm in diameter and six pairs of cupped washers which, when compressed with stainless steel nuts, were capable of generating a maximum force of 200kN.

Apiezon T-grease was used as a lubricant for the sliding surfaces of the cell at high temperatures (25 - 52°C), however, because of its stiffness, it was replaced with Apiezon H-grease at low temperatures (2 - 25°C).

The lower half of the cell was fixed while the top half was free to rotate, for aligning purposes, through a restricted arc with a differential spur gear and pinion.

Viton O-rings were inserted between the mating surfaces and the surfaces concentric with the cell axis, to work at high pressures up to approximately 30 atmospheres. All other non-moving metal-metal surface contacts were sealed by lead O-rings, prepared *in situ* by moulding lead wire into circular V-shaped grooves.

Two matched thermistors were placed to monitor the difference in concentration changes with time, at a distance of $L/6$ and $5L/6$ from one end, where L is the length of the cell.

Gas pressures were measured with a Bourdon Gauge which was calibrated against a dead weight tester.²²

3.11 Common features of Cells A_1 , A_2 and A_3

- (i) Flexible stainless steel tubing was used to connect the cells with the other parts of the apparatus.
- (ii) An Edwards diffusion pump, incorporated with an oil rotary pump, was used to evacuate the desired cell.

At low pressures (less than one atmosphere) the leak rate was better than 2×10^{-6} torr min⁻¹, while at high pressures (more than one atmosphere) the leak rate was less than 1×10^{-4} torr min⁻¹.

- (iii) Each cell was suspended, on an adjustable three point suspension, into a water bath containing approximately 500 litres of deionised water which was stirred vigorously (with a $\frac{1}{3}$ H.P. motor) to reduce thermal gradients inside the bath.
- (iv) The cell was aligned vertically with the help of a spirit level.
- (v) The temperature of the bath was controlled to within $\pm 0.0015^\circ\text{C}$ at low temperatures (2 - 20°C) and to within $\pm 0.001^\circ\text{C}$ at high temperatures (20 - 52°C).
- (vi) The flow of the gases into the system at various points, as required, was controlled by Nupro bellow valves (Crawford Fitting Co., Cleveland, Ohio).

The disadvantages of the shearing cell are:

- (1) Dufour effect.
- (2) Heat of mixing.

These effects occurred because of the non-ideality of the gases and have been explained before by various authors¹⁸⁻²¹.

3.12 *Experimental Procedure for the Loschmidt Cell*

Usually mixtures were prepared only in one half of the cell while the other half was filled with a pure gas, but if needed, the mixtures can be prepared in all four compartments.

The first gas was introduced into all the diffusion channels up to a certain desired pressure and then one half of the cell was closed, depending upon the density of the gas. The same gas continued to fill the other half of the cell up to the final pressure. The manifold was evacuated immediately after isolating the cell from it and refilled with the second gas at a pressure greater than that inside the cell. This gas was allowed to enter into the first half by opening proper valves and, with the aid of a successive dilution technique, the pressures in both halves were made equal.

Molefractions of the gases were calculated from their partial pressures, measured with a Bourdon Gauge.

After complete mixing of these gases the experiment was started by aligning the respective upper and lower compartments.

The variation in the difference of resistance between the thermistors with time was recorded and computed to calculate the diffusion coefficients.

3.13 Pressure Measurements

The pressure inside the cell was measured by the following two techniques:

1. *Silicone oil manometer:*

Low pressures (less than 25 Torr) were measured by a simple silicone oil manometer (Dow Corning 704). It was simply a U-shaped glass tube hooked to the upper bulb of the cell with swagelok fittings. The tube was partially filled

with a silicone oil, which was carefully 'degassed' with the aid of a small magnetically operated stirring device. The density of the degassed oil was determined with the help of a pycnometer¹¹.

An assembly of a movable telescope clamped on a cathetometer, which was placed vertically at all times, with the help of a spirit level in two perpendicular planes, was used to measure the meniscus of the oil. The telescope was aligned to give the same reading in each arm of the manometer when both sides were equally evacuated. The sharpness of the meniscus was confirmed by positioning a globe behind it.

The reproducibility of the cathetometer readings of the meniscus were ± 0.002 cm, thus giving a maximum error in the pressure measurements of 0.1%.

2. *Bourdon Gauge:*

The pressures of more than 25 Torr were measured by a Bourdon Gauge (Texas Instruments, Houston).

Inside this gauge there was a pressure transducer which consisted of a hollow quartz spiral, with a small mirror at the end, housed in a capsule with two outlets. One outlet connected the spiral to the cell and the other connected the rest of the capsule to the vacuum system. The pressure in the cell relative to vacuum could be determined by knowing the extent of unwinding of the spiral due to pressure difference across the walls. This degree of unwinding of the spiral was detected by a photocell placed inside the Texas Instrument and was registered on a decade counter with the help of a servo motor linked to it.

All capsules were calibrated using a dead weight tester to an accuracy of better than 0.1%; the reading on the decade counter could be converted into its pressure units by the use of these calibration curves.

The least-squares constants for the curves of different capsules used in this study are given in Table 3.4.

Table 3.4

Least-squares Constants for Bourdon Capsules

Tube No.	Calibrated Range	a_0	a_1	a_2	Av. dev. %
4176*	34 atm.	3.33740	3.7788×10^{-5}	0.0	± 0.02
4107	13 atm.	0.65567	3.2730×10^{-5}	-1.7449×10^{-8}	± 0.02
5588	10 atm.	0.64962	3.2955×10^{-5}	-2.7263×10^{-8}	± 0.01
2421	1 atm.	2.71176	-8.5315×10^{-5}	0.0	$\pm 0.02_s$

* In this case the Bourdon-tube consisted of an aluminium spiral.

3.14 Temperature Control

Each cell was completely immersed in a vigorously stirred bath of deionised water whose temperature was kept constant by following two techniques.

i. Temperatures higher than ambient were maintained with a mercury toluene thermoregulator which activated a thyatron circuit so switching the "on-off" current from the regulator to a 12 ohm stainless steel "pyrotenax" element mounted along the inner sides of the bath.

The major heat losses were overcome by the use of base heaters (35 ohm pyrotenax heating coil and hecla type normal

water heaters). They were attached to the A.C. voltage variator and the amount of current passed through them depends upon the temperature to be maintained.

ii. A similar method was employed to control the temperature below the ambient, except the cold water was circulated through the experimental bath instead of using the base heaters. The water was cooled in a separate bath (B1) using a refrigeration unit before circulating it through an experimental bath (B2) in which the cell was immersed. The extent of cooling the bath, B1, was controlled by adjusting the flow rate of refrigerant from the compressor with a bypass mechanism. The temperature of this bath was kept at 4 - 5°C below the temperature of bath B2. This was maintained by a temperature sensitive thermistor bridge which activated an "on-off" switch attached to the refrigerator, thus stopping or initiating the flow of refrigerant.

The water was constantly stirred and pumped by a water pump through a framework of copper coils placed inside bath B2. The temperature of the latter bath was controlled with a mercury toluene regulator as described above.

With this type of arrangement, the temperature of the bath was controlled to within $\pm 0.001^\circ$ over a range of 10 - 52°C. However, slightly higher fluctuations of the order of ± 0.0015 were observed below 10°C. These temperatures were measured with a mercury in glass thermometer which had been calibrated against a platinum resistance thermometer.

The front glass window was always covered with a polystyrene foam board to minimise the thermal fluctuations of the bath from its environments.

3.15 Determination of Diffusion Coefficients

In this section, a common method applicable to all the cells used for accurate determination of diffusion coefficients in binary gas mixtures will be described. It consists of a Wheatstone bridge in which two arms of the network are a pair of matched thermistors to monitor the composition of diffusing gases as a function of time.

Thermistors are usually composed of oxide semiconductor materials. Their resistance decreases exponentially with temperature, thus giving large and negative temperature coefficients of resistance (α). This is in contrast to most metals which have small and positive values for α . The temperature dependence of the thermistor material is given by

$$R_T = R_{T_w} \left[\exp \beta \left(\frac{1}{T} - \frac{1}{T_w} \right) \right] \quad \dots \quad 3.46$$

where T : temperature of the thermistor;
 R_{T_w} : the resistance of the thermistor at temperature T_w of the water bath; and
 β : is a constant related to the material of the thermistor.

The equilibrium resistance of the thermistor depends upon the rate at which the heat generated in it by passage of electric current is dissipated. This is largely controlled by the thermal conductivities of the surrounding gases and the temperature gradient operating, *in situ*, assuming negligible convection effects. Normally ambient temperature is held constant.

Thermal conductivities of various gases are different and any change in the composition of a gas around the thermistor will change its resistance. This difference in resistance of the two thermistors is proportional to the composition of the gases at the monitoring positions¹⁶. The method is more sensitive when thermal conductivities of two gases are considerably different, e.g. the thermal conductivity of helium is nearly ten times higher than that of argon.

In the actual circuit (Fig. 3.2) R_1 and R_2 are two thermistors* and R_3 and R_4 are matched $5k\Omega$ micacard resistors. A constant voltage V is applied across the circuit. This, however, can be changed in order to achieve the desired imbalance in the bridge. The difference in resistance $\Delta R(t)$ at a given time t between the two thermistors produces a potential drop V_{24} between the two arms of the bridge. The relation to calculate $\Delta R(t)$ is given by¹⁷

$$\Delta R(t) = \frac{R_3 V V_{24}}{V_{14} (V_{14} - V_{24})} \quad \dots \quad 3.47$$

A digital voltmeter measured both voltages V_{14} and V_{24} simultaneously when the bridge operated in an 'Out of balance', through an analogue scanner.

The data was recorded after the difference in resistance between the two thermistors was directly proportional to the difference in composition at two monitoring positions. Thus, in general, at the start of the diffusion experiment, recording of the data was withheld until V_{24} had fallen approximately to 25 mV. This corresponds to the $\Delta R(t)$ value close to 100Ω . From this point onwards 100 - 150 readings were taken at regular

* Type G112P thermistors used in this work were supplied by Fenwal Electronics, Inc. (Framingham, Massachusetts). The β value for the thermistors was 3500K. These had resistance of 8000Ω at 25°C and were matched to within 0.7% of the nominal value in helium.

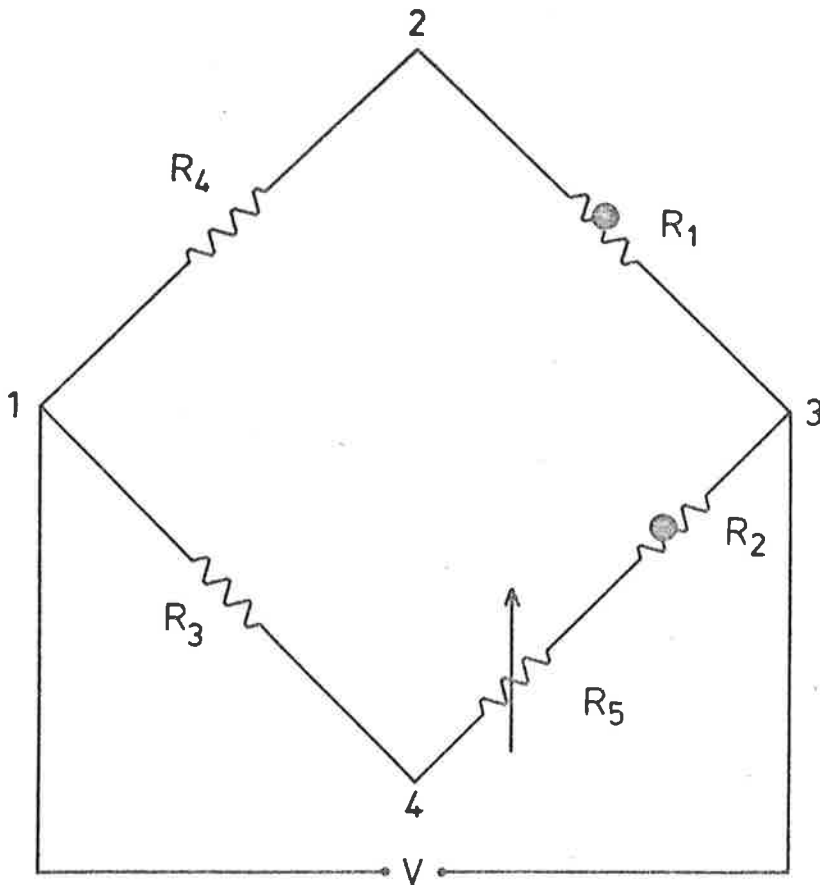


Figure 3.2: The Wheatstone Bridge Circuit.

time intervals to record the significant part of the resistance versus time curve. These time intervals were achieved with a crystal timer which produced pulses at preset time intervals, thus initiating a scan to record both V_{14} and V_{24} either on paper tape or a printer.

Diffusion coefficients were calculated by least-squares analysis of the data obtained, by using the following equation

$$\Delta R(t) - \Delta R(\infty) = A' \exp(-\pi^2 \mathcal{D}_{12} t/L^2) \quad \dots \quad 3.48$$

where A : is a constant;

L : length of the cell for the Loschmidt Cell and cell constant for a calibrated two bulb cell;

$\Delta R(t)$: the difference in resistance between two thermistors at certain time t ;

and $\Delta R(\infty)$: the difference in resistance between two thermistors after equilibrium.

The quantity $\Delta R(\infty)$ is a residual resistance between two thermistors and its value should be zero for a perfectly matched pair of thermistors. This value, however, was not zero and should be known accurately to calculate \mathcal{D}_{12} . In order to determine $\Delta R(\infty)$ a further twenty readings were taken near the end of the experiment after the system had reached equilibrium.

With the use of the above experimental procedures the reproducibility of the diffusion coefficients for all the cells was found to be better than $\pm 0.1\%$. The purity of each gas was greater than 99.9%.

REFERENCES

1. Ney, E.P. and Armistead, F.C., *Phys. Rev.* 71
(1947) 14.
2. Loschmidt, J., *Akad. Wiss. Wien* 61 (1870) 367.
3. Yabsley, M.A. and Dunlop, P.J., *Physica* 85A
(1976) 160.
4. Rayleigh, J.W.S., *The Theory of Sound II*, Dover
Publications, New York (1945) p.203 and p.491.
5. Barnes, C., *J. Appl. Phys.* 5 (1934) 4.
6. Gordon, A.R., *Ann. N.Y. Acad. Sci.* 46 (1945) 285.
7. Stokes, R.H., *J. Amer. Chem. Soc.* 72 (1950) 763.
8. Mason, E.A., Malinauskas, A.P. and Evans, R.B.,
J. Chem. Phys. 46 (1967) 3199.
9. Paul, R., *Phys. Fluids* 3 (1960) 905.
10. Annis, B.K., Humphreys, A.E. and Mason, E.A.,
Phys. Fluids 12 (1969) 78.
11. Yabsley, M.A., Ph.D. Thesis, University of Adelaide,
Australia (1975).
12. King, L.V., *Phil. Mag.* 21 (1947) 3.
13. Wirz, P., *Helv. Phys. Acta.* 20 (1947) 3.
14. Harned, H.S. and French, D.M., *Ann. N.Y. Acad. Sci.* 46
(1945) 267.

15. Staker, G.R. and Dunlop, P.J., *Chem. Phys. Letters* 42 (1976) 419.
16. Staker, G.R., Ph. D. Thesis, University of Adelaide, Australia (1976).
17. Yabsley, M.A. and Dunlop, P.J., *J. Phys.* E8 (1975) 834.
18. Ljunggren, S., *Arkiv Kemi* 24 (1965) 1.
19. Waldmann, L., *Z. Physik* 124 (1944) 175.
20. Waldmann, L., *Z. Physik* 124 (1944) 2.
21. Waldmann, L., *Z. Physik* 124 (1944) 30.
22. Bell and Howell, Type 6-201-0001 primary pressure standard.

CHAPTER 4

THE CONCENTRATION DEPENDENCE OF DIFFUSION

4.1 *Introduction*

In the past few years, Dunlop *et al.*¹⁻⁹ have reported the diffusion coefficients at 300K and near one atmosphere pressure for many binary systems containing helium which were precise enough but not accurate because of the incorrect use of thermistor bridge as indicated in 1975 by Yabsley and Dunlop¹⁰. In the present study, precise and accurate diffusion coefficients for the concentration dependence of several binary mixtures were measured in two bulb¹¹ and Loschmidt¹² cells with the help of the improved thermistor bridge described earlier¹⁰. By comparing the results obtained from these cells, it appeared that the end correction¹³⁻¹⁵, which is usually applied to the connecting tube, was not sufficiently accurate for precise work. The results for one of the systems (Ar - N₂) have been partially duplicated by using a Loschmidt cell and mass spectrometer¹⁶ to analyse the gas mixtures and are in excellent agreement with the thermistor bridge results.

4.2 *Results and Discussion of the Cells A₁ and A₃*

Yabsley *et al.*¹⁷ measured the diffusion coefficients for the systems He - Ar and He - O₂ at low pressures

($\approx 2 - 10$ Torr) and at 300K using tubes* 1 and 2 where Knudsen effects¹⁷ were important and, in support of Wirz¹⁸, gave a relation to calculate the end correction.

To continue this study, tube* 3 was used to perform similar experiments for the systems He - O₂, He - Ar and He - N₂. The results thus obtained using this tube are in good agreement with those of Yabsley and Dunlop¹⁷ and are plotted in Figures 4.1 - 4.3.

Because of the importance of Knudsen effects at low pressures, the extrapolation of the graph PD_{12} versus $(Pr)^{-1}$ was necessary to obtain $P\mathcal{D}_{12}$, where PD_{12} is the experimental diffusion coefficient at one atmospheric pressure, r is the radius of the tube and $P\mathcal{D}_{12}$ is the corrected value of diffusion coefficient at one atmosphere when $(Pr)^{-1} = 0$. To minimise the errors introduced by this extrapolation, tube* 4 was constructed so that;

- (a) convenient relaxation times could be obtained for the systems studied using pressures between 40 - 90 torr in the present cell; and
- (b) Knudsen effects could be neglected. These effects are less than 0.1%¹⁷ provided the value of $(Pr)^{-1}$ is less than $50 \text{ atm}^{-1} \text{ cm}^{-1}$.

The concentration dependence of the binary diffusion coefficients, \mathcal{D}_{12} , for the systems He - Ar, He - N₂, He - O₂, He - CO₂ and N₂ - Ar were measured at 300K in the present two bulb cell (A₁) using tube 4 and Loschmidt cell (A₃) which have been described earlier in Chapter 3. The $(Pr)^{-1}$ value for all the experiments performed in the two bulb cell (A₁) was between

* Tubes 1, 2, 3 and 4 are described in Chapter 3.

10 - 20 atm⁻¹ cm⁻¹ . The experimental values obtained with this cell for the above systems and the system He - Ne are listed in Tables 4.1 - 4.6.

It was not possible to measure the diffusion coefficients successfully for He - Ne system over the entire concentration range with the Loschmidt cell (A₃). The exact reasons for this failure are not known at this stage and more work needs to be carried out to establish this fact. All the experiments for the other five systems were performed at one atmosphere in this cell.

The experimental data for each system obtained from both the cells (two bulb (A₁) and Loschmidt (A₃)) were fitted to the empirical relation^{15,19}

$$D_{12} = D_{12}^0 \left[1 + \frac{a_1 x_2}{1 + a_2 x_2} \right] \quad \dots \quad 4.1$$

where D_{12}^0 is the limiting experimental diffusion coefficient, a_1 and a_2 are constants and x_2 is the molefraction of the heavy component.

The above equation 4.1 accurately reproduces the form of the concentration dependence of D_{12} predicted by the Chapman-Enskog theory. The parameters obtained from a "least-squares" analysis, together with the percentage average deviations (Av. dev. %) of the experimental points from the smooth curves are given in Table 4.7.

Graphical representation of the data from both the cells is presented in Figures 4.1 - 4.6.

Using the Wirz¹⁸ relation, it was difficult to correlate the data obtained from tubes 1 and 2 of Ref. [17]

Table 4.1^{a, b}

Concentration Dependence of the Diffusion
Coefficient for He/O₂ at 300K

(Two Bulb Apparatus Results)

x_2 (heavy)	P (atm)	$P\mathcal{D}_{12}$ (atm.cm ² .s ⁻¹)
0.1003	0.0594	0.7551
0.2498	0.0712	0.7603
0.3997	0.0890	0.7638
0.5010	0.1063	0.7647
0.7514	0.0709	0.7696
0.9003	0.0591	0.7712

^a x_2 is the molefraction of the heavy component,
P is the pressure in atmosphere at which the
experiments were performed and $P\mathcal{D}_{12}$ is the
numerical value of the diffusion coefficient
at one atmosphere when $(Pr)^{-1} = 0$.

^b These results are obtained with the cell (A₁)
using Tube 4.

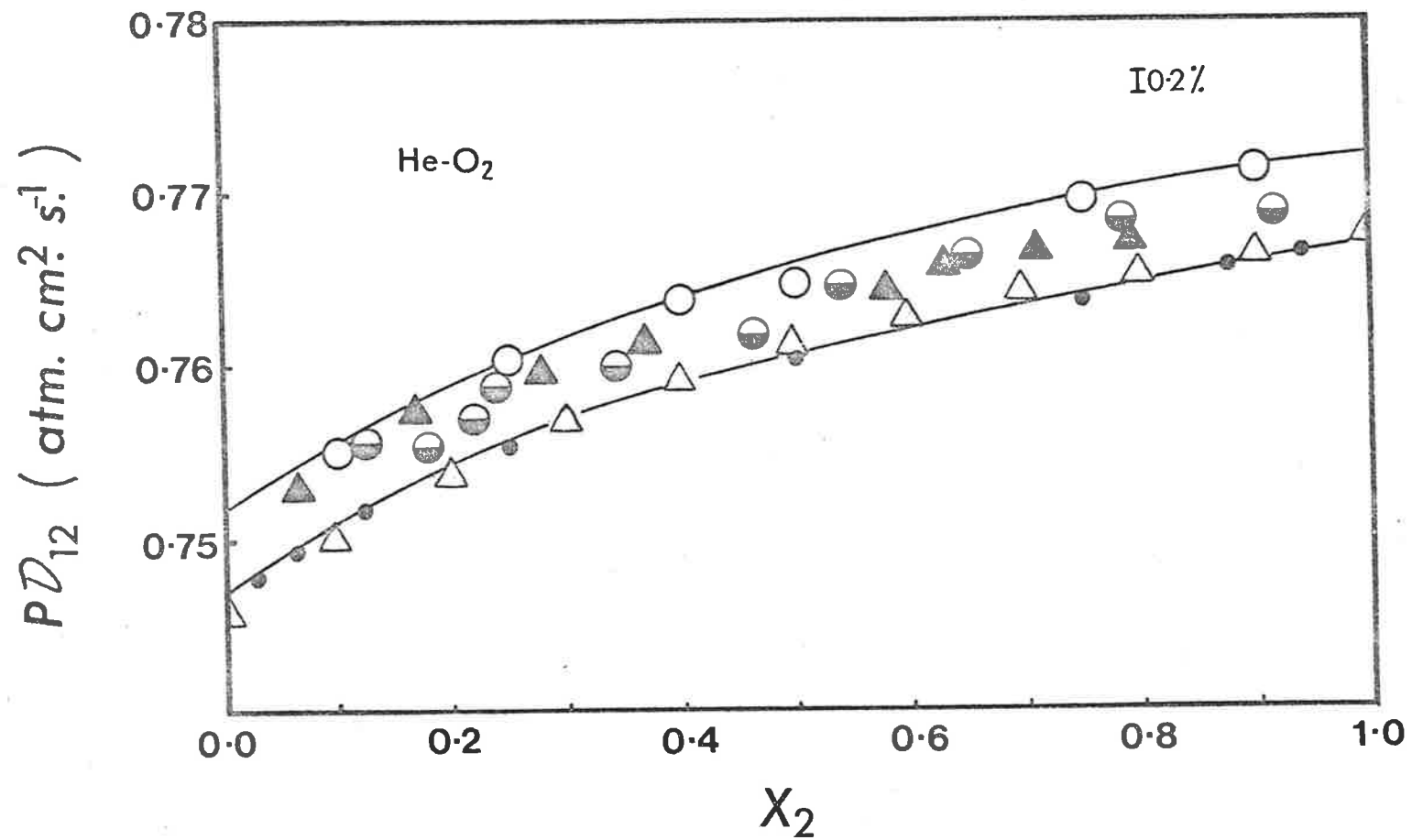


Figure 4.1: Concentration Dependence of the Diffusion Coefficient for the system He - O_2 at 300K.

- - Tube 4
- ◐ - Tubes 1 and 2, Ref. 10.
- ▲ - Tube 3
- - Loschmidt Cell
- △ - Chapman-Enskog Theory

Table 4.2^a

Concentration Dependence of the Diffusion
Coefficient for He/N₂ at 300K

(Two Bulb Apparatus Results)

x_2 (heavy)	P (atm)	$P\mathcal{D}_{12}$ (atm.cm ² .s ⁻¹)
0.0997	0.0923	0.7162
0.0998	0.0511	0.7166
0.1004	0.0731	0.7166
0.2493	0.0613	0.7217
0.4000	0.0767	0.7235
0.5007	0.0919	0.7250
0.5949	0.0774	0.7270
0.7406	0.0622	0.7288
0.9012	0.0730	0.7306
0.9056	0.0511	0.7303
0.9076	0.0913	0.7303

^a All symbols have their usual meanings (see Table 4.1).

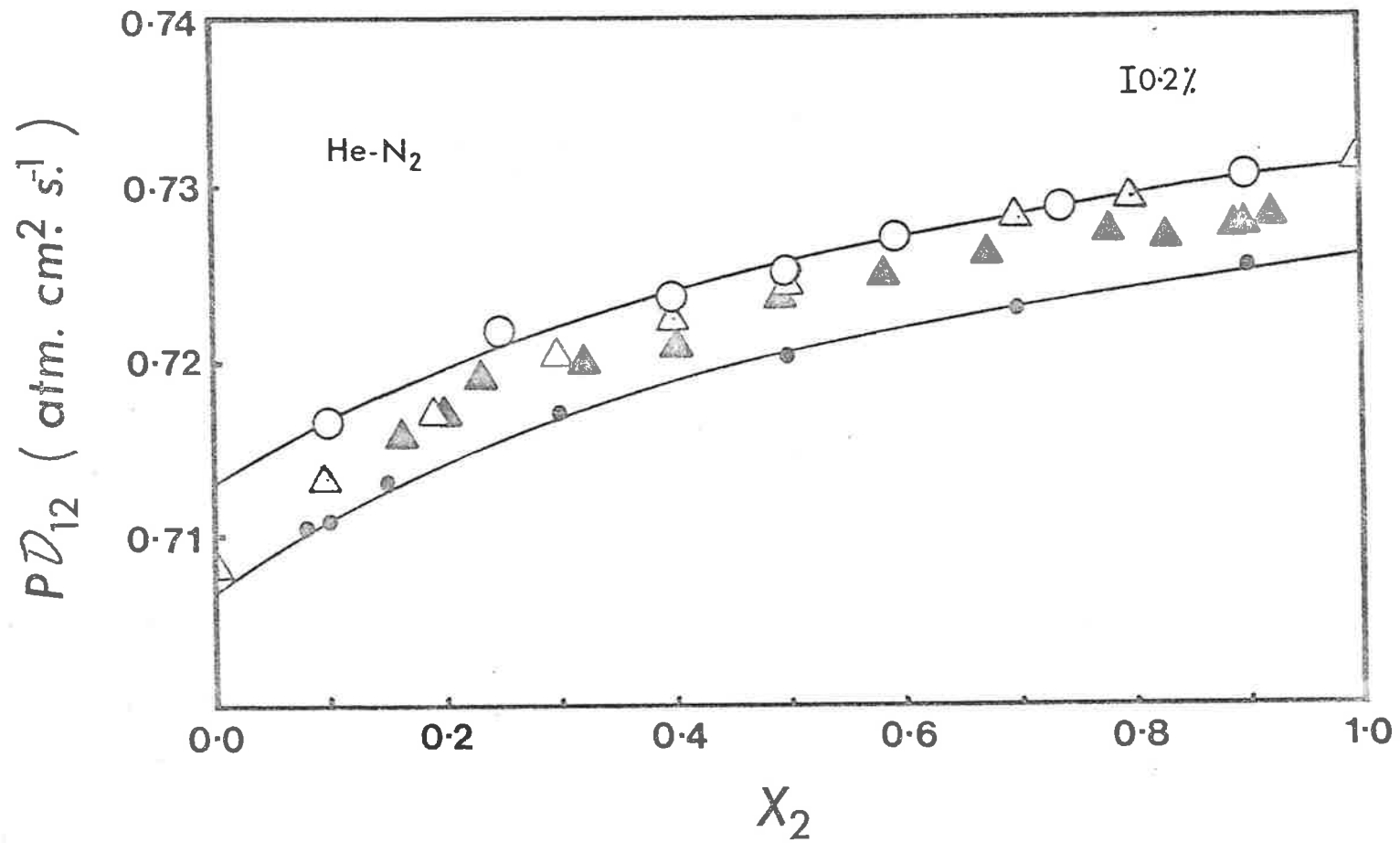


Figure 4.2: Concentration Dependence of the Diffusion Coefficient for the system He - N₂ at 300K.

- - Tube 4
- - Loschmidt Cell
- ▲ - Tube 3
- △ - Chapman-Enskog Theory

Table 4.3^a

*Concentration Dependence of the Diffusion
Coefficient for He/Ar at 300K*

(Two Bulb Apparatus Results)

x_2 (heavy)	P (atm)	$P\bar{D}_{12}$ (atm.cm ² .s ⁻¹)
0.1006	0.0595	0.7447
0.2498	0.0714	0.7514
0.3996	0.0892	0.7556
0.5010	0.1063	0.7574
0.6015	0.0886	0.7590
0.7510	0.0709	0.7617
0.9010	0.0591	0.7633

^a All symbols have their usual meanings
(see Table 4.1).

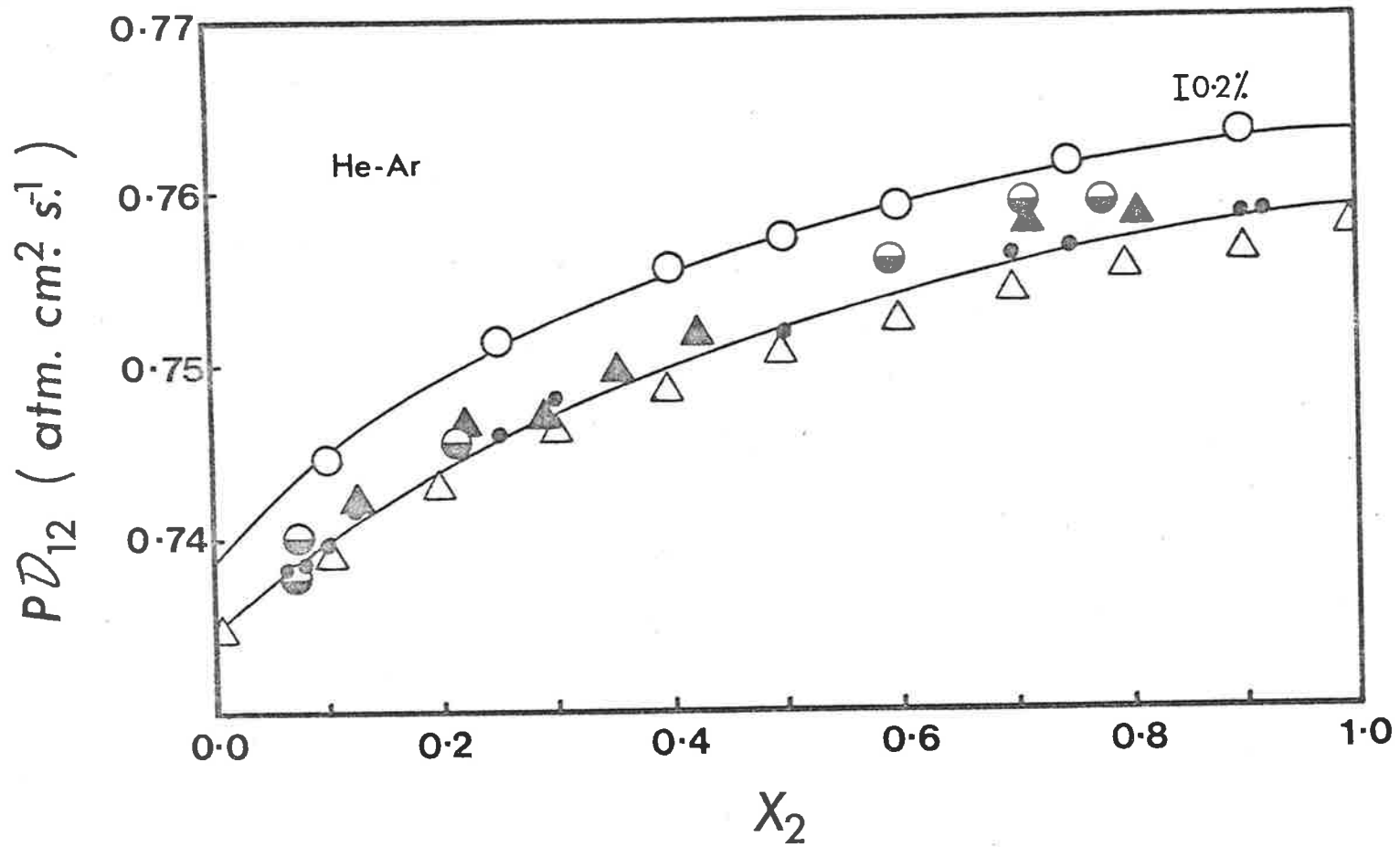


Figure 4.3: Concentration Dependence of the Diffusion Coefficients for the system He - Ar at 300K.

- - Tube 4 ◐ - Tubes 1 and 2, Ref.10. ▲ - Tube 3
 ● - Loschmidt Cell △ - Chapman-Enskog Theory

Table 4.4^a

*Concentration Dependence of the Diffusion
Coefficient for He/CO₂ at 300K*

(Two Bulb Apparatus Results)

x_2 (heavy)	P (atm)	$P\mathcal{D}_{12}$ (atm.cm ² .s ⁻¹)
0.1001	0.0593	0.6115
0.2500	0.0711	0.6161
0.3996	0.0888	0.6192
0.5019	0.0884	0.6200
0.6028	0.0884	0.6213
0.7525	0.0590	0.6225
0.9008	0.0592	0.6236

^a All symbols have their usual meanings
(see Table 4.1).

Table 4.5^a

*Concentration Dependence of the Diffusion
Coefficient for N₂/Ar at 300K*

(Two Bulb Apparatus Results)

x_2 (heavy)	P (atm)	$P\mathcal{D}_{12}$ (atm.cm ² .s ⁻¹)
0.1470	0.0537	0.2048
0.2999	0.0534	0.2050
0.3994	0.0534	0.2051
0.5005	0.0533	0.2052
0.6006	0.0536	0.2053
0.6999	0.0534	0.2056
0.8500	0.0534	0.2058

^a All symbols have their usual meanings
(see Table 4.1).

Table 4.6^a

*Concentration Dependence of the Diffusion
Coefficient for He/Ne at 300K*

(Two Bulb Apparatus Results)

x_2 (heavy)	P (atm)	$P\mathcal{D}_{12}$ (atm.cm ² .s ⁻¹)
0.1491	0.0657	1.1103
0.2475	0.0930	1.1142
0.3965	0.0660	1.1200
0.3975	0.0658	1.1217
0.4511	0.1172	1.1225
0.6024	0.0983	1.1261
0.7525	0.0930	1.1300
0.8021	0.0660	1.1310
0.9012	0.0657	1.1335

^a All symbols have their usual meaning
(see Table 4.1).

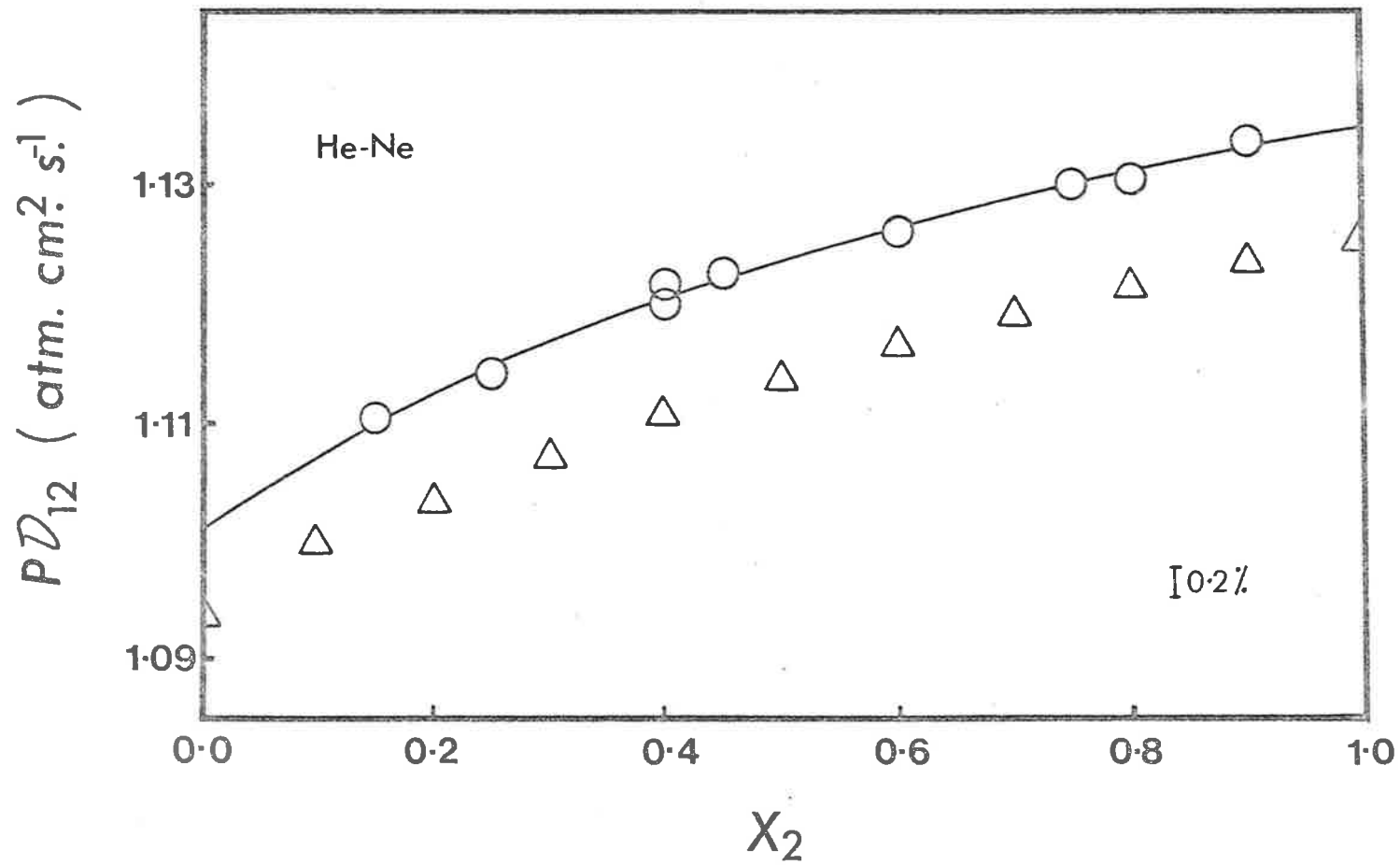


Figure 4.6: Concentration Dependence of the Diffusion Coefficient for the system He - Ne at 300K.

○ - Tube 4

△ - Chapman-Enskog Theory

Table 4.7

Least-squares Data for Eq. 4.1

	D_{12}^0 ($\text{cm}^2 \cdot \text{sec}^{-1}$)	a_1	a_2	Av. Dev. % ^a
<i>(a) Loschmidt cells</i>				
He-O ₂ ^b	0.7469	0.0564	1.1270	± 0.03 (15)
He-N ₂	0.7067	0.0676	1.4883	± 0.04 (26)
He-Ar	0.7344	0.0846	1.4825	± 0.06 (25)
He-CO ₂	0.6029	0.0905	2.3952	± 0.04 (12)
N ₂ -Ar	0.2034	0.0041	0.0000	± 0.04 (26)
<i>(b) Two-bulb cell</i>				
He-O ₂	0.7513	0.0583	1.0929	± 0.04 (6)
He-N ₂	0.7129	0.0576	1.2505	± 0.04 (11)
He-Ar	0.7385	0.1016	1.9275	± 0.02 (7)
He-CO ₂	0.6064	0.1082	2.7165	± 0.02 (7)
N ₂ -Ar	0.2046	0.0069	0.0000	± 0.02 (7)
He-Ne	1.1028	0.0503	0.7016	± 0.04 (10)

^a The figures in parentheses are the number of experimental points.

^b Previously reported in Ref. [10].

with the results obtained in this study using tubes 3 and 4. The data for tube 4 showed the greatest deviations but, because of the short length and large radius of this tube, it is extremely sensitive to the constants used in the experimental relation of Wirz. Thus it is possible that his relation might be valid in form, but is not accurate enough for present purposes (i.e. 0.1%).

It was noticed that even after allowing for the possible errors in the Wirz relation, the results obtained are approximately 0.5% higher than the results which were measured with a Loschmidt cell. Thus, it was concluded that either the method used to apply the end correction is incomplete or there is another important factor which is still to be discovered. It was therefore decided that, if possible, it would be more appropriate to calibrate the two-bulb cell with the accurate data available in the literature.

After applying the end correction as described in Ref. [17], the results obtained with tube 4 in the two bulb apparatus were precise but consistently higher by $0.71 \pm 0.10\%$ than the data in Table 4.7(a) obtained with the cells of the Loschmidt design.

A summary of these deviations between the data obtained from two different types of cells is given in Table 4.8.

From the above discussion it appears that, if Knudsen effects are neglected, any point selected from the data in Table 4.7(a) may be used to calibrate two-bulb cells with a precision of $\pm 0.1\%$.

Table 4.8

*Deviations Between the Data Obtained by the
Two Bulb Cell and the Loschmidt Cell*

System	$\% \Delta_{x_2=0}^a$	$\% \Delta_{x=.5}^a$	$\% \Delta_{x_2=1}^a$
He/Ar	.56	.72	.92
He/N ₂	.88	.71	.72
He/O ₂	.59	.67	.72
He/CO ₂	.58	.81	.82
N ₂ /Ar	.59	.73	.88

$$^a \Delta = \frac{(\overline{P\mathcal{D}}_{12})_{\text{TBA}} - (\overline{P\mathcal{D}}_{12})_{\text{Losch}}}{(\overline{P\mathcal{D}}_{12})_{\text{Losch}}}$$

4.3 Results from the Small Two Bulb Cell (A₂)

A small two bulb cell, described in Chapter 3, was calibrated using the data obtained in this laboratory²⁰ with a Loschmidt cell and was then used to measure the concentration dependence of the binary diffusion coefficients for the systems He - Kr, He - Xe, Ne - Kr, Ne - Xe, Ar - Kr, Ar - Xe, Ar - O₂, Ar - CO, Kr - CH₄ and CF₄ - CH₄ at 300K. The (Pr)⁻¹ values for all the experiments performed with this cell were less than 10 atm.⁻¹ cm.⁻¹ and hence Knudsen effects were neglected. The experimental results obtained for all the abovementioned systems, and the system Ne-Ar* were fitted to equation 4.1 and are summarised in Table 4.9.

* The diffusion coefficients for this system were measured with Loschmidt Cell (A₃).

Table 4.9

Least-square Parameters of Equation 4.1 for the
Following Systems in Small Two Bulb Cell (A_2) at 300K

System	D_{12}^0 # ($\text{cm}^2 \cdot \text{s}^{-1}$)	a_1	a_2	Av. Dev. %
He-Kr	0.6356	0.0785	1.0381	± 0.06
He-Xe	0.5429	0.0794	1.0677	± 0.07
Ne-Ar*	0.3234	0.0091	-	± 0.07
Ne-Kr	0.2629	0.0175	-	± 0.04
Ne-Xe	0.2212	0.0326	0.5313	± 0.02
Ar-Kr	0.1404	0.0026	-	± 0.05
Ar-Xe	0.1140	0.0017	-	± 0.06
Ar-CO	0.2067	0.0065	-	± 0.02
Ar-O ₂	0.2037	0.0024	-	± 0.04
Kr-CH ₄	0.1786	0.0008	-	± 0.02
CH ₄ -CF ₄	0.1455	0.0079	-	± 0.04

* The experiments for this system were performed in
Loschmidt cell (A_3).

D_{12}^0 is the limiting diffusion coefficient when
 $x_2 = 0$.

4.4 Theoretical Predictions for Concentration Dependence of D_{12}

The variation of the diffusion coefficients with composition was also predicted, for all the other systems under study except for $\text{CH}_4 - \text{CF}_4$ and $\text{Ar} - \text{CO}$, using Kihara's second approximation to the Chapman-Enskog theory which is given by equation 2.5.

The potential parameters $(\epsilon_{11}, \sigma_{11})$ for helium were obtained²¹ while for all other gases, these were calculated from the temperature dependence of viscosities²²⁻²⁶ and the values are given elsewhere²⁷. The potential parameters $(\epsilon_{12}, \sigma_{12})$ for the mixtures were also calculated using a similar technique but from the temperature studies of diffusion²⁸⁻³⁰. The collision integrals for all the gases and gas mixtures, except helium³¹, were obtained from the tables given by Klein *et al.*³².

The predicted values for these systems are listed in Tables 4.10 and 4.11 and are plotted along with the experimental values in Figures 4.1 - 4.10.

The concentration dependence of the diffusion coefficients can also be compared by determining the ratio of D_{12} at the two composition extremes. A summary of the ratios of the predicted and experimental values is given in Table 4.12. Experimental ratios are derived from the coefficients of Tables 4.7 and 4.9. As can be seen in Figures 4.1 - 4.11, there is reasonably good agreement between the experimental diffusion coefficients and their respective predicted values for all the systems except $\text{He} - \text{N}_2$ and $\text{He} - \text{CO}_2$. This non-reproducibility is probably due to the

Table 4.10^a: Predicted Diffusion Coefficients for the Rare Gas Mixtures at 300K using Kihara's Second Approximation

	He-Ne	He-Ar	He-Kr	He-Xe	Ne-Ar	Ne-Kr	Ne-Xe	Ar-Kr	Ar-Xe
x_2	(PD ₁₂) _{Pred.} (atm.cm. ² s ⁻¹)								
0.0000	1.0940	0.7342	0.6358	0.5435	0.3232	0.2628	0.2213	0.1406	0.1141
0.1000	1.0988	0.7392	0.6418	0.5490	0.3238	0.2637	0.2223	0.1407	0.1141
0.2000	1.1031	0.7431	0.6462	0.5528	0.3242	0.2645	0.2231	0.1407	0.1142
0.3000	1.1070	0.7463	0.6496	0.5555	0.3246	0.2651	0.2238	0.1408	0.1142
0.4000	1.1104	0.7488	0.6522	0.5576	0.3250	0.2657	0.2243	0.1408	0.1142
0.5000	1.1135	0.7509	0.6543	0.5592	0.3253	0.2661	0.2247	0.1408	0.1143
0.6000	1.1164	0.7527	0.6561	0.5605	0.3256	0.2665	0.2251	0.1409	0.1143
0.7000	1.1189	0.7543	0.6576	0.5616	0.3258	0.2668	0.2254	0.1409	0.1143
0.8000	1.1213	0.7556	0.6588	0.5625	0.3261	0.2671	0.2257	0.1409	0.1144
0.9000	1.1234	0.7567	0.6599	0.5633	0.3263	0.2674	0.2259	0.1410	0.1144
1.0000	1.1253	0.7577	0.6608	0.5639	0.3265	0.2676	0.2261	0.1410	0.1144

^a x_2 is the molefraction of the heavy component and PD₁₂ is the numerical value of the diffusion coefficient at one atmosphere.

Table 4.11^a: Predicted Diffusion Coefficients for the Following Mixtures at 300K using Kihara's Second Approximation

	He-O ₂	He-N ₂	He-CO ₂	Ar-N ₂	Ar-O ₂	Kr-CH ₄
x ₂	(PD ₁₂) _{Pred} (atm.cm. ² s ⁻¹)					
0.0000	0.7455	0.7080	0.6036	0.2029	0.2031	0.1784
0.1000	0.7501	0.7132	0.6094	0.2030	0.2031	0.1785
0.2000	0.7538	0.7171	0.6136	0.2031	0.2032	0.1786
0.3000	0.7567	0.7202	0.6168	0.2031	0.2032	0.1787
0.4000	0.7591	0.7228	0.6192	0.2032	0.2032	0.1788
0.5000	0.7611	0.7248	0.6212	0.2032	0.2032	0.1789
0.6000	0.7628	0.7266	0.6228	0.2033	0.2033	0.1789
0.7000	0.7642	0.7280	0.6241	0.2034	0.2033	0.1790
0.8000	0.7654	0.7293	0.6252	0.2034	0.2033	0.1791
0.9000	0.7665	0.7304	0.6262	0.2035	0.2034	0.1791
1.0000	0.7675	0.7313	0.6270	0.2035	0.2034	0.1792

^a x₂ is the molefraction of the heavy component and PD₁₂ is the numerical value of the diffusion coefficient at one atmosphere.

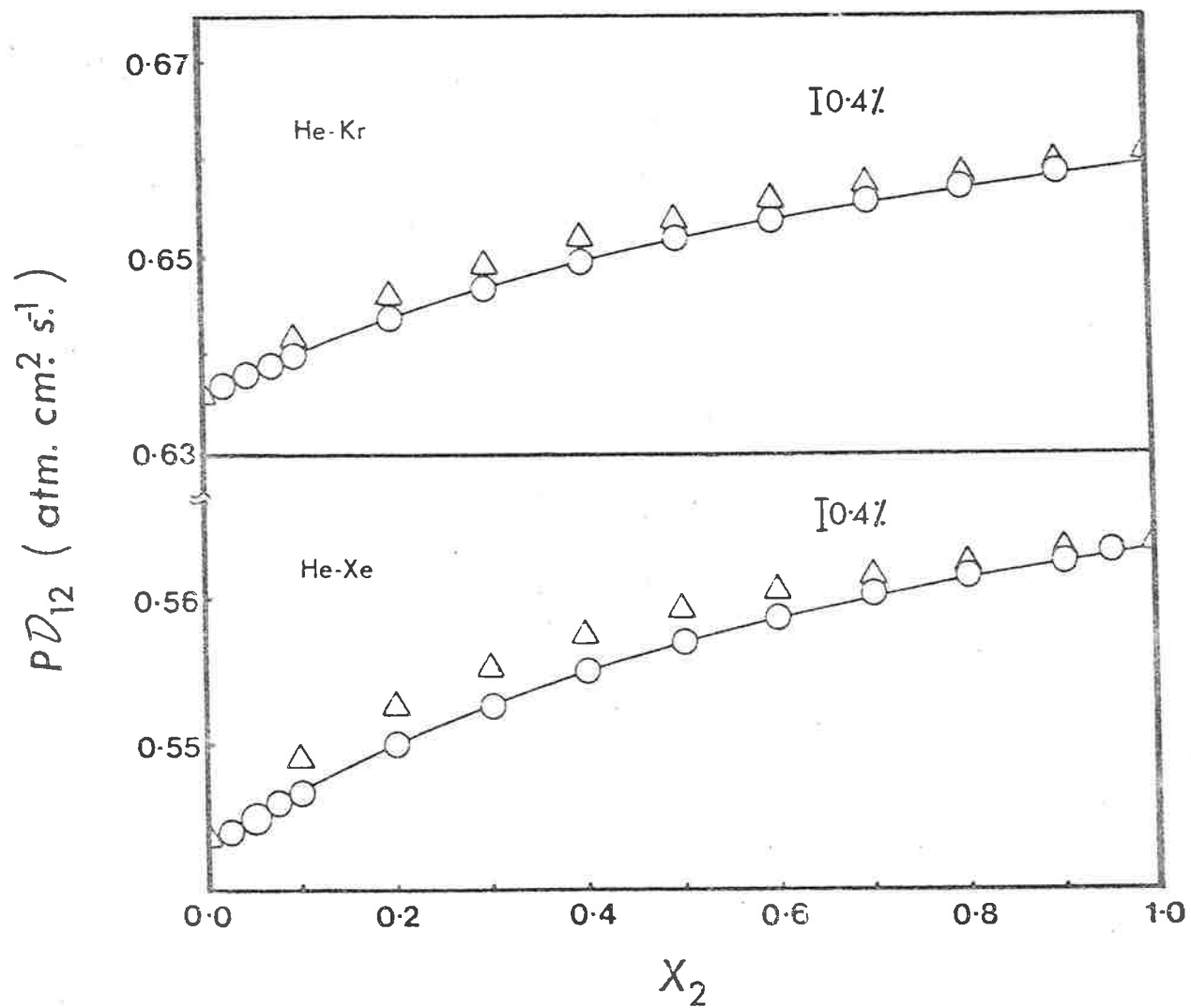


Figure 4.7: Concentration Dependence of the Diffusion Coefficient for the systems He - Kr and He - Xe at 300K.

○ - Small Two Bulb Cell

△ - Chapman Enskog Theory

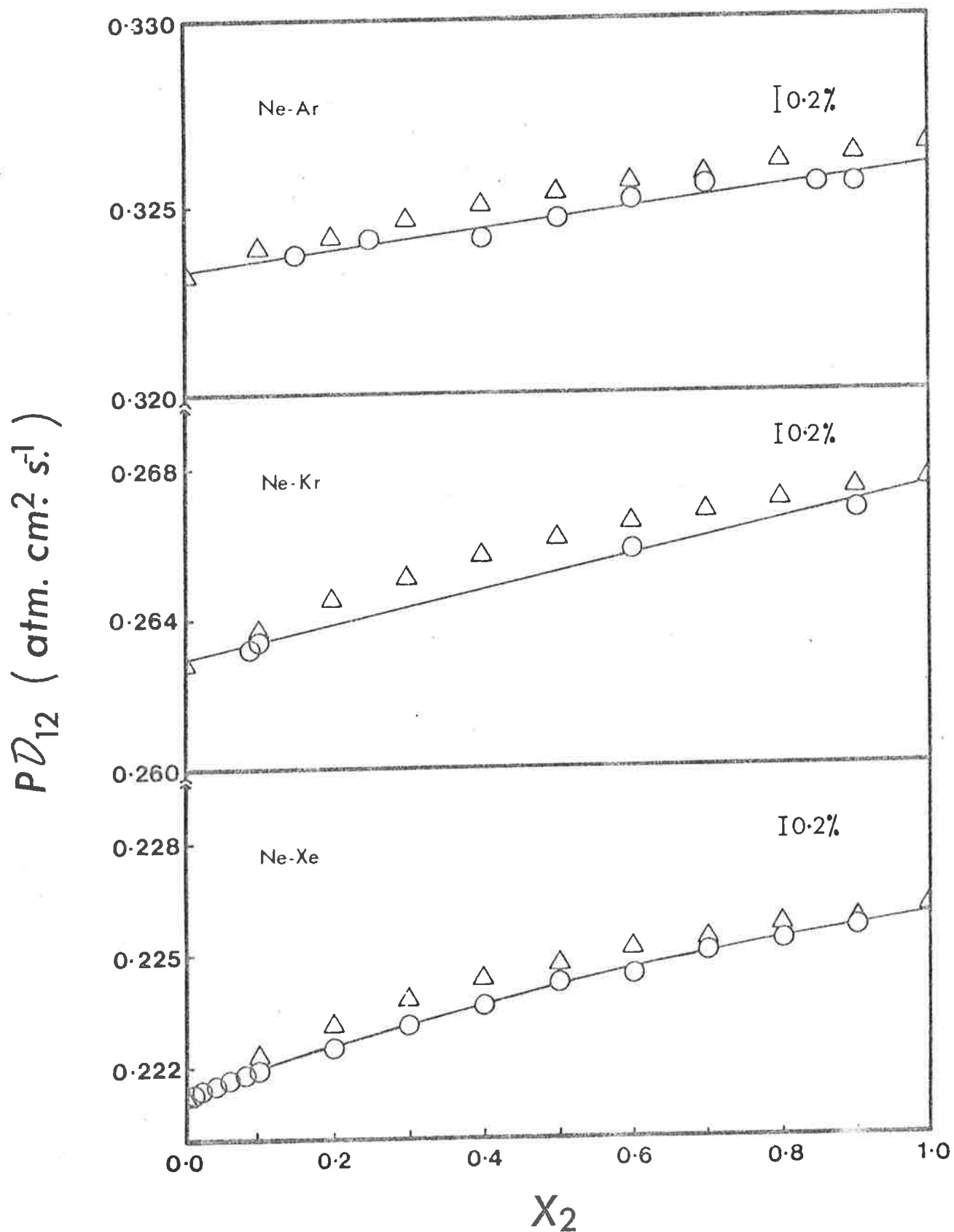


Figure 4.8: Concentration Dependence of the Diffusion Coefficient for the systems Ne - Ar, Ne - Kr and Ne - Xe at 300K.

- - Small Two Bulb Cell
 △ - Chapman-Enskog Theory

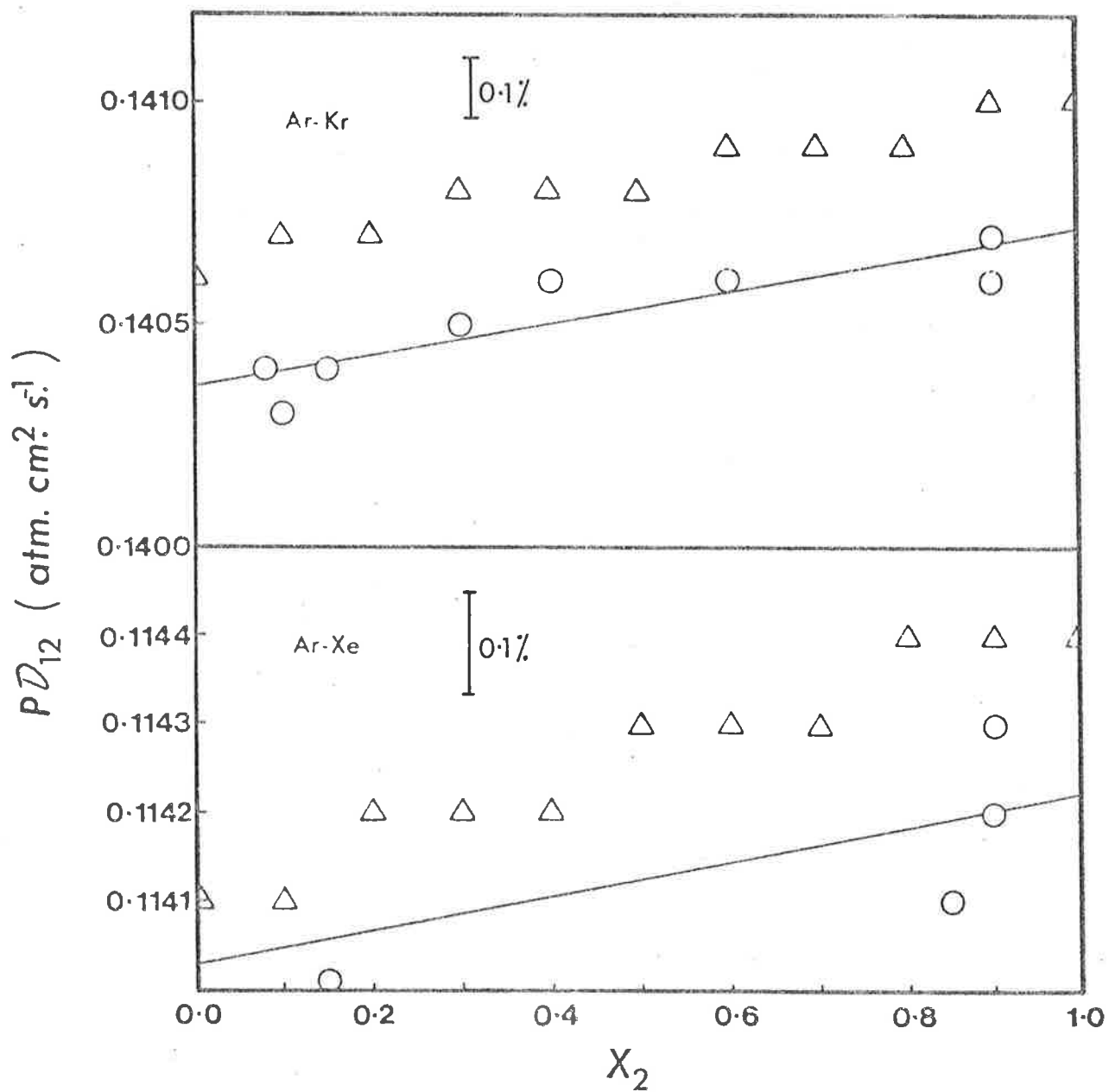


Figure 4.9: Concentration Dependence of the Diffusion Coefficients for the systems Ar - Kr and Ar - Xe at 300K.

- - Small Two Bulb Cell
- △ - Chapman-Enskog Theory

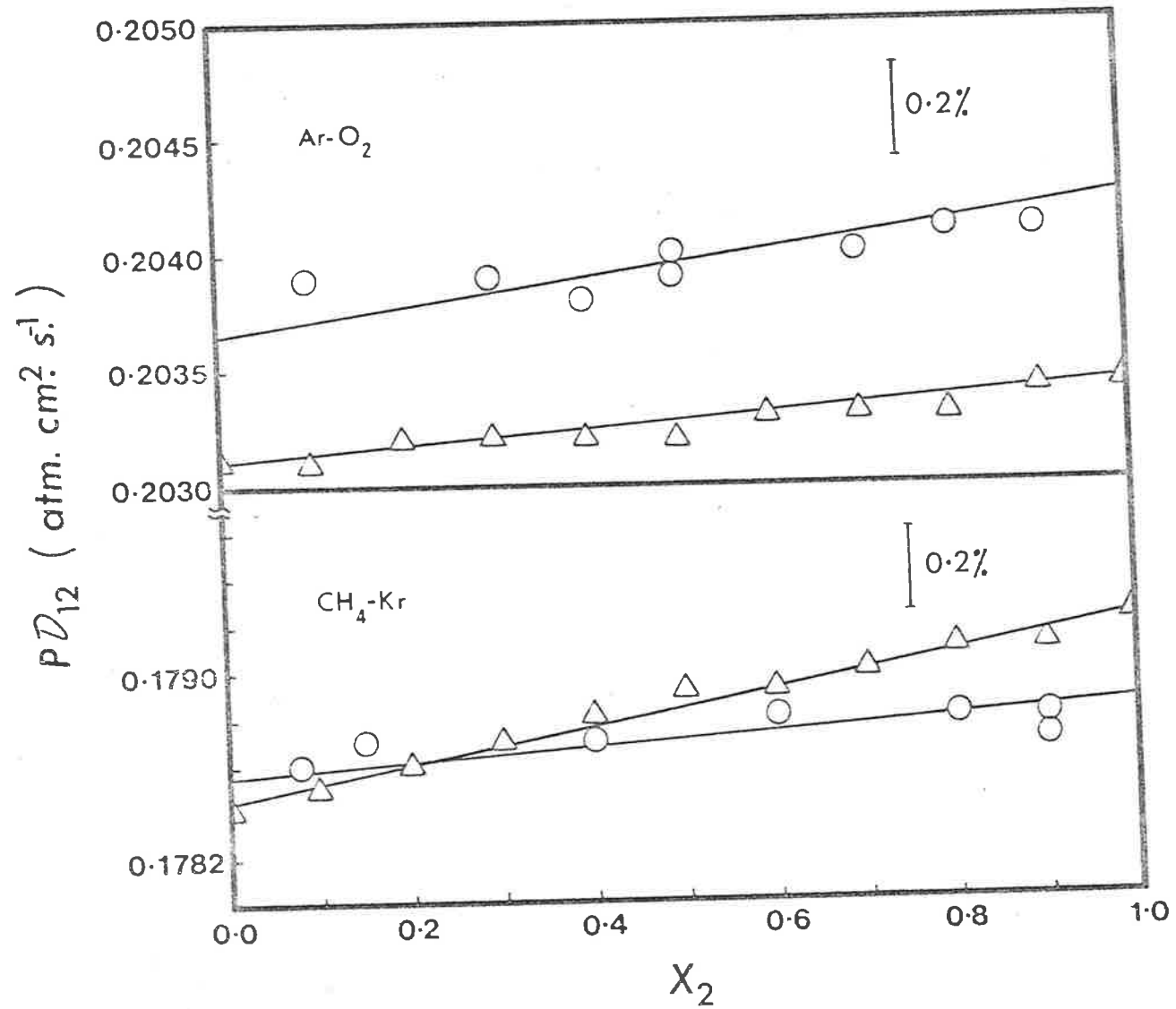


Figure 4.10: Concentration Dependence of the Diffusion Coefficient for the systems Ar - O₂ and CH₄ - Kr.

\circ - Small Two Bulb Cell \triangle - Chapman-Enskog Theory

Table 4.12^a

Comparison of Experimental and Predicted Values of
 $(PD_{12})_{x_2=1} / (PD_{12})_{x_2=0}$

System	A ₁ T.B.A.	A ₂ S.T.B.A.	A ₃ Loschmidt	Predicted
He-Ne	1.029	-	-	1.029
He-Ar	1.038	1.034	1.034	1.032
He-Kr	-	1.038	-	1.039
He-Xe	-	1.038	-	1.038
Ne-Ar	-	-	1.009	1.010
Ne-Kr	-	1.017	-	1.018
Ne-Xe	-	1.021	-	1.022
Ar-Kr	-	1.003	-	1.003
Ar-Xe	-	1.002	-	1.003
He/N ₂	1.026	-	1.027	1.033
He/O ₂	1.028	-	1.026	1.029
He/CO ₂	1.029	-	1.027	1.039
Kr/CH ₄	-	1.001	-	1.004
N ₂ /Ar	1.007	-	1.004	1.003
O ₂ /Ar	-	1.002	-	1.001

^a x_2 is the molefraction of the heavy component and PD_{12} is the numerical value of the diffusion coefficient at one atmosphere.

failure of the [m,6,8] intermolecular potential to fit these results.

4.5 *Concentration Dependence of Diffusion Coefficient for He - Ar at 277K and 323.15K*

Finally the diffusion coefficients for the system He - Ar were measured as a function of composition at one atmosphere and at 277.0K and 323.15K with the Loschmidt cell (A_3).

The experimental data at both the temperatures, together with the predicted values (using equation 2.5), are given in Tables 4.13 and 4.14. The former data was fitted to the equation 4.1 and the constants thus obtained are summarised in Table 4.15.

The experimental results and the predicted values are compared graphically in Figure 4.11 and by calculating the ratios at two composition extremes in Table 4.16, which show an excellent agreement with one another.

The analysis of the above data indicates that:

- (i) the mutual diffusion coefficient varies 25% over the temperature range of 46K; and
- (ii) the variation in concentration dependence of D_{12} over this range is less than 0.1%.

Table 4.13^a

Experimental and Predicted Values of the Diffusion
Coefficient for He-Ar System at 277K

x_2	$(P\mathcal{D}_{12})_{\text{exp}}$ (atm.cm. ² s ⁻¹)	x_2	$(P\mathcal{D}_{12})_{\text{pred}}$ (atm.cm. ² s ⁻¹)
0.0703	0.6456	0.0000	0.6417
0.1001	0.6470	0.1000	0.6460
0.3003	0.6544	0.2000	0.6494
0.3999	0.6560	0.3000	0.6521
0.4000	0.6550	0.4000	0.6544
0.4998	0.6575	0.5000	0.6562
0.5000	0.6575	0.6000	0.6577
0.6000	0.6582	0.7000	0.6591
0.6996	0.6610	0.8000	0.6602
0.6998	0.6608	0.9000	0.6612
0.7998	0.6616	1.0000	0.6621
0.8999	0.6628		

^a All symbols have their usual meaning (see Table 4.12)

Table 4.14^a

Experimental and Predicted Values of the Diffusion Coefficient for He-Ar System at 323.15K

x_2	$(PD_{12})_{exp}$ (atm.cm. ² s ⁻¹)	x_2	$(PD_{12})_{Pred}$ (atm.cm. ² s ⁻¹)
0.0703	0.8363	0.0000	0.8322
0.1001	0.8375	0.1000	0.8380
0.3003	0.8463	0.2000	0.8425
0.4003	0.8492	0.3000	0.8460
0.5000	0.8516	0.4000	0.8490
0.5998	0.8540	0.5000	0.8514
0.6997	0.8555	0.6000	0.8534
0.8000	0.8578	0.7000	0.8551
0.8997	0.8594	0.8000	0.8566
		0.9000	0.8580
		1.0000	0.8591

^a All symbols have their usual meaning (see Table 4.12).

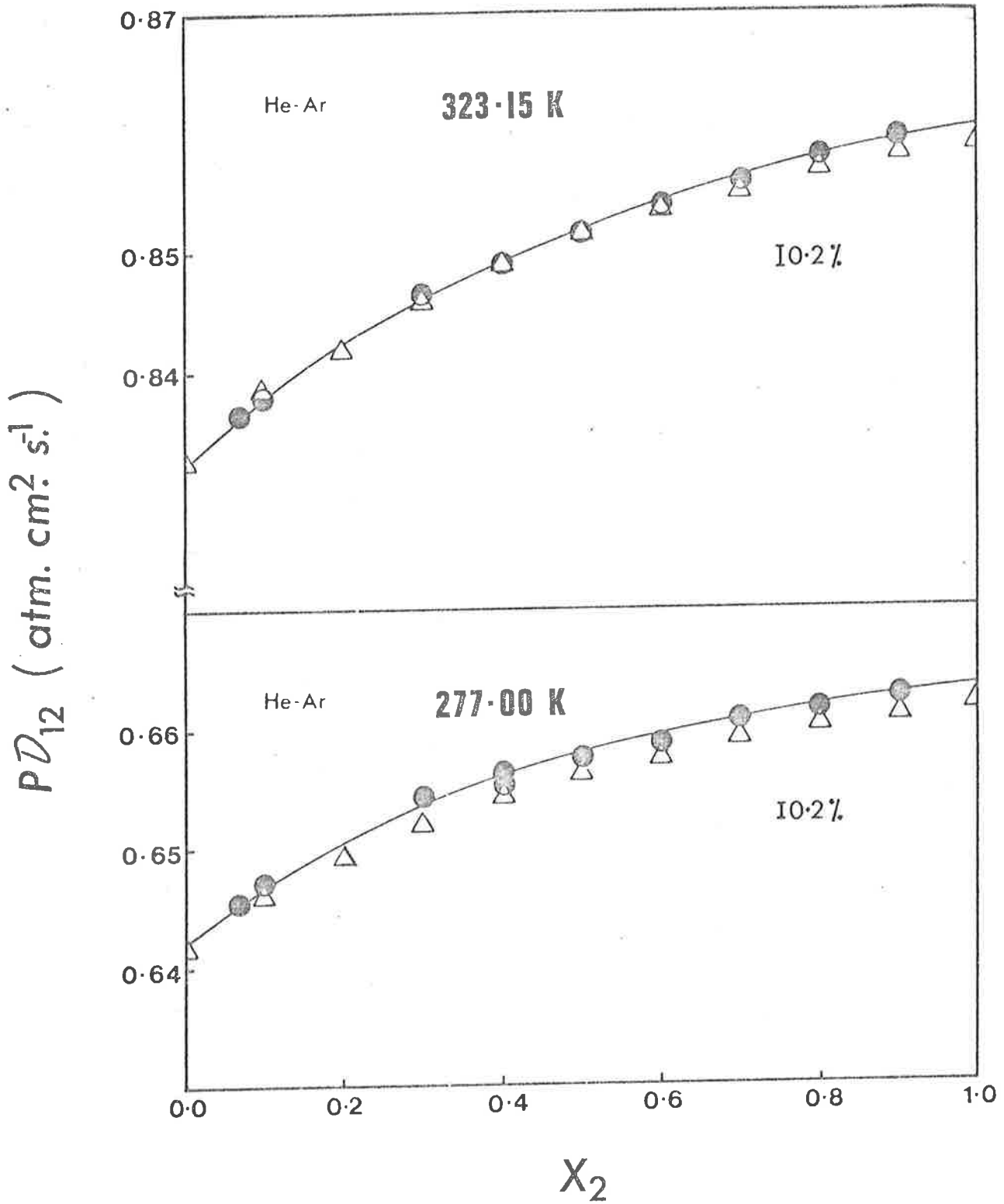


Figure 4.11: Concentration Dependence of Diffusion Coefficient for the system He - Ar at 323.15K and 277.00K.

● - Loschmidt Cell △ - Chapman-Enskog Theory

Table 4.15

Least-Square Parameters of Equation 4.1 for the System He-Ar

T K	D_{12}^0 # (cm. ² s ⁻¹)	a ₁	a ₂	Av. Dev. %
277.00	0.6423	.0859	1.5916	± 0.03
323.15	0.8321	.0765	1.2353	± 0.02

D_{12}^0 is the limiting diffusion coefficient when $x_2 = 0$.

Table 4.16^a

Comparison of Experimental and Predicted Values of
 $(PD_{12})_{x_2=1} / (PD_{12})_{x_2=0}$ for He/Ar

T K	Experimental	Predicted
277.00	1.033	1.032
323.15	1.034	1.032

^a All symbols have their usual meaning
 (see Table 4.12).

REFERENCES

1. Carson, P.J., Dunlop, P.J. and Bell, T.N., *J. Chem. Phys.* 56 (1972) 531.
2. Yabsley, M.A. and Dunlop, P.J., *Phys. Lett.* A38 (1972) 247.
3. Carson, P.J., Yabsley, M.A. and Dunlop, P.J., *Chem. Phys. Lett.* 15 (1972) 436.
4. Carson, P.J. and Dunlop, P.J., *Chem. Phys. Lett.* 14 (1972) 377.
5. Harris, K.R., Bell, T.N. and Dunlop, P.J., *Can. J. Phys.* 50 (1972) 1644.
6. Harris, K.R., Bell, T.N. and Dunlop, P.J., *Can. J. Chem.* 50 (1972) 1874.
7. Yabsley, M.A., Carson, P.J. and Dunlop, P.J., *J. Phys. Chem.* 77 (1973) 703.
8. Staker, G.R., Yabsley, M.A., Symons, J.M. and Dunlop, P.J., *Chem. Soc. Faraday Trans. I* 70 (1974) 825.
9. Staker, G.R., Dunlop, P.J., Harris, K.R. and Bell, T.N., *Chem Phys. Lett.* 32 (1975) 561.
10. Yabsley, M.A. and Dunlop, P.J., *J. Phys.* E8 (1975) 834.

11. Ney, E.P. and Armistead, F.C., *Phys. Rev.* 71
(1947) 14.
12. Loschmidt, J., *Akad. Wiss. Wien* 61 (1870) 367.
13. Rayleigh, J.W.S., *The Theory of Sound II*, Dover
Publications, New York (1945) p.203 and
p.491.
14. King, L.V., *Philos. Mag.* 21 (1936) 128.
15. Marrero, T.R. and Mason E.A., *J. Phys. Chem. Ref.*
Data 1 (1972) 3.
16. Shankland, I.R. and Dunlop, P.J., *Chem. Phys. Lett.*
39 (1976) 557.
17. Yabsley, M.A. and Dunlop, P.J., *Physica* 85A
(1976) 160.
18. Wirz, P., *Helv. Phys. Acta* 20 (1947) 3.
19. Amdur, I. and Schatzki, T.F., *J. Chem. Phys.* 29
(1958) 1.
20. Arora, P.S., Shankland, I.R., Bell, T.N., Yabsley,
M.A. and Dunlop, P.J., *Rev. Sci. Instr.* 48
(1973) 673.
21. Mason, E.A. and Rice, W.E., *J. Chem. Phys.* 22
(1954) 522.
22. Kestin, J., Ro, S.T. and Wakeham, W.A., *J. Chem.*
Phys. 56 (1972) 4114.

23. Kestin, J., Ro, S.T. and Wakeham, W.A., *J. Chem. Phys.* 56 (1972) 4119.
24. Kestin, J., Ro, S.T. and Wakeham, W.A., *J. Chem. Phys.* 56 (1972) 5837.
25. Kestin, J., Khalifa, H.E., Ro, S.T. and Wakeham, W.A., *Physica* 88A (1977) 242.
26. Hellemans, J.M., Kestin, J. and Ro, S.T., *Physica* 65 (1973) 362.
27. Arora, P.S., Symons, J.M., Martin, M.L. and Dunlop, P.J., *Chem. Phys. Lett.* 62 (1979) 396.
28. Arora, P.S., Carson, P.J. and Dunlop, P.J., *Chem. Phys. Lett.* 54 (1978) 117.
29. Arora, P.S., Robjohns, H.L. and Dunlop, P.J., *Physica* 95A (1979) 561.
30. Arora, P.S., Robjohns, H.L., Shankland, I.R. and Dunlop, P.J., *Chem. Phys. Lett.* 59 (1978) 478.
31. Taylor, W.L., *J. Chem. Phys.* 57 (1972) 832.
32. Klein, M., Hanley, H.J.M., Smith, F.J. and Holland, P., *Tables of Collision Integrals and Second Virial Coefficients for the [m,6,8] Intermolecular Potential Function*, National Bureau of Standards Circular, NSRD-NBS47, 1974.

CHAPTER 5ATHE TEMPERATURE DEPENDENCE OF DIFFUSION5A.1 *Introduction*

Information regarding intermolecular forces between gas atoms may be obtained from gaseous transport properties and compressibility measurements as well as from molecular scattering and crystal data¹. The potential parameters for like molecules can be obtained directly from the study of the coefficients of viscosity of pure gases as a function of temperature² but corresponding information about forces between unlike molecules obtained directly from measurements on gaseous mixtures is very meagre. The most direct method of probing the potential function for unlike interactions is the study of the temperature dependence of mutual diffusion coefficients since these depend only on the force fields of the unlike diffusing molecules and, in the first approximation, are independent of the forces between the like pairs whereas viscosity, thermal conductivity, thermal diffusion and virial coefficients of binary mixtures depend directly on both like and unlike interactions to the same approximation. It is for this reason that the determination of binary diffusion coefficients inherently gives a better indication of the force law between pairs of unlike molecules than can be obtained from any other physical measurement.

Recently Van Heijningen *et al.*^{3,4} and Hogervorst⁵⁻⁸ calculated the potential parameters from the binary diffusion coefficients measured over the temperature ranges of 65.4 - 400K and 300 - 1400K, respectively, using both the Lennard-Jones [12-6] and the [exp-6] models, but the agreement between the experimental and the predicted values (using their parameters) for the transport properties of binary noble gas mixtures was not good enough for the present accuracy.

Kestin and co-workers^{10,21-29} calculated ~~potential~~^{scaling} parameters by the application of their extended law of corresponding states^{9,10} and the viscosity data measured over a wide temperature range approximately 700K (298.15 - 973.15K). The details of the predicted values of second virial coefficients, viscosities and diffusion coefficients (using their parameters) for noble gas mixtures will be discussed later in this chapter.

In this laboratory, Carson and Dunlop¹¹ tried to obtain the potential energy parameters by measuring the diffusion coefficients over a small range of temperature (≈ 50 K) for Lennard-Jones[12-6] potential. They used the two point interpolation method to calculate the collision integrals at various temperatures. This method was not accurate enough and hence resulted in the failure of the project.

For the present study, the binary diffusion coefficients of rare and polyatomic gas mixtures were measured over a small temperature range of fifty degrees. Using the experimental data together with some excellent second virial coefficients, the potential parameters (ϵ_{12}

and σ_{12}) of the mixed interactions were obtained which predict almost all the data available in the literature within the experimental errors. The potential selected for this purpose was the group of [m,6,8] potentials proposed by Klein and Hanley^{12,13}. These authors applied this group of potentials to various rare and polyatomic gases and suggested that [11,6,8, $\gamma = 3$] potential was the best among the [m,6,8] group because of its better predictions about the transport data than any other member of this group. However, in the present study the calculated potentials varied from [9,6,8, $\gamma = 0$] for Ar - CO to [12,6,8, $\gamma = 2.5$] for Ar - Xe. These potentials may not be unique but they predict the best transport and second virial coefficient data in the literature, as good as or better than any other potentials which have been proposed for these systems. The method to calculate the potential parameters for pure gases and their binary gas mixtures is discussed, in detail, in this chapter. The various transport properties (e.g. viscosity, thermal diffusion coefficient, self diffusion coefficient, second virial coefficients, diffusion coefficients at low and high temperatures) have been predicted using the best calculated potentials among the [m,6,8] group which show slightly better agreement than those given by the extended law of corresponding states.

5A.2 *Experimental and Results*

The diffusion coefficients for all the binary noble gas mixtures (except Kr - Xe) and for the systems He - N₂, He - CO₂, He - O₂, Ar - CO, Ar - N₂, Ar - O₂, CH₄ - Kr and CH₄ - CF₄, each of which contains at least one polyatomic molecule, were measured at constant molefraction as a function of temperature between 275-323K. The molefraction, x_2 , of the *heavy* component was chosen to be as small as possible but large enough to give reasonable out of balance reading on the digital voltmeter. The experiments for binary gas systems He - Ne, He - Ar, Ne - Ar and N₂ - Ar were performed at one atmosphere pressure in a Loschmidt cell (A₃) while for all other systems they were performed in two bulb cell (A₂) and a large pressure range (40 - 300 torr) was used in order to

- (i) keep the experiments to the similar lengths of time;
- (ii) eliminate the Knudsen effects.

The experimental results and the molefraction, at which a particular binary system was studied, are given in Appendix 3. The binary diffusion coefficients were obtained in duplicate either at every two degree interval or at every four degree interval from 277 to 323K, averaged and converted to a value corresponding to one atmosphere pressure and then fitted to a polynomial in temperature, T, given by

$$D_{12} = b_1 + b_2T + b_3T^2 \quad \dots \quad 5A.1$$

The coefficients for each system together with the percentage average deviations of the experimental points from the

smooth curves are given in Table 5A.1. The concentration dependence of D_{12} for each system at 300K was measured and has been discussed in Chapter 4. The Chapman-Enskog theory for binary diffusion indicates that over a range of 50K the variation in the concentration dependence of D_{12} is less than 0.1%. This fact has been supported experimentally with a He - Ar mixture as shown in Chapter 4.

5A.3 Calculations of the Potential Parameters for Unlike Interactions

Theoretical Chapman-Enskog equation 2.3 for the diffusion coefficient may be rearranged to the form

$$[D_{12}]_m \cdot f_D^{(m)} \cdot P = \frac{3}{8\sqrt{\pi}} \left[\frac{k^3 (M_1 + M_2)}{2M_1 M_2} \right]^{1/2} \frac{1}{\sigma_{12}^2} \cdot \frac{T^{3/2}}{\Omega_{12}^{(1,1)*}(T^*)} \quad \dots \quad 5A.2$$

The quantity $f_D^{(m)}$ is a very small correction factor which was applied to yield the theoretical first approximation after extrapolating the smoothed experimental results to $x_2 = 0$ using equation 4.1.

For the first approximation, the equation 5A.2 can be written as

$$[D_{12}]_1 \cdot P = \frac{3}{8\sqrt{\pi}} \left[\frac{k^3 (M_1 + M_2)}{2M_1 M_2} \right]^{1/2} \frac{1}{\sigma_{12}^2} \cdot \frac{T^{3/2}}{\Omega_{12}^{(1,1)*}(T^*)} \quad \dots \quad 5A.3$$

i.e. $Y_i = \theta \cdot X_i$

where $\theta = \frac{3}{8\sqrt{\pi}} \left[\frac{k^3 (M_1 + M_2)}{2M_1 M_2} \right]^{1/2} \frac{1}{\sigma_{12}^2}$ and $X_i = T^3 / \Omega_{12}^{(1,1)*}(T^*)$

Table 5A.1: Least-squares Coefficients for Equation 5A.1.

System	x_2^a	$b_1 \times 10^2$	$b_2 \times 10^3$	$b_3 \times 10^6$	Av. dev. %
He-Ne*	0.15	- 1.5186	1.30600	8.0695	± 0.06
He-Ar*	0.15	- 6.9068	1.23353	4.8998	± 0.05
He-Kr#	0.10	-12.3666	1.52792	3.3999	± 0.03
He-Xe#	0.10	- 0.6411	0.61811	4.0915	± 0.05
Ne-Ar*	0.15	- 6.1238	0.70962	1.9148	± 0.04
Ne-Kr#	0.15	- 2.2749	0.39265	1.8708	± 0.07
Ne-Xe#	0.08	- 8.2455	0.75183	0.8749	± 0.04
Ar-Kr#	0.15	+ 0.0630	0.06087	1.3502	± 0.05
Ar-Xe#	0.15	- 2.0482	0.18420	0.8822	± 0.10
He-N ₂ #	0.20	-15.2693	1.80450	3.6177	± 0.04
He-O ₂ #	0.15	-35.9205	3.16733	1.7869	± 0.09
He-CO ₂ #	0.15	- 8.1267	1.23002	3.5624	± 0.06
Ar-N ₂ *	0.50	- 7.4946	0.63930	0.9653	± 0.05
Ar-O ₂ #	0.50	- 5.0619	0.46192	1.2870	± 0.04
Ar-CO#	0.35	- 2.8714	0.33599	1.5034	± 0.06
Kr-CH ₄ #	0.15	- 4.3961	0.36896	1.2438	± 0.03
CH ₄ -CF ₄ #	0.15	- 3.2028	0.29646	0.9876	± 0.03

^a x_2 is a molefraction of the heavy component.

* Experiments were performed with Loschmidt cell (A_3).

Experiments were performed with small two bulb cell (A_2).

The contribution of θ to the temperature dependence is very little at low molefractions. Equation 5A.3 suggests a simpler method of determining the potential parameters than that given by Van Heijningen *et al.*^{3,4} and by Hogervorst⁶.

Equation 5A.3 implies that for a given set of values for Y_i and X_i , the plot of Y_i versus X_i is a straight line passing through the origin. For an experimental set of $[D_{12}]_1$ and T values, a corresponding set of (Y_i, X_i) values was calculated by assuming an approximate value of ϵ_{12} . It was repeated for a series of ϵ_{12} values and the value which resulted in the best least-squares fit of (Y_i, X_i) passing through the origin was selected, this value thus corresponds to the minimum standard error. The optimum value of σ_{12} was then calculated from the slope of the best fit. The potential parameters (ϵ_{12} and σ_{12}) calculated by this method for all the systems mentioned in the beginning, together with their error limits obtained by applying an F-test to the standard error of the best fit, are given in Tables 5A.2 and 5A.3. In Figure 5A.1 a graph is plotted between a series of (ϵ_{12}/k) values and their respective percentage errors in slope, θ , for a binary mixture Ar - Kr which clearly shows a single minimum corresponding to the best value of (ϵ_{12}/k) for that system.

The collision integrals for the above calculations were taken from the tables given by Klein *et al.*¹⁴ At a particular temperature these collision integrals were obtained by fitting the required portion of the curve T^* versus

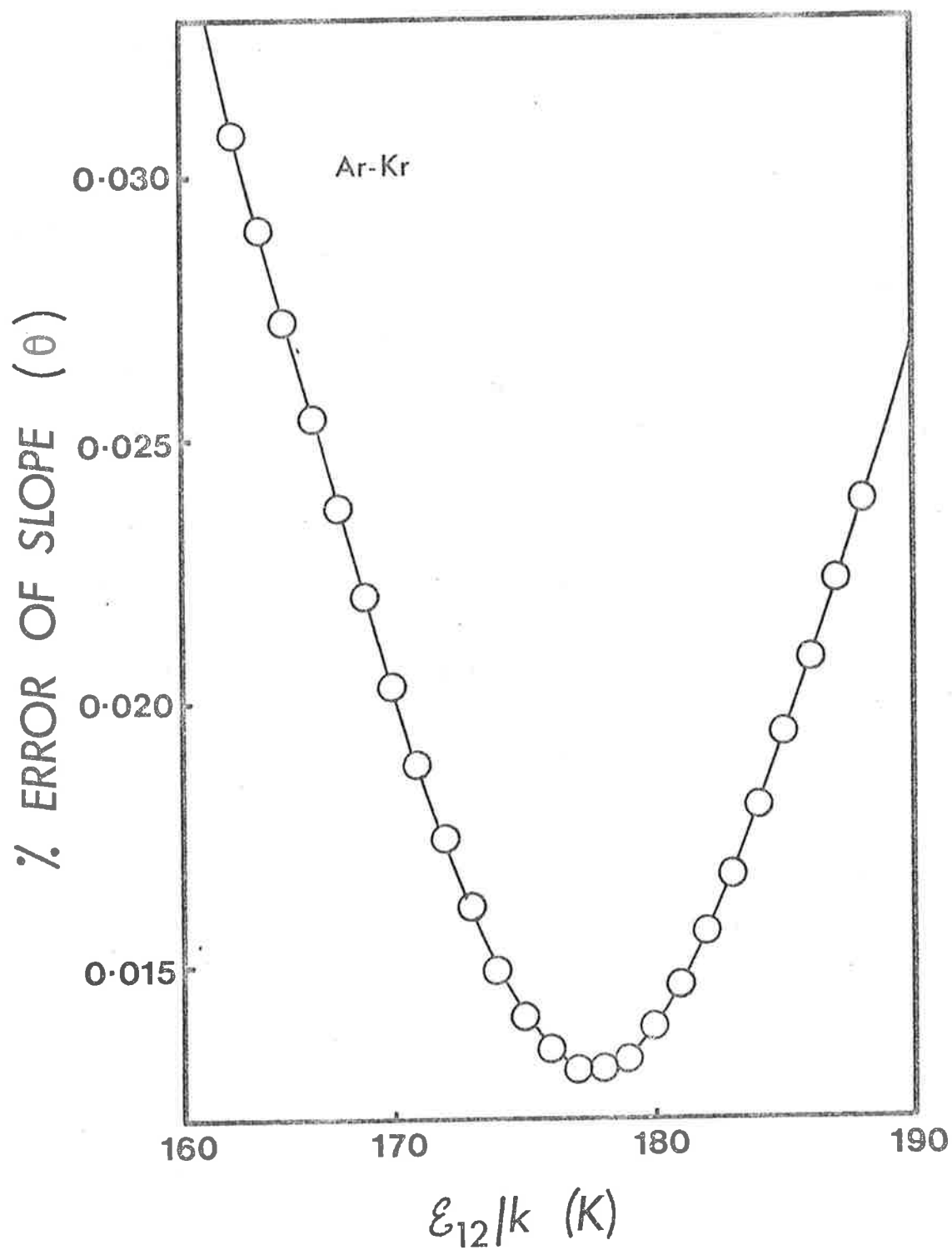


Figure 5A.1: A Typical Fit of the Temperature Dependence Data for Ar-Kr system.

Table 5A.2: Tests of $[m,6,8]$ Potentials for Noble Gas Mixtures^{a,b}

	He-Ne	He-Ar	He-Kr	He-Xe	Ne-Ar
Potential	(10,6,8, $\gamma=2$)	(9,6,8, $\gamma=2$)	(11,6,8, $\gamma=0$)	(9,6,8, $\gamma=3$)	(11,6,8, $\gamma=3$)
(ϵ_{12}/k) (K)	21.0 \pm 2.0	22.5 \pm 2.0	24.0 \pm 2.0	21.5 \pm 2.0	74.0 \pm 2.0
σ_{12} (Å)	2.661 \pm 0.005	3.213 \pm 0.005	3.330 \pm 0.005	3.678 \pm 0.005	3.308 \pm 0.005
Av. Error, B_{12} (cm ³) ^{15,16}	-1.0 (123-323)	\pm 0.6 (123-323)	\pm 1.1 (148-323)	\pm 0.6 (173-323)	-1.0 (123-323)
Av. % Error, η_{mix} ^{10,21-24}	\pm 0.2 (298-973)	-0.2 (298-993)	-0.3 (298-873)	\pm 0.3 (298-773)	+0.1 (298-973)
Av. % Error, η_{mix} ^{30,31}	-	\pm 0.4 (120-1600)	-	-	-
Av. % Error, \mathcal{D}_{12} ⁴	+1.1 (65-295)	+0.6 (90-400)	+1.2 (112-400)	+1.2 (169-400)	\pm 0.5 (90-400)
Av. % Error, \mathcal{D}_{12} ⁶	\pm 0.6 (300-1400)	+2.4 (300-1400)	+0.5 (300-1100)	+1.9 (300-1000)	\pm 0.5 (300-1400)
Av. % Error, α_T ⁴⁹	-	-	-	-	\pm 2.6 (110-270)
Av. % Error, α_T ³⁵	\pm 1.7 (306)	\pm 1.5 (278-306)	-	-	\pm 1.5 (278-306)

Continued...

Table 5A.2: Continued

	Ne-Kr	Ne-Xe	Ar-Kr	Ar-Xe
Potential	(11,6,8, $\gamma=3$)	(12,6,8, $\gamma=2.5$)	(11,6,8, $\gamma=3$)	(12,6,8, $\gamma=2.5$)
(ϵ_{12}/k) (K)	79.0 \pm 2.0	87.0 \pm 2.0	177.5 \pm 2.0	212.5 \pm 2.0
σ_{12} (Å)	3.186 \pm 0.005	3.359 \pm 0.005	3.417 \pm 0.005	3.558 \pm 0.005
Av. Error, B_{12} (cm ³) ^{15,16}	-1.4 (148-323)	-3.2 (173-323)	-1.0 (148-323)	+1.0 (173-323)
Av. % Error, η_{mix} ^{10,21-24}	-0.2 (298-973)	\pm 0.2 (298-773)	-0.2 (298-973)	\pm 0.2 (298-773)
Av. % Error, η_{mix} ^{30,31}	-	-	\pm 0.2 (120-1600)	-
Av. % Error, D_{12} ⁴	\pm 1.2 (111-400)	+0.6 (169-400)	+0.7 (169-400)	+0.6 (169-400)
Av. % Error, D_{12} ⁶	\pm 0.5 (300-1400)	+0.4 (300-1400)	+1.7 (300-1400)	+0.4 (300-1400)
Av. % Error, α_T ⁴⁹	-	-	-18.0 (200-267)	-
Av. % Error, α_T ³⁵	-	-	-	-

- a After consulting the original data the following average experimental errors were adopted:
 B_{12} , 1.5 - 2.0 cm³; η_{mix} (Kestin *et al.*), 0.25%; η_{mix} (Smith and co-workers), 1%; D_{12} (van Heijningen *et al.*), 1%; D_{12} (Hogervorst) 1-1.5%; α_T (Gr w and Wakeham), 3%; α_T (Symons *et al.*), 1.5-2%.
- b The temperature range in degrees kelvin used in each study is given in brackets beneath each entry.

Table 5A.3: Tests of $[m,6,8]$ potentials for Binary Gas Mixtures^{a,b}

	He-N ₂	He-O ₂	He-CO ₂	Ar-N ₂	Ar-O ₂	Ar-CO	CH ₄ -Kr	CH ₄ -CF ₄
Potential	(11,6,8,γ=0)	(9,6,8,γ=1)	(12,6,8,γ=0.5)	(9,6,8,γ=4)	(9,6,8,γ=0)	(9,6,8,γ=0)	(11,6,8,γ=1)	(10,6,8,γ=1)
(ϵ_{12}/k) (K)	21.0±2.0	25.5±2.0	25.0±2.0	99.5±2.0	102.0±3.0	86.0±3.0	171.0±3.0	127.0±3.0
σ_{12} (Å)	3.262±0.005	3.179±0.005	3.394±0.005	3.546±0.005	3.477±0.007	3.606±0.007	3.622±0.007	4.221±0.007
Av. dev.	0.4	±2.52	±0.6	+1.4	-1.0	±3.4	+4.7	±1.4
B ₁₂ (cm ³) ¹⁵⁻¹⁹	(123-323)	(90-298)	(223-298)	(123-323)	(90)	(123-323)	(123-273)	(223-623)
Av. % dev.	+0.4	+0.4	±0.2	+0.3	±0.1	-	+0.6	+0.7
η_{mix} ²⁵⁻²⁹	(298-973)	(298-678)	(298-973)	(298-767)	(298-770)	-	(298-478)	(296-473)
Av. % dev.	-	-	-	-	-	-	-	+0.9
η_{mix} ^{30, 31}	-	-	-	-	-	-	-	(150-1100)

- a After consulting the original data the following average experimental errors were adopted:
 B₁₂ (Brewer and Douslin), 1.5-2.0 cm³; B₁₂ (Knobler et al.), 2.0-3.0 cm³; η_{mix} (Kestin et al.),
 0.25%; η_{mix} (Smith and co-workers), 2%.
- b The temperature range in degrees Kelvin is given in brackets beneath each entry.

$\Omega_{ij}^{(\ell, s)}$ to the polynomials up to order twenty and selecting the one with a minimum standard error

$$\Omega_{ij}^{(\ell, s)} = a + bT^* + cT^{*2} + \dots uT^{*20} \quad \dots \quad 5A.4$$

where a, b, c, \dots, u are the constants and T^* is the reduced temperature.

When this method was applied to all the systems, pairs of parameters were obtained for each system for a series of [m,6,8] potentials. It was impossible to determine which pair of parameters was best since all reproduced the experimental data equally well. To decide the best pair of parameters, the second virial coefficients for each pair were calculated using the following expression

$$B_{12} = \frac{2}{3} \pi N \sigma_{12}^3 B_{12}^* , \quad \dots \quad 5A.5$$

where N is the Avogadro's number; B_{12}^* is the reduced second virial coefficient whose value was taken from the tabulation of Klein *et al.*¹⁴. These calculated values of B_{12} were then compared with the excellent experimental data of Brewer^{15,16}, Douslin *et al.*¹⁷, Knobler *et al.*¹⁸ and the compilation of Dymond and Smith¹⁹. The differences between the values calculated with the appropriate [m,6,8] potential and the corresponding experimental values of B_{12} for rare gas mixtures are listed in Table 5A.4 whereas the same for all other gas pairs are presented in Table 5A.5.

The second virial coefficients have also been calculated with the potential parameters obtained by Kestin *et al.*^{10,21-24} using the extended law of corresponding states theory and viscosity data. The differences between the

Table 5A.4: Differences $(B_{12}^{\text{calc}} - B_{12}^{\text{exp}})$ for the Data of Brewer^{15, 16} ^a

T K	He-Ne		He-Ar		He-Kr		He-Xe		Ne-Ar		Ne-Kr		Ne-Xe		Ar-Kr		Ar-Xe	
	A	B	A	B	A	B	A	B	A	B	A	B	A	B	A	B	A	B
323.2	-0.8	0.8	0.1	- 5.5	1.1	1.6	-0.3	7.9	-0.8	1.6	-0.1	- 3.0	-2.2	-1.7	-1.4	-2.6	1.5	1.9
298.2	-0.7	0.9	0.0	- 6.0	-	-	-	-	-0.9	1.8	-	-	-	-	-	-	-	-
273.2	-0.6	1.0	0.6	- 5.8	2.7	3.2	0.5	9.1	-0.5	2.4	-0.5	- 3.5	-2.0	-1.5	-1.1	-3.6	1.8	2.1
248.2	-0.7	0.9	0.2	- 6.8	-	-	-	-	-	-	-	-	-	-	-	-	-	-
223.2	-0.8	0.9	0.2	- 7.5	0.6	1.0	-0.1	9.5	-0.6	2.9	-0.5	- 4.5	-3.2	-2.6	-1.2	-4.9	1.2	2.2
198.2	-0.8	0.8	-0.2	- 8.7	0.4	0.6	-0.7	8.5	-1.0	2.9	-1.2	- 5.7	-4.3	-3.7	-1.0	-5.7	0.0	1.3
173.2	-1.0	0.7	-0.4	-10.1	0.1	0.6	-1.6	9.8	-1.4	3.0	-1.8	- 7.3	-4.1	-3.7	-1.2	-6.8	0.5	3.7
148.2	-1.3	0.6	-1.1	-12.2	-1.9	-1.2	-	-	-2.0	3.2	-3.7	-10.7	-	-	0.2	-7.7	-	-
123.2	-1.6	1.1	-2.9	-16.3	-	-	-	-	-3.2	2.8	-	-	-	-	-	-	-	-

^a Column A gives differences in $\text{cm}^3 \cdot \text{mol}^{-1}$ between values calculated with the appropriate [m,6,8] potential and the corresponding experimental values. Column B gives differences in $\text{cm}^3 \cdot \text{mol}^{-1}$ between values calculated with the extended law of corresponding states and the corresponding experimental values.

Table 5A.5: Differences ($B_{12}^{calc} - B_{12}^{exp}$) for the Gas Mixtures^{a,b}

T K	He-N ₂	He-O ₂	He-CO ₂	Ar-N ₂	Ar-O ₂	Ar-CO	CH ₄ -Kr	CH ₄ -CF ₄ [#]
623.15	-	-	-	-	-	-	-	-2.21
598.15	-	-	-	-	-	-	-	-2.12
573.15	-	-	-	-	-	-	-	-1.91
548.15	-	-	-	-	-	-	-	-2.06
523.15	-	-	-	-	-	-	-	-1.85
498.15	-	-	-	-	-	-	-	-1.65
473.15	-	-	-	-	-	-	-	-1.41
448.15	-	-	-	-	-	-	-	-1.35
423.15	-	-	-	-	-	-	-	-0.98
398.15	-	-	-	-	-	-	-	-0.76
373.15	-	-	-	-	-	-	-	-0.59
348.15	-	-	-	-	-	-	-	+0.04
323.15	-0.29	-	-	-0.53	-	-	-	+0.36
298.15	-0.23	-1.32	-1.67	-0.90	-	-	-	+1.19
273.15	+0.37	-	-	-1.31	-	-0.95	-1.98	+2.21
248.15	+0.16	-	+0.04	-0.94	-	-	-	-
223.15	+0.60	-	-0.04	-0.55	-	-0.56	-1.24	-
198.15	+0.55	-	-	-0.21	-	-	-	-
173.15	-0.34	-	-	+0.07	-	+1.72	+1.67	-
148.15	-1.00	-	-	+1.71	-	+4.40	+5.06	-
123.15	+0.33	-	-	+6.17	-	+9.45	+13.63	-
90.00	-	+3.71*	-	-	-1.0*	-	-	-

^a The experimental data was taken from Ref. [15,16] except for, #, which was taken from Ref. [17], and * which was taken from Ref. [18].

^b The numerical values given in this table are in cm³.mol⁻¹.

calculated values with the corresponding states theory and the corresponding experimental values for rare gas pairs are also given in Table 5A.4 which clearly indicates that the former predicted values give a better agreement with the experimental data than the latter.

The potential parameters were then tested (Tables 5A.2 and 5A.3) by predicting binary viscosities, diffusion coefficients at much higher and lower temperatures (for rare gas mixtures), thermal diffusion factors and the concentration dependences of D_{12} for comparison with the most accurate data in the literature. The calculations for the thermal conductivities have not been included here for the reason given by Kestin *et al.*²⁰. The concentration dependences of D_{12} have been discussed in Chapter 4, whereas all other transport properties will be discussed in the following sections.

5A.4 *Calculations of Viscosities*

The viscosities of all binary mixtures were calculated using the Chapman-Enskog equation 2.18 and the percentage differences between the values calculated with appropriate [m,6,8] potential and the corresponding experimental values are listed in Tables 5A.6 and 5A.7. The experimental data chosen for comparison from the literature were those of Kestin *et al.*^{10,21-29} and Smith *et al.*^{30,31}. The viscosities for the rare gas mixtures were also calculated with the potential parameters obtained^{10,21-24} from the viscosity data using the assumed extended law of corresponding states

Table 5A.6: Percentage Deviations $[(\eta_{\text{mix}}^{\text{calc}} - \eta_{\text{mix}}^{\text{exp}}) / \eta_{\text{mix}}^{\text{exp}}] \times 100$ for the Binary Viscosity Data of Kestin and co-workers^{10,21-24} a, b, c.

T K	He-Ne		He-Ar		He-Kr		He-Xe		Ne-Ar		Ne-Kr		Ne-Xe		Ar-Kr		Ar-Xe	
	A	B	A	B	A	B	A	B	A	B	A	B	A	B	A	B	A	B
298.2	0.6	0.5	-0.2	0.0	-0.1	-0.1	-0.3	-0.4	0.2	0.1	-0.1	0.7	0.2	0.8	0.1	0.2	0.2	0.5
373.2	0.2	0.0	-	-	-	-	±0.2	-0.4	0.1	0.1	-0.1	0.8	-0.4	0.2	-0.2	±0.1	-0.6	0.2
473.2	0.0	-0.2	-0.4	-0.2	-0.6	-0.6	±0.2	-0.3	0.1	0.1	-0.3	0.8	0.0	0.8	-0.2	±0.1	-0.1	1.0
573.2	-0.1	-0.2	-0.2	±0.2	-0.5	-0.5	±0.3	±0.2	0.1	0.2	-0.2	0.7	-	-	-0.1	0.3	-	-
673.2	-0.2	-0.3	-	-	-	-	±0.3	±0.3	0.0	0.1	-0.2	0.8	-	-	-0.2	0.2	-	-
773.2	-0.1	-0.1	0.2	0.2	-0.3	-0.3	±0.3	-0.6	0.1	0.1	-0.3	0.8	-0.3	0.8	-0.2	0.2	0.2	0.2
873.2	-0.1	0.1	-0.2	-0.2	-0.3	-0.2	-	-	0.0	0.2	-0.3	0.9	-	-	-0.1	0.4	-	-
973.2	0.0	0.2	-	-	-	-	-	-	0.0	0.2	-0.4	0.8	-	-	-0.4	0.1	-	-

- a Column A gives percentage differences between values calculated with the appropriate [m,6,8] potential and the corresponding experimental values. Column B gives percentage differences between values calculated with the extended law of corresponding states and the corresponding experimental values.
- b The values listed for each temperature are averages over the concentrations reported in the literature.
- c The He-Xe values were obtained by smoothing the data in Ref. [10].

Table 5A.7: Percentage Deviations $[(\eta_{mix}^{calc} - \eta_{mix}^{exp}) / \eta_{mix}^{exp}] \times 100$ for the Binary Gas Mixtures^{a, b}

T K	He-N ₂	He-O ₂	He-CO ₂	Ar-N ₂	Ar-O ₂	Ar-CO	CH ₄ -Kr	CH ₄ -CF ₄
296.15	-	-	-	-	-	-	-	- 0.98
298.15	- 0.59	+ 1.05	- 0.31	- 0.70	+ 0.35	-	+ 0.76	-
323.15	-	-	-	-	-	-	-	- 0.77
328.15	-	-	-	-	-	-	+ 0.42	-
367.15	-	-	-	- 0.32	-	-	-	-
371.15	-	-	- 0.11	-	-	-	-	-
368.15	-	-	-	-	± 0.05	-	-	-
373.15	- 0.46	-	-	-	-	-	+ 0.44	- 0.63
378.15	-	0.23	-	-	-	-	-	-
422.15	-	-	-	-	-	-	-	- 0.73
423.15	-	-	-	-	-	-	+ 0.69	-
467.15	-	-	-	± 0.04	-	-	-	-
468.15	-	-	-	-	- 0.10	-	-	-
473.15	- 0.35	-	-	-	-	-	+ 0.68	- 0.65
475.15	-	-	± 0.12	-	-	-	-	-
478.15	-	+ 0.13	-	-	-	-	-	-
571.15	-	-	-	- 0.20	-	-	-	-
573.15	- 0.33	+ 0.42	-	-	-	-	-	-
575.15	-	-	± 0.21	-	-	-	-	-
576.15	-	-	-	-	± 0.05	-	-	-
667.15	-	-	-	-	+ 0.15	-	-	-
673.15	- 0.36	-	+ 0.35	- 0.28	-	-	-	-
678.15	-	+ 0.34	-	-	-	-	-	-
767.15	-	-	-	- 0.26	-	-	-	-
770.15	-	-	-	-	± 0.0	-	-	-
773.15	- 0.40	-	+ 0.22	-	-	-	-	-
873.15	- 0.44	-	+ 0.22	-	-	-	-	-
973.15	- 0.49	-	+ 0.35	-	-	-	-	-

^a The experimental data was taken from References [25-29].

^b The values listed for each temperature are averages over the concentrations reported in the literature.

of Kestin *et al.*^{9,10} and the percentage differences between the calculated and the experimental values for these mixtures are listed in Table 5A.6, which show slightly poorer agreement than the former.

The viscosities for two ternary systems (He - Ne - Kr and He - Ar - Kr) were computed using equation 2.23 and compared with the corresponding experimental data given by Kestin *et al.*²⁷. The potential parameters used for these calculations were taken from Table 5A.2. A summary of the predicted and the experimental results²⁷ is given in Table 5A.8. The agreement between these values is excellent.

Table 5A.8

Percentage Deviations $[(\eta_{mix}^{calc} - \eta_{mix}^{exp}) / \eta_{mix}^{exp}] \times 100$
for the Ternary Gas Mixtures^a

T K	He-Ne-Kr	He-Ar-Kr
298.15	+ 0.09	- 0.27
373.15	- 0.09	- 0.43
573.15	- 0.18	- 0.18
673.15	+ 0.07	0.0
873.15	-	- 0.49

^a The experimental data was taken from Ref. [27].

In all cases discussed in this section, the experimental values for pure gases were used to calculate the

η_{mix} instead of those predicted by the first Chapman-Enskog approximation. In this way, the calculated values of η_{mix} depend only on the unlike interactions which is a good compromise between the first and the second approximation^{32,33}.

As expected, Table 5A.7 shows slightly larger deviations than those in Table 5A.6. It is because of the fact that [m,6,8] potentials might not be good enough to describe the intermolecular forces involved in the systems containing polyatomic molecules as accurately as such forces in mixtures of noble gases.

The interaction viscosity coefficient, η_{12} , for the systems containing polyatomic molecules were calculated, to analyse the experimental data of Kestin and co-workers²⁵⁻²⁹, using a method proposed by Maitland and Smith³⁰. This parameter, η_{12} , was essentially independent of concentration for all these gas mixtures except $\text{CH}_4 - \text{Kr}$. From this study, it appears that there may be some error for one of the mixtures²⁷ used to study $\text{CH}_4 - \text{Kr}$. The large deviations between the predicted and the experimental values²⁷ for $\text{CH}_4 - \text{CF}_4$ may be due to the fact that each molecule has twelve internal degrees of freedom.

Because of the excellent agreement between the predicted and the experimental viscosities of rare gas systems and the reasonable agreement for the systems containing polyatomic molecules, it would seem that a combination of binary diffusion and second virial coefficient data provides an excellent method for predicting viscosity data for the same systems. From the above discussion it appears that this method predicts viscosity coefficients more accurately

than viscosity data can be used to predict binary diffusion coefficients.

5A.5 *Calculations for Diffusion Coefficients at Very High and Low Temperatures*

The potential parameters obtained from the present study were utilized to calculate the binary diffusion coefficients at much higher and lower temperatures for rare gas mixtures using Kihara's second approximation (eq. 2.5). A similar data was produced using the potential parameters calculated by Kestin and co-workers^{10,21-24} with the help of their corresponding states theory and viscosity results. The predicted values, by the above two methods, were compared with the experimental values of Van Heijningen *et al.*⁴ at low temperatures and Hogervorst⁶ at high temperatures which show an excellent agreement within the experimental errors except for He - Ar ^{and He - Kr}. The percentage deviations between the values calculated with the appropriate [m,6,8] potential and the corresponding experimental values together with the percentage deviations between the values calculated with the extended law of corresponding states and the corresponding experimental values are listed in Table 5A.9 for low temperatures and in Table 5A.10 for high temperatures. As can be seen from these tables, the values predicted by the present method show slightly better agreement, for all the gas pairs except He - Ar and He - Xe at high temperatures, with the experimental results than the ones predicted by the corresponding states theory.

Table 5A.9: Percentage Deviations $[(D_{12}^{\text{calc}} - D_{12}^{\text{exp}}) / D_{12}^{\text{exp}}] \times 100$ - van Heijningen et al.^{4 a}

T K	He-Ne		He-Ar		He-Kr		He-Xe		Ne-Ar		Ne-Kr		Ne-Xe		Ar-Kr		Ar-Xe	
	A	B	A	B	A	B	A	B	A	B	A	B	A	B	A	B	A	B
65.4	1.0	-2.2	-	-	-	-	-	-	-	-	-	-	-	-	-	-	-	-
77.4	0.0	-1.3	-	-	-	-	-	-	-	-	-	-	-	-	-	-	-	-
90.2	0.5	-0.9	1.1	-9.1	-	-	-	-	-1.0	-3.5	-	-	-	-	-	-	-	-
111.7	-	-	-	-	1.8	-0.4	-	-	-	-	-2.9	-3.6	-	-	-	-	-	-
169.3	1.4	1.8	0.4	-3.3	1.2	0.0	0.3	1.8	-0.6	1.6	0.6	-3.3	0.5	-1.2	0.8	-1.3	1.3	1.3
231.1	-	-	-	-	-	-	2.5	3.2	-	-	-	-	0.9	0.2	0.6	-1.2	1.0	1.1
295.0	2.6	1.9	0.6	-0.5	0.3	0.1	1.0	1.0	0.1	-0.1	1.0	-0.8	0.4	0.2	0.7	-0.8	-0.1	-0.1
400.0	-	-	0.2	-0.2	1.7	1.6	1.2	0.4	0.4	0.6	-0.2	-0.8	0.7	1.3	0.8	-0.1	0.1	-0.1

a Column A gives percentage differences between values calculated with the appropriate [m,6,8] potential and the corresponding experimental values. Column B gives percentage differences between values calculated with the extended law of corresponding states and the corresponding experimental values.

Table 5A.10: Percentage Deviations $[(D_{12}^{\text{calc}} - D_{12}^{\text{exp}})/D_{12}^{\text{exp}}] \times 100$ - Hogervorst^{6 a}

T K	He-Ne		He-Ar		He-Kr		He-Xe		Ne-Ar		Ne-Kr		Ne-Xe		Ar-Kr		Ar-Xe	
	A	B	A	B	A	B	A	B	A	B	A	B	A	B	A	B	A	B
300	-0.6	-1.2	0.5	-1.1	0.6	+0.3	1.1	1.3	-0.2	-0.2	0.3	-1.2	1.0	0.9	0.0	-1.0	0.0	0.0
400	-0.6	-1.6	0.8	0.0	1.2	+1.1	1.3	0.4	0.4	-0.6	0.2	-0.7	0.9	1.4	1.2	0.1	-0.3	-0.4
500	-0.2	-1.4	1.0	0.0	0.4	0.0	0.8	-0.3	0.3	1.3	0.1	0.2	1.0	2.0	1.7	1.4	0.2	0.0
600	-0.6	-2.0	1.3	0.2	0.8	+0.3	1.2	-0.5	-0.2	0.3	0.1	0.8	0.8	2.4	2.0	1.8	0.3	0.5
700	0.2	-1.4	2.1	0.6	0.8	+0.4	1.8	-0.2	-0.5	0.1	0.2	1.4	0.7	2.4	1.9	2.2	0.9	1.0
800	0.4	-1.5	2.3	0.5	0.0	-0.6	2.2	0.0	0.7	1.3	-0.5	0.7	0.0	2.0	2.1	2.7	0.1	0.7
900	0.3	-1.6	2.6	0.4	0.0	-0.8	3.0	0.6	0.5	1.2	-1.2	0.6	0.0	2.1	1.9	2.7	0.8	1.7
1000	0.6	-1.2	3.0	0.8	0.4	-0.4	3.0	0.8	0.5	1.7	-1.0	0.5	-0.2	2.1	2.1	3.1	0.5	1.6
1100	1.0	-0.8	3.6	1.0	0.7	-0.2	-	-	0.4	0.9	-0.9	0.8	0.0	2.0	2.4	3.6	0.5	1.7
1200	0.7	-0.8	3.6	0.7	-	-	-	-	0.0	0.6	-0.7	1.1	0.0	2.6	2.7	4.6	0.1	1.7
1300	1.6	-0.2	3.8	0.6	-	-	-	-	-	-	-0.2	0.6	-1.0	0.7	0.0	2.3	2.4	4.7
1400	1.2	-0.3	4.0	0.8	-	-	-	-	0.7	1.4	-0.9	0.8	-0.3	2.4	2.0	3.7	0.3	2.1

^a Column A gives percentage differences between values calculated with the appropriate [m,6,8] potential and the corresponding experimental values. Column B gives percentage differences between values calculated with the extended law of corresponding states and the corresponding experimental values.

5A.6 *Calculations of Thermal Diffusion Coefficients*

The concentration dependence of the thermal diffusion factors ($\bar{\alpha}_T$) for the systems He - Ne, He - Ar, Ne - Ar, He - N₂ and He - CO₂ were calculated to the second approximation at 306K by the method of Mason³⁴ described earlier (eq. 2.32). The calculated values of $\bar{\alpha}_T$ were compared with the experimental values of Symons *et al.*³⁵ for each system at three molefractions together with their estimated errors, in each $\bar{\alpha}_T$, assuming an error of ± 0.00003 in each of the two equilibrium molefractions measured at the end of an experiment are given in Table 5A.11.

The estimated experimental percentage errors and the percentage deviations between the experimental and the predicted $\bar{\alpha}_T$ values, $\Delta\%$, are quite similar (Table 5A.11) for the noble gas mixtures (He - Ne, He - Ar and Ne - Ar) while for others (He - N₂ and He - CO₂), these values are quite different.

As can be seen from equation 2.32, $\bar{\alpha}_T$ depends on both the like as well as the unlike interactions of the molecules. A method to calculate [m,6,8] potential parameters for unlike interactions, by combining the accurate binary diffusion and the cross term virial coefficients, was described earlier in this chapter. A similar method was used to obtain [m,6,8] potential parameters for like interactions by combining the most accurate viscosity data and second virial coefficients. For helium both exp-6^{36,37} and Beck's^{38,39} potentials were tested and it was seen that the former always gave slightly better agreement with the experimental results.

Table 5A.11

Comparison of Experimental³⁵ and Predicted Thermal
Diffusion Factors at 306 K

	He-Ne	He-Ar	Ne-Ar	He-N ₂	He-CO ₂
			(x ₂ =0.9)		
$\bar{\alpha}_T$ (exp)	0.27 ₁	0.28 ₅	0.15 ₀	0.25 ₀	0.30 ₀
$\bar{\alpha}_T$ (calc)	0.25 ₉	0.27 ₁	0.14 ₇	0.27 ₇	0.29 ₄
$\Delta\%$	-4.4	-4.9	-2.6	+10.8	+2.0
Est. % Error	4.5	2.3	4.3	2.2	1.5
			(x ₂ =0.5)		
$\bar{\alpha}_T$ (exp)	0.31 ₈	0.38 ₀	0.17 ₈	0.35 ₄	0.41 ₉
$\bar{\alpha}_T$ (calc)	0.31 ₃	0.37 ₂	0.17 ₈	0.38 ₂	0.42 ₂
$\Delta\%$	-1.6	-2.1	0.0	+7.9	+0.7
Est. % Error	1.3	0.6	1.3	0.6	0.4
			(x ₂ =0.1)		
$\bar{\alpha}_T$ (exp)	0.38 ₆	0.57 ₈	0.21 ₆	0.60 ₉	0.68 ₄
$\bar{\alpha}_T$ (calc)	0.40 ₀	0.59 ₁	0.22 ₂	0.61 ₅	0.74 ₇
$\Delta\%$	+3.6	+2.2	+2.7	+1.0	+9.2
Est. % Error	3.2	1.1	3.0	0.9	0.6

5A.7 *Calculations of the Potential Parameters for Like Interactions*

To obtain the potential parameters for pure gases, a small correction was applied to the smooth experimental viscosity data reported by Kestin and co-workers^{23,28,29,40,41} to yield the theoretical first approximation. The Chapman-Enskog equation 2.16 for first approximation can be written as

$$[\eta]_1 = \frac{5}{16\sqrt{\pi}} [M k]^{1/2} \frac{1}{\sigma^2} \cdot \frac{T^{1/2}}{\Omega^{(2,2)*}(T^*)} , \quad \dots \quad 5A.6$$

$$Y_i = \theta \cdot X_i ,$$

$$\theta = \frac{5}{16\sqrt{\pi}} [M k]^{1/2} \frac{1}{\sigma^2} .$$

The force constants calculated, with the above equation 5A.6 and the method described in Section 5A.3, for like interactions between Ne - Ne, Ar - Ar, Kr - Kr, Xe - Xe, N₂ - N₂, O₂ - O₂, CO₂ - CO₂ and CH₄ - CH₄, are listed in Table 5A.12.

The second virial coefficients calculated using the potential parameters were compared with their corresponding experimental values reported by Brewer^{15,16} and Dymond and Smith¹⁹ and are presented in Tables 5A.13 and 5A.14 respectively. At low temperatures, the differences $[B_{11}^{calc} - B_{11}^{exp}]$ are quite large for diatomic and polyatomic gases which indicate that the $[m,6,8]$ intermolecular potential function becomes less effective with the increase of the

Table 5A.12: Tests of $[m,6,8]$ Potentials for Pure Gases^{a, b}

	Ne	Ar	Kr	Xe	N ₂	O ₂	CO ₂	CH ₄
Potential	(9,6,8,γ=1)	(11,6,8,γ=3)	(11,6,8,γ=2.5)	(11,6,8,γ=3)	(12,6,8,γ=1.5)	(11,6,8,γ=1.5)	(11,6,8,γ=0)	(12,6,8,γ=1)
(ϵ_{11}/k)(K)	27.0±2.0	152.5±3.0	206.0±3.0	295.0±3.0	116.0±3.0	131.0±3.0	235.0±3.0	172.0±3.0
σ_{11} (Å)	2.908±0.005	3.302±0.007	3.533±0.007	3.831±0.007	3.561±0.007	3.354±0.007	3.781±0.007	3.669±0.007
Av. Error, B ₁₁ (cm ³) ^{15,16}	+0.45 (123-323)	±2.12 (123-323)	±0.24 (123-323)	+3.70 (173-323)	±3.90 (123-323)	±0.35 (173-323)	±9.21 (223-298)	±5.22 (123-298)
Av. Error, B ₁₁ (cm ³) ¹⁹	+1.15 (60-600)	±0.91 (81-600)	±2.85 (110-600)	±0.52 (275-650)	±6.39 (75-700)	±5.74 (90-400)	±6.24 (273-423)	±10.46 (110-600)
Av. % Error, [D] ₁ ⁴²	±1.33 (77-353)	±0.69 (77-353)	-	-	-6.43 (77-353)	-6.75 (77-353)	-3.45 (77-353)	-7.93 (77-353)
Av. % Error, [D] ₁ ⁴³	+2.72 (77-1400)	-	-	-	-	-	-	-
Av. % Error, [D] ₁ ⁴⁴	-	-	+1.47 (195-1036)	-	-	-	-	-
Av. % Error, [D] ₁ ⁴⁵	-	-	-4.96 (232-470)	-	-	-	-	-
Av. % Error, [D] ₁ ⁴⁶	-	-	+2.78 (300)	-	-	-	-	-
Av. % Error, [D] ₁ ⁴⁷	-	-	-	+1.99 (194-378)	-	-	-	-

^a After consulting the original data the following average experimental errors were adopted: B₁₁ (Brewer), 1.5-2.0 cm²; B₁₁ (Dymond and Smith), 1.0-3.0 cm³ for noble gases and 2.0-5.0 for diatomic and polyatomic gases: [D]₁ (Winn), 1.0-3.0%; [D]₁ (Weissman et al.), 2.0%; [D]₁ (Trappeniers) 0.1%; [D]₁ (Amdur et al.), 1.0-2.0%.

^b The temperature range in degrees kelvin used in each study is given in brackets beneath each entry.

Table 5A.13: Differences $(B_{11}^{\text{calc}} - B_{11}^{\text{exp}})^a$ for the Data of Brewer^{15,16}

T(K)	Ne	Ar	Kr	Xe	N ₂	O ₂	CO ₂	CH ₄
323.15	+ 0.04	+ 0.34	+ 0.03	+ 1.77	- 0.31	- 0.64	-	-
298.15	+ 0.38	+ 0.34	+ 0.52	+ 2.59	0.00	0.00	- 1.68	+ 0.10
273.15	+ 0.42	+ 0.43	- 0.06	+ 2.06	+ 0.53	- 0.35	- 3.52	+ 0.43
248.15	+ 0.51	- 0.34	-	-	+ 1.08	-	+ 5.00	-
223.15	+ 0.61	+ 0.31	- 0.28	+ 3.85	+ 1.91	+ 0.25	+26.65	+ 1.64
198.15	+ 0.61	+ 0.30	- 0.03	4.49	+ 2.45	-	-	+ 2.61
173.15	+ 0.41	- 0.20	+ 0.15	7.47	+ 2.54	- 0.47	-	+ 5.47
148.15	+ 0.17	- 0.42	- 0.28	-	+ 3.62	-	-	+ 8.95
123.15	+ 0.92	-16.36	+ 0.56	-	+22.69	-	-	+17.35

^a The numerical values given in this table are in $\text{cm}^3 \cdot \text{mol}^{-1}$.

Table 5A.14: Differences ($B_{11}^{\text{calc}} - B_{11}^{\text{exp}} = \delta$)^a for the Compilation of Dymond and Smith¹⁹

Ne		Ar		Kr		Xe		N ₂		O ₂		CO ₂		CH ₄	
T(K)	δ	T(K)	δ	T(K)	δ	T(K)	δ	T(K)	δ	T(K)	δ	T(K)	δ	T(K)	δ
600	+ 0.3	600	- 0.5	600	+ 0.6	650	- 0.2	700	- 0.5	400	- 0.2	423.30	-11.17	600	- 1.4
400	+ 0.8	500	- 0.2	500	+ 0.1	550	- 1.4	600	- 0.9	350	+ 0.5	418.21	-11.07	500	- 0.4
300	+ 0.6	400	+ 0.2	400	- 1.2	450	+ 0.6	500	0.0	300	- 0.1	412.99	-11.20	400	- 0.7
200	+ 1.0	300	+ 0.6	300	- 0.7	400	+ 0.2	400	- 0.3	250	- 1.9	398.17	- 9.94	350	0.0
150	+ 1.5	250	+ 0.5	250	- 0.1	350	0.0	300	- 0.3	200	- 2.8	372.93	- 8.64	300	- 0.1
125	+ 1.7	200	- 0.3	200	- 0.3	325	- 0.3	250	+ 0.2	175	- 1.2	348.42	- 7.23	275	+ 0.9
100	+ 2.0	150	- 2.0	170	+ 0.3	300	+ 0.7	200	+ 1.0	150	+ 2.7	322.87	- 4.88	250	+ 2.2
80	+ 1.6	125	+ 0.6	150	+ 0.7	275	- 0.6	150	+ 3.5	125	+ 4.5	313.26	- 3.78	225	+ 3.4
70	+ 1.3	110	- 0.4	140	+ 1.7			125	+ 5.6	110	+ 8.0	305.24	- 2.50	200	+ 5.0
60	+ 0.7	100	- 1.4	130	+ 2.7			110	+15.3	100	+12.5	304.20	- 2.33	180	+ 8.4
		95	- 2.3	120	+ 4.9			100	+10.6	90	+28.7	303.06	- 1.98	160	+15.0
		90	- 0.7	115	+ 7.9			90	+14.4			298.21	- 1.72	150	+17.9
		85	+ 0.3	110	+15.9			80	+16.6			273.16	+ 4.70	140	+21.1
		81	+ 2.7					75	+20.2					130	+24.4
														120	+25.7
														110	+40.7

^a The numerical values given in this table are in cm³.mol⁻¹ .

internal degrees of freedom of the molecules and a more flexible potential function is required to explain these deviations.

5A.8 *Calculations of Self Diffusion Coefficients*

The self diffusion coefficients of eight different gases at various temperatures were calculated using the Chapman-Enskog equation 2.8 with the most likely values of the parameters (Table 5A.12). A comparison (Tables 5A.15 and 5A.16) was made between the experimental results obtained by various workers⁴²⁻⁴⁷ and the values calculated from [m,6,8] potentials which show a reasonably good agreement for the noble gases (Ne, Ar, Kr, Xe) whereas for other gases (N₂, O₂, CO₂, CH₄), as expected, the agreement was not as good.

As can be seen from the Tables 5A.2, 5A.3 and 5A.12, the potentials varied from [9,6,8, $\gamma = 0$] to [12,6,8, $\gamma = 2.5$] which indicates that if the [m,6,8] group is assumed to characterise gases or binary gas systems, then more than one member of the group is necessary. Thus it appears that these systems are not conformal in terms of any particular member of the [m,6,8] group. A similar conclusion was recently given by Maitland and Wakeham⁴⁸ who obtained potentials by direct inversion of gaseous transport coefficients. In order to illustrate this fact the potential parameters for the systems He - Ne, He - Ar, He - Kr and He - Xe were calculated using [11,6,8, $\gamma = 3$] potential and then the second virial coefficients were predicted for comparison with the data of Brewer^{15,16}. The results were listed in Table 5A.17 which show that the deviations between the calculated

Table 5A.15

Percentage Deviations $[(D)_1^{\text{calc}} - (D)_1^{\text{exp}} / (D)_1^{\text{exp}}] \times 100$
 for the Data of Winn⁴²

T(K)	Ne	Ar	N ₂	O ₂	CO ₂	CH ₄
353.15	- 1.40	- 0.81	- 4.88	- 6.64	0.00	- 4.40
298.15	+ 0.78	-	- 4.25	-10.78	- 2.65	- 7.08
295.15	-	0.00	-	-	-	-
273.15	- 0.88	- 0.64	- 6.49	- 5.88	- 4.93	- 8.25
194.65	- 1.17	- 1.20	-10.57	- 9.81	- 6.20	- 0.40
90.15	-	0.00	- 5.95	-	-	-19.54
77.65	+ 2.44	+ 1.49	-	- 0.65	-	-

Table 5A.16: Percentage Deviations $[(D)_1^{\text{calc}} - (D)_1^{\text{exp}} / (D)_1^{\text{exp}}] \times 100$ for the Data
Published in the Literature⁴³⁻⁴⁷

Ne ⁴³		Kr ⁴⁴		Kr ⁴⁵		Kr ⁴⁶		Xe ⁴⁷	
T(K)	% Dev.	T(K)	% Dev.	T(K)	% Dev.	T(K)	% Dev.	T(K)	% Dev.
1400.0	+ 4.90	1036.1	- 2.46	470.0	- 9.84	300.0	+ 2.78	378.0	+ 1.22
1200.0	+ 5.10	717.5	0.00	414.0	- 6.18			329.9	+ 2.63
738.0	+ 3.50	479.7	+ 2.14	343.0	- 5.19			300.5	+ 1.56
597.3	+ 4.00	366.5	+ 0.69	295.0	- 3.96			293.0	+ 2.58
573.0	+ 1.36	305.2	- 0.96	296.0	- 2.02			273.2	+ 1.25
446.0	+ 1.38	195.7	+ 2.58	288.0	- 3.16			194.7	- 2.72
300.2	+ 1.49			273.0	- 1.19				
77.4	0.00			243.0	- 6.94				
				232.0	- 6.15				

and the experimental values are much higher than the experimental errors.

Table 5A.17

Differences ($B_{12}^{\text{calc}} - B_{12}^{\text{exp}}$) Obtained by Assuming an
(11,6,8, $\gamma = 3$) Potential Derived from Our Diffusion
Data Alone^a

T (K)	He-Ne	He-Ar	He-Kr	He-Xe
323.2	- 3.1	- 4.8	- 0.6	- 7.7
298.2	- 3.1	- 5.2	-	-
273.2	- 3.2	- 5.0	- 0.8	- 8.0
248.2	- 3.5	- 5.8	-	-
223.2	- 3.8	- 6.3	- 1.5	-10.0
198.2	- 4.2	- 7.4	- 2.0	-12.9
173.2	- 4.8	- 8.4	- 2.4	-13.8
148.2	- 5.7	-10.1	- 4.6	-
123.2	- 6.3	-13.2	-	-

^a The values listed in each column have unit of $\text{cm}^3 \cdot \text{mol}^{-1}$.

The abovementioned fact can also be seen graphically in Figure 5A.2 by plotting a deviation graph similar to the one reported by Maitland and Wakeham⁴⁸ which shows a significant deviation from conformality at low separations.

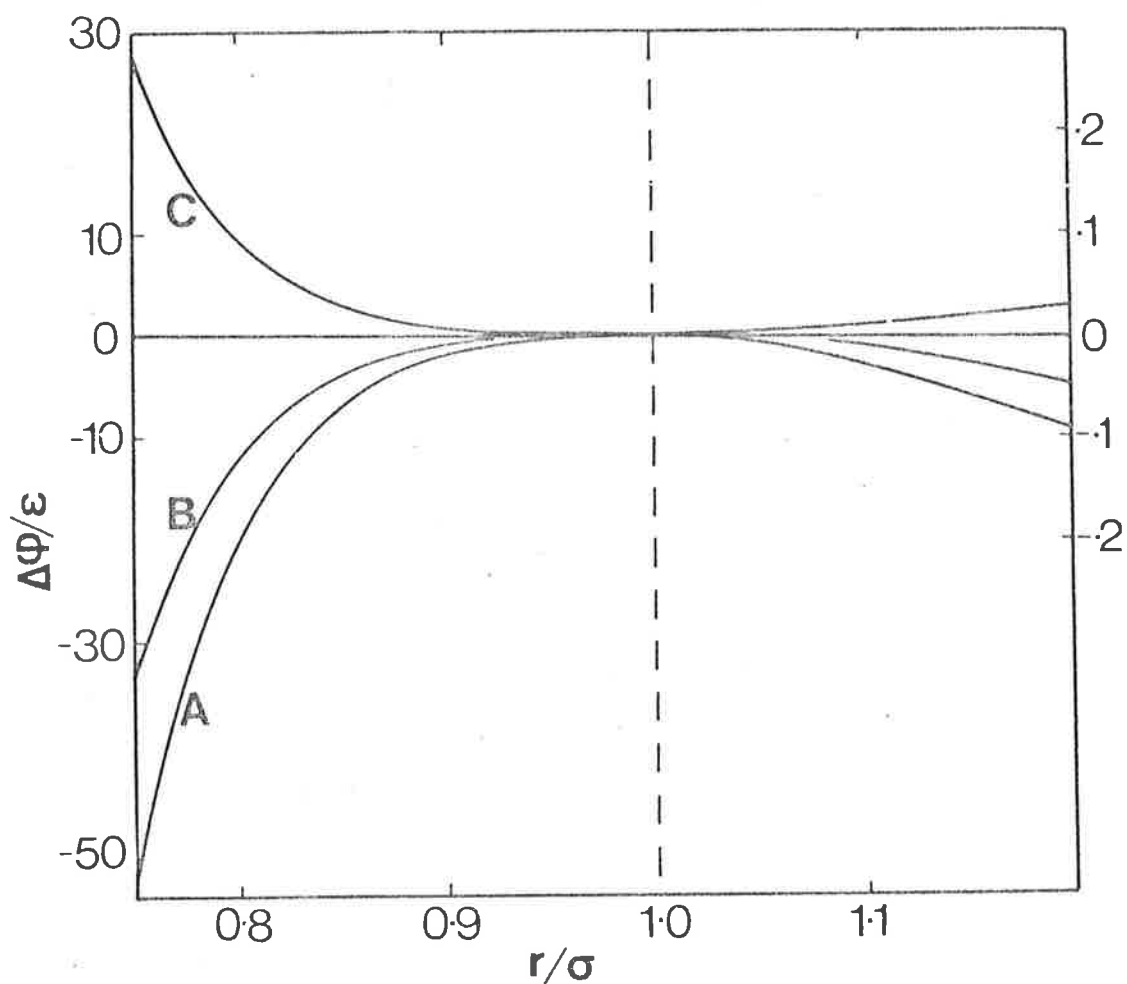


Figure 5A.2: Deviations, $(\Delta\phi/\epsilon)$, of Several Potentials From the $(11,6,8,\gamma = 3)$ as a Function of the Reduced Separation (r/σ) : A, for the $(9,6,8,\gamma = 2)$; B, for the $(10,6,8,\gamma = 2)$; C, for the $(12,6,8,\gamma = 2.5)$. The left hand ordinate applies to $(r/\sigma) < 1$, the right hand ordinate to $(r/\sigma) > 1$. The order A, B, C applies on both sides of the graph.

REFERENCES

1. Hirschfelder, J.O., Curtiss, C.F. and Bird, R.B.,
Molecular Theory of Gases and Liquids (John Wiley and Sons, Inc., New York, 1954).
2. Hirschfelder, J.O., Bird, R.B. and Spotz, E.L.,
J. Chem. Phys. 16 (1948) 968. *Chem. Revs.*
44 (1949) 205.
3. Van Heijningen, R.J.J., Feberwee, A., Van Oosten, A.
and Beenakker, J.J.M., *Physica* 32 (1966) 1649.
4. Van Heijningen, R.J.J., Harpe, J.P. and Beenakker,
J.J.M., *Physica* 38 (1968) 1.
5. Hogervorst, W. and Freudenthal, J., *Physica* 37
(1967) 97.
6. Hogervorst, W., *Physica* 51 (1971) 59.
7. Hogervorst, W., *Physica* 51 (1971) 77.
8. Hogervorst, W., *Physica* 51 (1971) 90.
9. Kestin, J., Ro, S.T. and Wakeham, W.A., *Physica*
58 (1972) 165.
10. Kestin, J., Khalifa, H.E. and Wakeham, W.A.,
Physica 90A (1978) 215.
11. Carson, P.J., *Ph. D. Thesis*, University of Adelaide.
(1974).

12. Klein, M. and Hanley, H.J.M., *J. Chem. Phys.* 53
(1970) 4722.
13. Hanley, H.J.M. and Klein, M., *J. Phys. Chem.* 76
(1972) 1743.
14. Klein, M., Hanley, H.J.M., Smith, F.J. and Holland, P.,
*Tables of Collision Integrals and Second Virial
Coefficients for the [m,6,8] Intermolecular
Potential Function*, U.S. National Bureau of
Standards Circular, NSRDS-NBS47 (1974).
15. Brewer, J., *Determination of Mixed Virial Coefficients*,
Report No. MRL-2915-C, Air Force Office of Scient-
ific Research, No. 67-2795 (1967).
16. Brewer, J. and Vaughn, G.W., *J. Chem. Phys.* 50
(1969) 2960.
17. Douslin, D.R., Harrison, R.H. and Moore, R.T.,
J. Phys. Chem. 71 (1967) 3477.
18. Knobler, C.M., Beenakker, J.J.M. and Knaap, H.F.P.,
Physica 25 (1959) 909.
19. Dymond, J.H. and Smith, E.B., *The Virial Coefficients
of Gases* (Clarendon Press, Oxford, 1969).
20. Kestin, J., Ro, S.T. and Wakeham, W.A., *Physica*
58 (1972) 165.
21. Kalelkar, A.S. and Kestin, J., *J. Chem. Phys.* 52
(1970) 4248.

22. Kestin, J., Wakeham, W. and Watanabe, K., *J. Chem. Phys.* 53 (1970) 3773.
23. Kestin, J., Ro, S.T. and Wakeham, W.A., *J. Chem. Phys.* 56 (1972) 5837.
24. Kestin, J., Ro, S.T. and Wakeham, W.A., *J. Chem. Phys.* 56 (1972) 4086.
25. Kestin, J., Ro, S.T. and Wakeham, W.A., *J. Chem. Phys.* 56 (1972) 4036.
26. Hellemans, J.M., Kestin, J. and Ro, S.T., *J. Chem. Phys.* 57 (1972) 4038.
27. Kestin, J., Khalifa, H.E. and Wakeham, W.A., *J. Chem. Phys.* 67 (1977) 4254.
28. Kestin, J., Khalifa, H.E., Ro, S.T. and Wakeham, W.A., *Physica* 88A (1977) 242.
29. Hellemans, J.M., Kestin, J. and Ro, S.T., *Physica* 65 (1973) 362.
30. Maitland, G.C. and Smith, E.B., *J. Chem. Soc. Faraday Trans. I* 70 (1974) 1191.
31. Gough, D.W., Matthews, G.P. and Smith, E.B., *J. Chem. Soc. Faraday Trans. I* 72 (1976) 645.
32. Saxena, S.C. and Joshi, R.K., *Physica* 29 (1963) 870.
33. Saxena, S.C. and Joshi, R.K., *Indian J. Phys.* 38 (1963) 479.

34. Mason, E.A., *J. Chem. Phys.* 27 (1957) 75.
35. Symons, J.M., Martin, M.L. and Dunlop, P.J.,
J.C.S. Faraday I 75 (1979) 621.
36. Mason, E.A. and Rice, W.E., *J. Chem. Phys.* 22
(1954) 522.
37. Taylor, W.L., *J. Chem. Phys.* 57 (1972) 832.
38. Taylor, W.L. and Keller, J.M., *J. Chem. Phys.*
54 (1971) 648.
39. Barker, J.A., in: *Rare Gas Solids, Vol. I*,
Klein, M.L. and Venables, J.A., eds., Academic
Press, New York, 1976.
40. Kestin, J., Ro, S.T. and Wakeham, W.A., *J. Chem.*
Phys. 56 (1972) 4119.
41. Kestin, J., Ro, S.T. and Wakeham, W.A., *J. Chem.*
Phys. 56 (1972) 4114.
42. Winn, B.E., *Phys. Rev.* 80 (1950) 1024.
43. ^{ei}Wiessman, S., *J. Chem. Phys.* 16 (1973) 1425.
44. ^{ei}Wiessman, S. and Dubro, G.A., *The Physics of*
Fluids 13 (1970) 2689.
45. Wendt, R.P., Mundy, J.N., ^{ei}Wiessman, S. and Mason, E.A.,
The Physics of Fluids 6 (1963) 572.
46. Trappeniers, N.T. and Michels, J.P.J., *Chemical*
Physics Letters 18 (1973) 1.

47. Amdur, I. and Schatzki, T.F., *J. Chem. Phys.* 27
(1957) 1049.
48. Maitland, G.C. and Wakeham, W.A., *Molecular
Physics* 35 (1978) 1443.
49. Grew, K.E. and Wakeham, W.A., *J. Phys.* B4
(1971) 1548.

CHAPTER 5B

THE TEMPERATURE DEPENDENCE OF DIFFUSION IN
ALMOST LORENTZIAN GAS MIXTURES

5B.1 *Introduction*

The thermal diffusion factor, α_T , of gas mixtures depends upon the interactions between the like and the unlike molecules and can be calculated from temperature studies of transport processes as explained earlier (see section 5A.6). Holleran and Hulburt¹ gave a relation between the reduced collision integral², C^* , and the temperature derivatives of the diffusion coefficients which in turn relates the thermal diffusion process with that of diffusion. In 1968, Monchick and co-workers³ derived expressions relating the temperature dependence of diffusion to the thermal diffusion factor for mixtures of molecules having internal degrees of freedom. These equations were simplified by Vugts *et al.*⁴ and can be written as:

$$\alpha_T = (6C_{12}^* - 5) \frac{S_2 x_1 - S_1 x_2}{x_1^2 Q_1 + x_2^2 Q_2 + x_1 x_2 Q_{12}} + \frac{1}{5} (6\tilde{C}_{21} - 5) \quad \dots \quad 5B.1$$

$$2 \left[2 - \left(\frac{\partial \ln [D]_2}{\partial \ln T} \right)_p \right] = (6C_{12}^* - 5) + \frac{2}{5} (6\tilde{C}_{21} - 5), \quad \dots \quad 5B.2$$

where the quantity $(6C_{12}^* - 5)$ is well known as a leading factor in the above equations and the term $(6\tilde{C}_{12} - 5)$ is equal to zero if one of the components of a binary mixture

under study has no rotational degree of freedom (e.g. a rare gas). The expressions to calculate Q_i 's are given in Appendix 1 whereas the quantities S_i 's are defined by an expression (2.31).

Van de Ree^{5,6} also presented a simple method (Van de Ree theory based on the thermodynamics of irreversible processes) to calculate α_T from the temperature derivatives of diffusion coefficients and derived similar equations given by Monchick *et al.*³. Both these theoretical aspects (Monchick *et al.*³ and Van de Ree^{5,6}) are based on the Wang Chang, Uhlenbeck and De Boer⁷ approach in which spin polarisation is neglected.

Mason and Smith⁸ gave a new approximation scheme to calculate the thermal diffusion factor, α_2 , for almost Lorentzian gas mixture* which converges faster than the method suggested by Chapman-Cowling⁹. The final expression given by Mason and Smith⁸ can be written as:

$$\alpha_2 = \alpha_L + \sum_{j=2}^{\infty} \mu_j M^{j/2} \quad \dots \quad 5B.3$$

where α_2 is the thermal diffusion factor as $x_1 \rightarrow 0$, α_L is the exact Lorentzian thermal diffusion factor, M is the mass ratio (M_1/M_2) and μ_j 's are the higher-order coefficients of the expansion in powers of $M^{1/2}$. The value of first coefficient (μ_1) was found to be zero whereas the expressions to calculate the next few coefficients ($\mu_2 - \mu_5$), both for a Chapman-Enskog and a Kihara approximation, are given elsewhere⁸.

* A Lorentzian gas mixture is a mixture where the lighter component 1 is in trace concentration ($x_1 \ll x_2$) and the molecular weight of the bulk component 2 is very large as compared to the molecular weight of component 1 ($M_2 \gg M_1$).

The exact Lorentzian thermal diffusion factor, α_L , can be given¹⁰ (in terms of definite integrals) as

$$\alpha_L = 5/2 - (I_2/I_1) \quad \dots 5B.4a$$

where

$$I_n = \int_0^{\infty} e^{-\gamma^2} \gamma^{2n+1} [S_{12}^{(1)}]^{-1} d\gamma \quad \dots 5B.4b$$

in which $S_{12}^{(1)}$ is the cross section for diffusion and $\gamma^2 = \frac{1}{2}\mu v^2/kT$ is the dimensionless kinetic energy of a pair of colliding molecules.

Mason¹⁰ also derived an expression to calculate the exact Lorentzian diffusion coefficient, D_L , which can be expressed as

$$D_L = \frac{4(2\pi k^3 T^3/\mu)^{1/2}}{3\pi^2 \rho \sigma^2} \int_0^{\infty} e^{-\gamma^2} [S_{12}]^{-1} \gamma^3 d\gamma \quad \dots 5B.5$$

In the same publication¹⁰, Mason gave a relation between the quantities α_L and the temperature derivative of D_L at constant pressure which can be written as:

$$\alpha_L = \left[2 - \left(\frac{\partial \ln D_L}{\partial \ln T} \right)_p \right] \quad \dots 5B.6$$

On putting the above value of α_L in equation 5B.3, the expression for α_2 becomes

$$\alpha_2 = \left[2 - \left(\frac{\partial \ln D_L}{\partial \ln T} \right)_p \right] + \sum_{j=2}^{\infty} \mu_j M^{j/2} \quad \dots 5B.7$$

If the light component of a gas mixture has some internal degree of freedom (e.g. molecular gas), the term $[\frac{1}{5}(6\tilde{C}_{21} - 5)]$ linked to partial internal heat conductivity has to be added to the above equation.

In this chapter, a study of the temperature dependence of the binary diffusion coefficients for the systems He - Ar, He - Kr, H₂ - Ar and D₂ - Ar have been made. The thermal diffusion factors for the same mixtures have been calculated using the relation 5B.6 and compared with data available in the literature.

5B.2 *Experimental and Results*

The binary diffusion coefficients, D_{12} , were measured in duplicate at one atmosphere pressure every two degrees interval (He - Ar, H₂ - Ar and D₂ - Ar) and every four degrees interval (He - Kr) from 277K to 323K with the Loschmidt cell (cell A₃) described earlier in Chapter 3. The details of the experimental procedure and the method to calculate the diffusion coefficients have also been explained in Chapter 3.

The experimental results and the molefractions, x_2^* , at which a particular system was studied are given in Table 5B.1. The data for each system was then least-squared to a simple empirical relation:

$$[D_{12}] = A + BT + CT^2 \quad \dots \quad 5B.8$$

The value of the constants A, B and C obtained together with their percentage average deviations of the experimental points from the smooth curves are listed in Table 5B.2. The present data is accurate to within $\pm 0.1\%$.

* x_2 is the molefraction of heavy component.

Table 5B.1: Experimental Results for the Temperature Dependence of the Diffusion Coefficients in Almost Lorentzian Mixtures

He-Ar		He-Kr		H ₂ -Ar		D ₂ -Ar	
0.9000		0.9750		0.9000		0.9000	
T	($P\bar{D}_{12}$)	T	($P\bar{D}_{12}$)	T	($P\bar{D}_{12}$)	T	($P\bar{D}_{12}$)
(K)	(atm.cm. ² s ⁻¹)	(K)	(atm.cm. ² s ⁻¹)	(K)	(atm.cm. ² s ⁻¹)	(K)	(atm.cm. ² s ⁻¹)
277.00	0.6620	277.00	0.5758	277.00	0.7298	277.00	0.5280
279.09	0.6705	281.00	0.5896	279.00	0.7392	279.00	0.5348
281.00	0.6780	284.90	0.6048	281.00	0.7486	281.00	0.5412
284.90	0.6944	293.05	0.6353	284.90	0.7674	284.90	0.5554
288.85	0.7105	297.04	0.6488	288.85	0.7867	288.85	0.5690
293.05	0.7278	301.16	0.6648	293.05	0.8060	293.05	0.5828
297.04	0.7450	305.16	0.6794	297.04	0.8253	297.04	0.5973
300.00	0.7585	309.13	0.6945	300.00	0.8412	300.00	0.6086
301.15	0.7634	313.37	0.7107	301.15	0.8469	301.15	0.6126
303.15	0.7721	317.33	0.7254	303.15	0.8560	303.15	0.6200
305.15	0.7808	321.34	0.7418	305.15	0.8666	305.15	0.6268
307.13	0.7894	323.45	0.7500	307.13	0.8761	307.13	0.6340
309.13	0.7976			309.13	0.8872	309.13	0.6414
311.13	0.8065			313.26	0.9072	311.13	0.6485
313.26	0.8159			315.16	0.9170	313.26	0.6563
315.16	0.8243			317.16	0.9270	315.16	0.6635
317.16	0.8331			319.12	0.9373	317.16	0.6716
319.12	0.8415			321.12	0.9483	319.12	0.6783
321.12	0.8504			323.14	0.9580	321.12	0.6860
323.14	0.8596					323.14	0.6939

^a x_2 is the molefraction of heavy component.

Table 5B.2

Least-square Coefficients for Eq. 5B.8

System	^a x ₂	A × 10 ²	B × 10 ³	C × 10 ⁶	Av.dev.%
He - Ar	0.9000	-1.6441	1.86041	4.0500	± 0.03
He - Kr	0.9750	-1.8821	1.91386	3.0477	± 0.04
H ₂ - Ar	0.9000	-1.4790	1.63999	5.5183	± 0.04
D ₂ - Ar	0.9000	-6.9321	0.92528	4.4439	± 0.02

^a x₂ is the molefraction of heavy component.

5B.3 Calculations for Exact Lorentzian Thermal Diffusion Factor (α_L)

For a Lorentzian gas mixture with no internal degree of freedom, the thermal diffusion factor can be calculated using equation 5B.6. The experimental data can also be represented by a more practical form as:

$$\ln[D_{12}] = a_1 + a_2 \ln T \quad \dots 5B.9$$

The value of the constants a_1 and a_2 together with their percentage average deviations of the experimental points with respect to the empirical fit are listed in Table 5B.3.

The partial differentiation of the above equation 5B.9 with respect to $\ln T$ gives:

$$\left(\frac{\partial \ln D_{12}}{\partial \ln T} \right)_p = a_2 \quad \dots 5B.10a$$

Table 5B.3

Least-square Coefficients for Eq. 5B.9

System	x_2^a	a_1	a_2	Av.dev.%
He - Ar	0.9000	- 9.9546	1.6967	± 0.04
He - Kr	0.9750	-10.1220	1.7018	± 0.05
H ₂ - Ar	0.9000	-10.2616	1.7686	± 0.05
D ₂ - Ar	0.9000	-10.6105	1.7731	± 0.04

^a x_2 is the molefraction of heavy component.

The Chapman-Enskog theory² for binary diffusion indicates (Table 5B.4) that over a temperature range of 50K and at high molefractions of the heavy component 2, the quantity $(\partial \ln D_{12} / \partial \ln T)_p$ is independent of concentration. Therefore, in the present calculations, the temperature derivatives of the equation 5B.9 are assumed to be equal to the temperature derivatives of the exact Lorentzian diffusion coefficient.

$$\left(\frac{\partial \ln D_{12}}{\partial \ln T} \right)_p = \left(\frac{\partial \ln D_L}{\partial \ln T} \right)_p = a_2 \quad \dots 5B.10b$$

from which α_L can be calculated ($\alpha_L = 2 - a_2$).

The calculated values of α_L (using the above method) for the systems He - Ar and He - Kr at 300K were compared (Table 5B.5) with the experimental values recently obtained by Dunlop *et al.*¹¹ in this laboratory. The agreement between these values is quite good and hence supports the Mason's approximation scheme⁸.

Table 5B.4

Predicted Values of the Ratios $(\partial \ln D_{12} / \partial \ln T)_P$ for the Systems He - Ar and He - Kr using Chapman-Enskog Theory^a

x_2^b	He - Ar		He - Kr	
	$\left(\frac{\partial \ln D_{12}}{\partial \ln T}\right)_P$	$\left[2 - \left(\frac{\partial \ln D_{12}}{\partial \ln T}\right)_P\right]$	$\left(\frac{\partial \ln D_{12}}{\partial \ln T}\right)_P$	$\left[2 - \left(\frac{\partial \ln D_{12}}{\partial \ln T}\right)_P\right]$
0.1000	1.689	0.311	1.675	0.325
0.5000	1.691	0.309	1.676	0.324
0.9000	1.692	0.308	1.677	0.323
1.0000	1.692	0.308	1.677	0.323

^a The binary diffusion coefficients were generated after every five degrees from 275 to 325K using Kihara's second approximation and were least-square by an equation 5B.9.

^b x_2 is the molefraction of heavy component.

Table 5B.5

Comparison Between the Calculated and the literature^a Values of α_L at 300K

Systems	α_L^{calc}	$\alpha_L^{\text{(lit)}}$
He - Ar	0.303 ± 0.020	0.276 ± 0.010
He - Kr	0.298 ± 0.020	0.290 ± 0.010
H ₂ - Ar	0.231 ± 0.015	0.262 ± 0.005
D ₂ - Ar	0.227 ± 0.015	0.252 ± 0.005

^a Literature values for the systems He - Ar and He - Kr have been taken from Ref. (11) whereas those for H₂ - Ar and D₂ - Ar together with estimated errors were obtained by least-squaring the calculated values given by Wahby et al.¹³

For the other two systems $H_2 - Ar$ and $D_2 - Ar$ there is no reliable data available in the literature except that of Van de Ree *et al.*¹² at 420K. Wahby, Boerboom and Los¹³ calculated the exact Lorentzian thermal diffusion factor from the temperature dependence of diffusion for few binary gas mixtures including $H_2 - Ar$ and $D_2 - Ar$ at 420K and showed an excellent agreement with the experimental data of Van de Ree *et al.*¹². Wahby *et al.*¹³ then predicted the temperature dependence of α_L from 237K to 420K. For the sake of comparison at 300K, these calculated values¹³ of α_L were interpolated and, as expected, the agreement for these two systems is not so good (Table 5B.5).

REFERENCES

1. Holleran, E.M. and Hulburt, H.M., *J. Chem. Phys.* 19 (1951) 232.
2. Hirschfelder, J.O., Curtiss, C.F. and Bird, R.B., *Molecular Theory of Gases and Liquids*, Wiley (new York, 1954) Chapter 7 and 8.
3. Monchick, L., Sandler, S.I. and Mason, E.A., *J. Chem. Phys.* 49 (1968) 1178.
4. Vugts, H.F., Boerboom, A.J.H. and Los, J., *Physica* 51 (1971) 311.
5. Van de Ree, J., *Physica* 37 (1967) 584.
6. Van de Ree, J. and Scholtes, T., *J. Chem. Phys.* 57 (1972) 122.
7. Wang Chang, C.S., Uhlenbeck, G.E. and De Boer, J., *Studies in Statistical Mechanics II*, North-Holland Publ. Comp. (Amsterdam, 1964).
8. Mason, E.A. and Smith, F.J., *J. Chem. Phys.* 44 (1966) 3100.
9. Chapman, S. and Cowling, T.G., *The Mathematical Theory of Non-Uniform Gases* (Cambridge, 1939).
10. Mason, E.A., *J. Chem. Phys.* 27 (1957) 782.
11. Dunlop et al. (to be published).

12. Van de Ree, J. and Los, J., *Physica* 75 (1974) 548.
13. Wahby, A.S.M., Boerboom, A.J.H. and Los, J., *Physica* 75 (1974) 560.

CHAPTER 6THE PRESSURE DEPENDENCE OF DIFFUSION

6.1 Introduction

Mutual diffusion coefficients at 300K were measured by Staker and Dunlop¹ and Bell *et al.*² in a Loschmidt cell described earlier¹, over a small pressure range of 1 - 9 atmospheres for sixteen systems containing helium. For the present work, the same cell was modified to extend its range of pressure up to approximately 25 atmospheres by placing O-rings between the mating surfaces and concentric with the cell axis. The details of the cell, experimental procedure and the method used to derive the binary diffusion coefficients from the raw experimental data have been described in Chapter 3.

All experiments were performed, in duplicate, by allowing pure helium from the top compartment to diffuse into a mixture containing 70% helium resulting in a final molefraction, x_2 , of the *heavy* component equal to 0.15. The use of small initial concentration differences in the cell ensured that (a) negligible pressure changes occurred during all the experiments, so that the diffusion coefficients measured corresponded to the volume of the frame of reference^{3,4}. Moreover, at high pressures (greater than three atmospheres), the pressure of the bottom compartments was made equal to that of the top compartments by letting the gas in or out from the bottom half of the cell depending upon the sign of the pressure of mixing for the system under study.

(b) the thermistors used in the bridge circuit only yield consistent results⁵ in gas mixtures which have thermal conductivities reasonably close to helium, the gas in which they were tested by the manufacturer.

Small corrections (less than 0.1%) were sometimes necessary to adjust the results to the chosen molefraction.

All diffusion coefficients reported in this chapter are believed to be accurate to 0.1%. Even though the modified cell operated perfectly up to 25 atmospheres, it was not always possible to maintain a precision up to this point. Presumably the heat of mixing, the Dufour effect and convection from the thermistor surface all play a part in this loss of precision.

6.2 *Experimental and Results*

The pressure dependences of the binary diffusion coefficients, D_{12} , for the systems He - Ar, He - N₂, He - O₂ and He - CO₂ were measured, at constant composition ($x_2 = 0.15$) and two temperatures (300.00 and 323.15K) in a modified Loschmidt cell (A₃).

The experimental results are tabulated in Table 6.1. Using a least-squares procedure, this data was fitted to the expression:

$$PD_{12} = (PD_{12})_0 (1 + \theta P) \quad \dots \quad 6.1$$

where D_{12} is the binary diffusion coefficient, P is the pressure in atmospheres, $(PD_{12})_0$ is the limit of the quantity (PD_{12}) at $P = 0$ and θ is the slope describing the pressure dependence. The values of the intercepts $(PD_{12})_0$ and the

TABLE 6.1: Pressure Dependence Results at Two Temperatures for the Systems ^{a,b}

T =	He/Ar		He/N ₂		He/O ₂		He/CO ₂	
	300.00K	323.15K	300.00K	323.15K	300.00K	323.15K	300.00K	323.15K
P (atm)	(PD ₁₂) × 10 ⁴ (atm. m. ² s ⁻¹)							
1	0.7423	0.8399	0.7126	0.8069	0.7516	0.8511	0.6081	0.6886
2	-	-	0.7129	-	-	-	-	-
3	0.7416	0.8399	0.7130	0.8060	0.7516	0.8501	0.6066	0.6865
4	-	-	0.7128	-	-	-	-	-
5	0.7413	0.8401	0.7128	0.8060	0.7511	0.8497	0.6050	0.6853
6	-	-	0.7124	-	-	-	-	-
7	0.7409	0.8397	0.7125	0.8059	0.7513	0.8498	0.6023	0.6837
8	-	-	0.7123	-	-	-	-	-
9	0.7411	0.8400	0.7123	0.8067	0.7505	0.8500	0.6013	0.6827
10	-	-	0.7120	-	0.7505	-	0.6003	-
11	0.7410	0.8402	0.7122	0.8068	0.7506	0.8503	0.5982	0.6811
12	-	-	0.7122	-	0.7505	-	0.5975	-
13	0.7410	0.8410	0.7121	0.8070	0.7507	0.8502	0.5975	-
14	0.7408	-	0.7117	-	0.7496	-	0.5974	-
15	0.7408	-	-	-	-	-	-	-
16	-	-	0.7120	-	0.7501	-	-	-
17	-	-	-	-	-	-	-	-
18	-	-	0.7121	-	0.7502	-	-	-
19	-	-	-	-	-	-	-	-
20	-	-	0.7130	-	0.7502	-	-	-

a Actual pressures lie within 0.05% of these values.

b Given value is the average of the four experiments.

coefficients θ , together with their standard deviations, are summarised in Table 6.2.

Using the second virial coefficients^{6,7} in Table 6.3, a set of quantities, $n\mathcal{D}_{12}$, were calculated from the corresponding quantities, $P\mathcal{D}_{12}$, where the number density n was related to the pressure P by the following relation

$$n = P/[kT(1 + B_m'P)]. \quad \dots \quad 6.2$$

The second pressure virial coefficient B_m' of the mixture is given by:

$$B_m' = B_{11}x_1^2 + B_{22}x_2^2 + 2x_1x_2B_{12} \quad \dots \quad 6.3$$

where B_{11} and B_{22} are the second virial coefficients of the components 1 and 2 respectively;

x_1 and x_2 are the molefractions of the components 1 and 2 respectively;

and B_{12} is the second virial coefficient of the mixture.

The data (n versus $n\mathcal{D}_{12}$) was fitted to the relation

$$n\mathcal{D}_{12} = (n\mathcal{D}_{12})_0 (1 + B_D n) \quad \dots \quad 6.4$$

where B_D is an experimental "virial coefficient" for binary diffusion.⁸ The parameters obtained by the above equation are listed in Table 6.2 while the graphical representation of the same data is presented in Figures 6.1 - 6.4.

TABLE 6.2: Least-square Parameters for Eqs. 6.1 and 6.4 and Diffusion "Virial Coefficients"^a

	He-Ar		He-N ₂		He-O ₂		He-CO ₂	
	300.00K	323.15K	300.00K	323.15K	300.00K	323.15K	300.00K	323.15K
$(PD_{12})_0 \times 10^4$	0.741 ₉	0.839 ₆	0.712 ₇	0.806 ₁	0.751 ₆	0.850 ₄	0.609 ₂	0.689 ₀
S.D. $\times 10^8$	1.9	2.5	1.7	3.6	2.0	3.6	3.3	2.2
$\theta \times 10^4$	-1.12	0.81	-0.48	0.58	-1.20	-0.42	-14.91	-10.36
S.D. $\times 10^4$	0.26	0.37	0.22	0.56	0.22	0.53	0.62	0.44
$(nD_{12})_0 \times 10^{-21}$	1.815	1.907	1.744	1.831	1.839	1.932	1.490	1.565
S.D. $\times 10^{-18}$	0.4	0.6	0.4	0.8	0.5	0.8	0.8	0.5
$B_D \times 10^{29}$	-2.58	-1.79	-2.48	-2.05	-2.53	-2.25	-8.12	-6.65
S.D. $\times 10^{29}$	0.10	0.16	0.09	0.25	0.09	0.23	0.26	0.19
$(B_D^a)_{\text{exp}} \times 10^{29}$	-1.70	-1.53	-1.48	-1.34	-1.55	-1.43	-6.79	-6.02
$(B_D^T)_{\text{exp}} \times 10^{29}$	-0.88	-0.26	-1.00	-0.71	-0.98	-0.82	-1.33	-0.62
$(B_D^T)_{\text{calc}} \times 10^{29}$	-1.72	-1.67	-1.82	-1.78	-1.59	-1.73	-3.10	-2.83

^a Units: $(PD_{12})_0$, atm m² s⁻¹; θ , atm⁻¹; $(nD_{12})_0$, m⁻¹ s⁻¹; all B_D values, m³.

TABLE 6.3: Second Pressure Virial Coefficients and Effective Distance Parameters ^{a, b}

	$B_{ii} \times 10^4$		$B_{12} \times 10^4$		$B^E \times 10^4$		σ_{ii}^{EFF}	
	(atm ⁻¹)		(atm ⁻¹)		(atm ⁻¹)		(nm)	
	300.00K	323.15K	300.00K	323.15K	300.00K	323.15K	300.00K	323.15K
He	4.75	4.39	-	-	-	-	0.210	0.210
Ar	-6.34	-4.16	7.34	6.94	8.1 ₄	6.8 ₃	0.320	0.312
N ₂	-1.71	-0.09	8.62	8.13	7.1 ₀	5.9 ₈	0.337	0.331
O ₂	-6.30	-4.37	6.66	6.39	7.4 ₄	6.3 ₈	0.295	0.323
CO ₂	-49.62	-38.92	10.14	9.56	32.5 ₈	26.8 ₃	0.496	0.470

^a All virial coefficients are taken from references 6 and 7.

^b The subscript 1 is used to denote He; all other gases are denoted by the subscript 2.

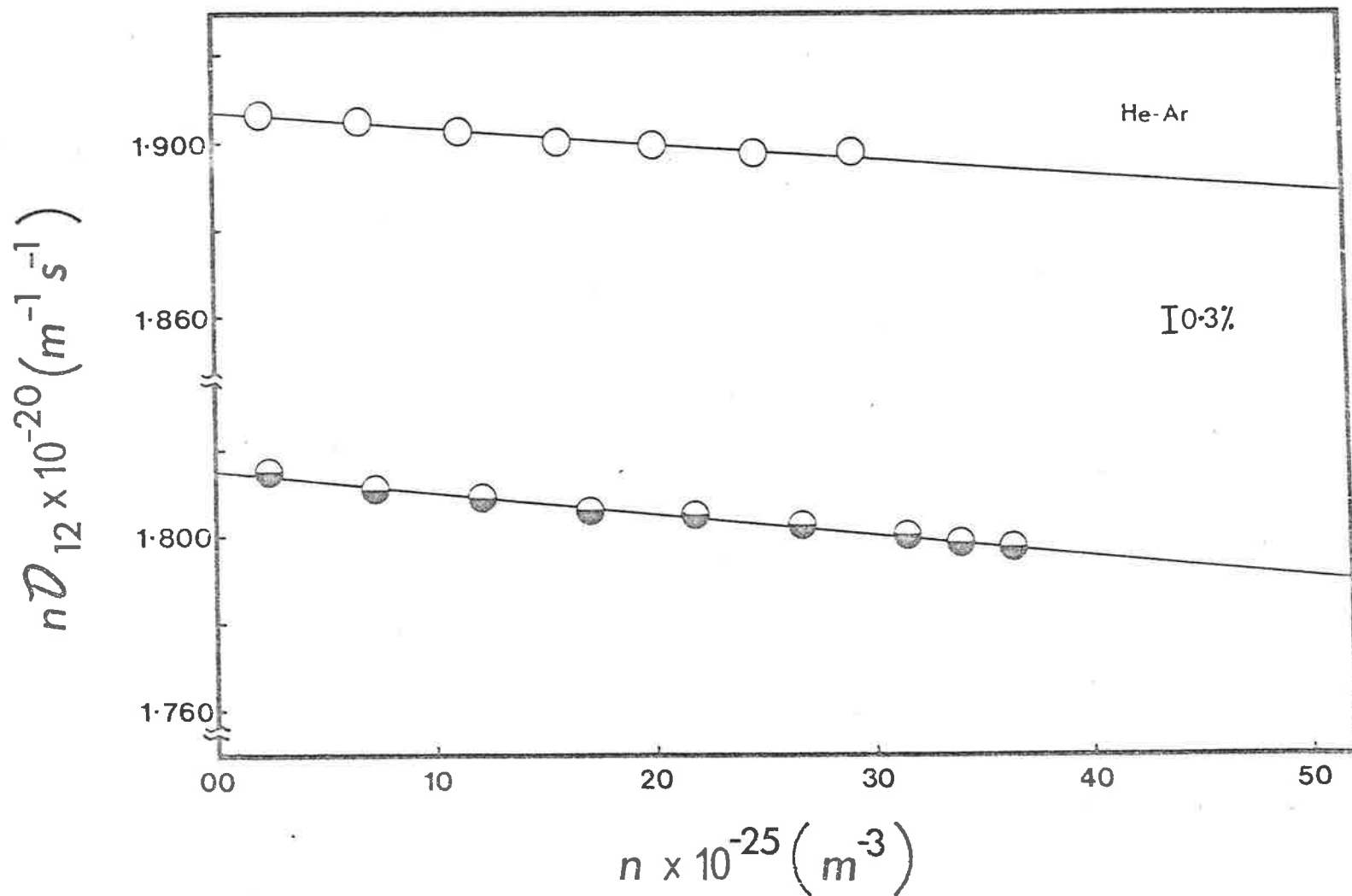


Figure 6.1: Density Dependence of the Diffusion Coefficient (n vs. nD_{12}) for the system He - Ar.

● - 300.00K

○ - 323.15K

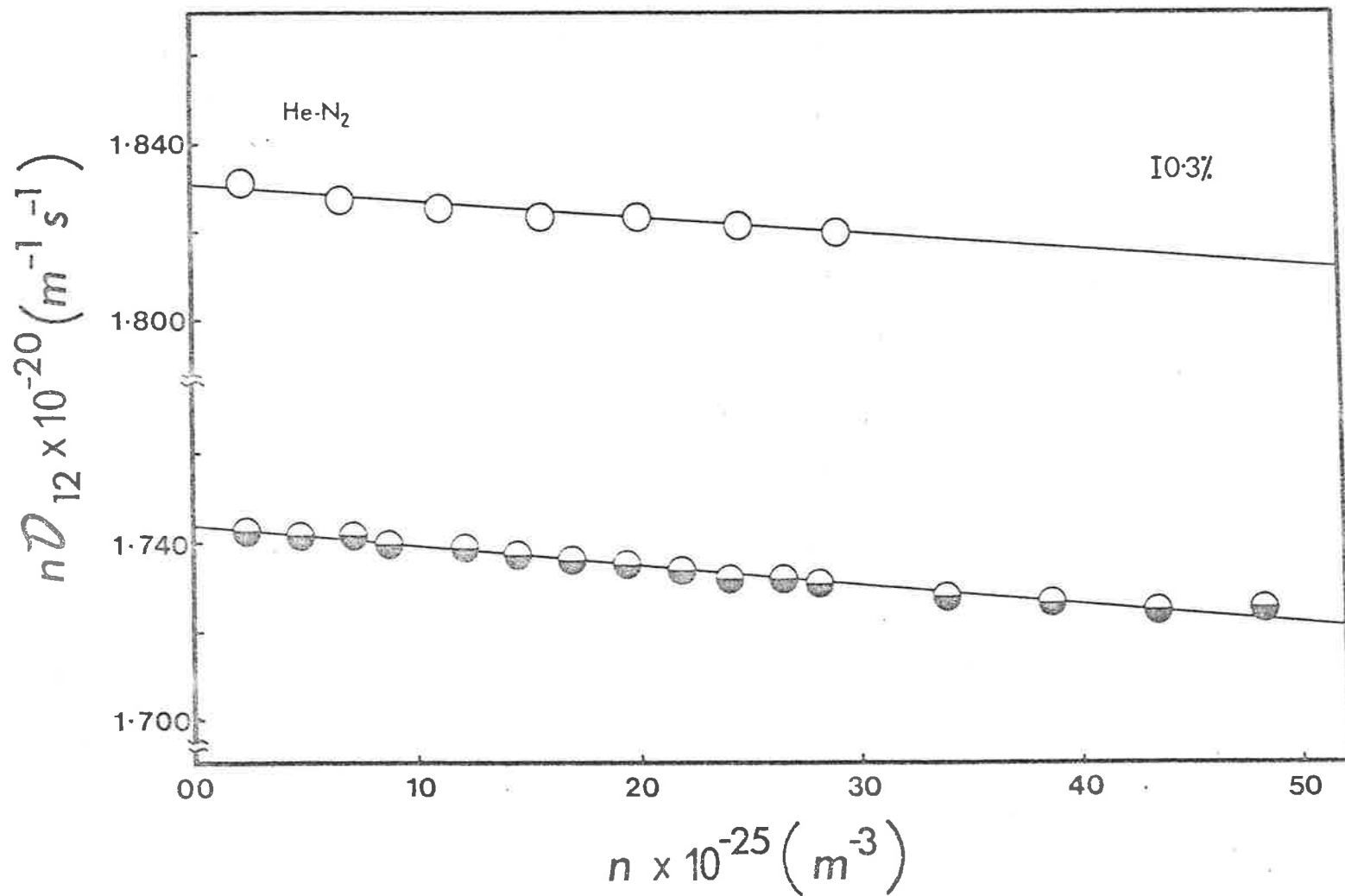


Figure 6.2: Density Dependence of the Diffusion Coefficient (n vs. nD_{12}) for the system He - N₂.

● - 300.00K

○ - 323.15K

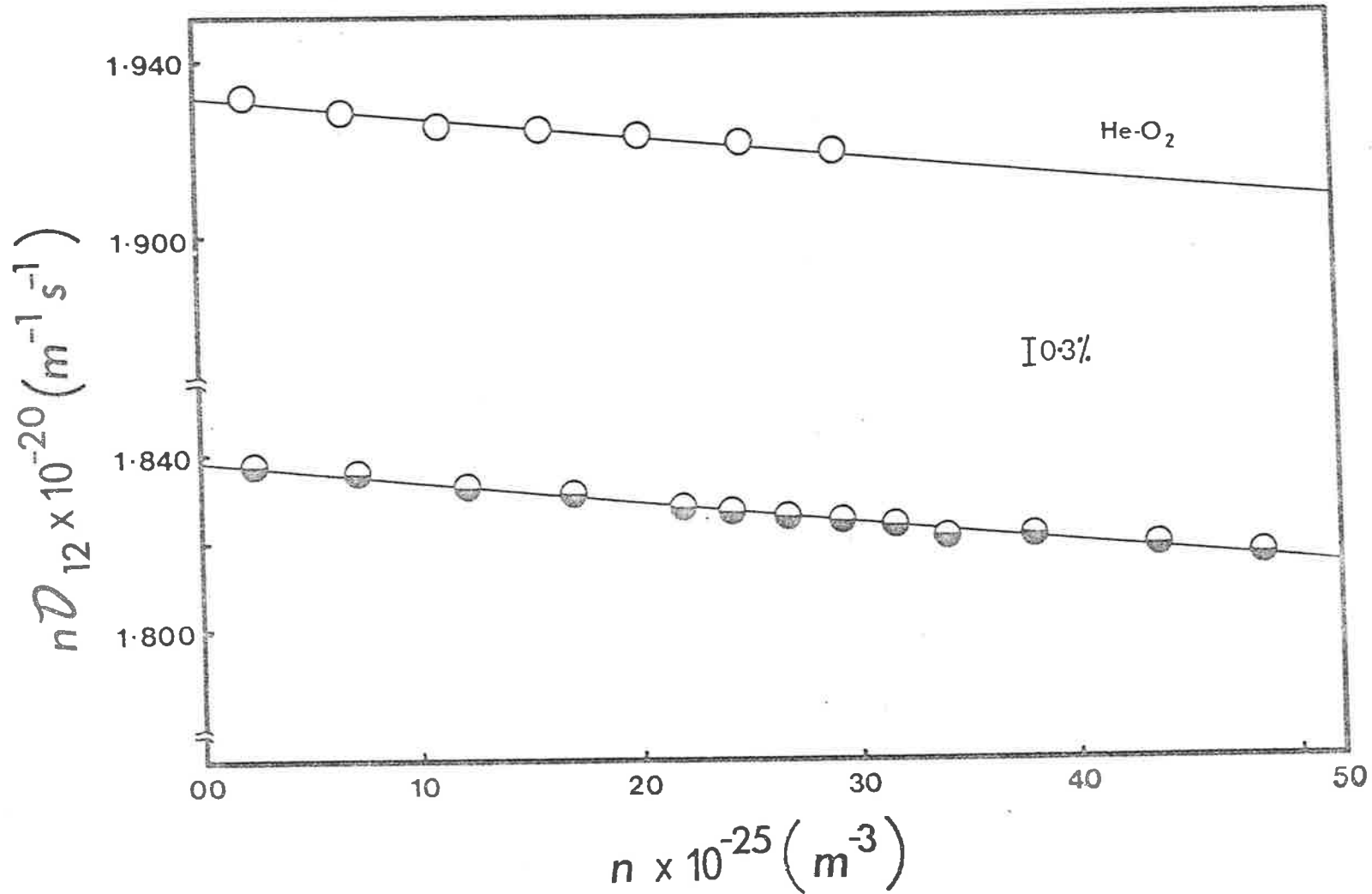


Figure 6.3: Density Dependence of the Diffusion Coefficient (n vs. nD_{12}) for system He - O₂.

● - 300.00K

○ - 323.15K

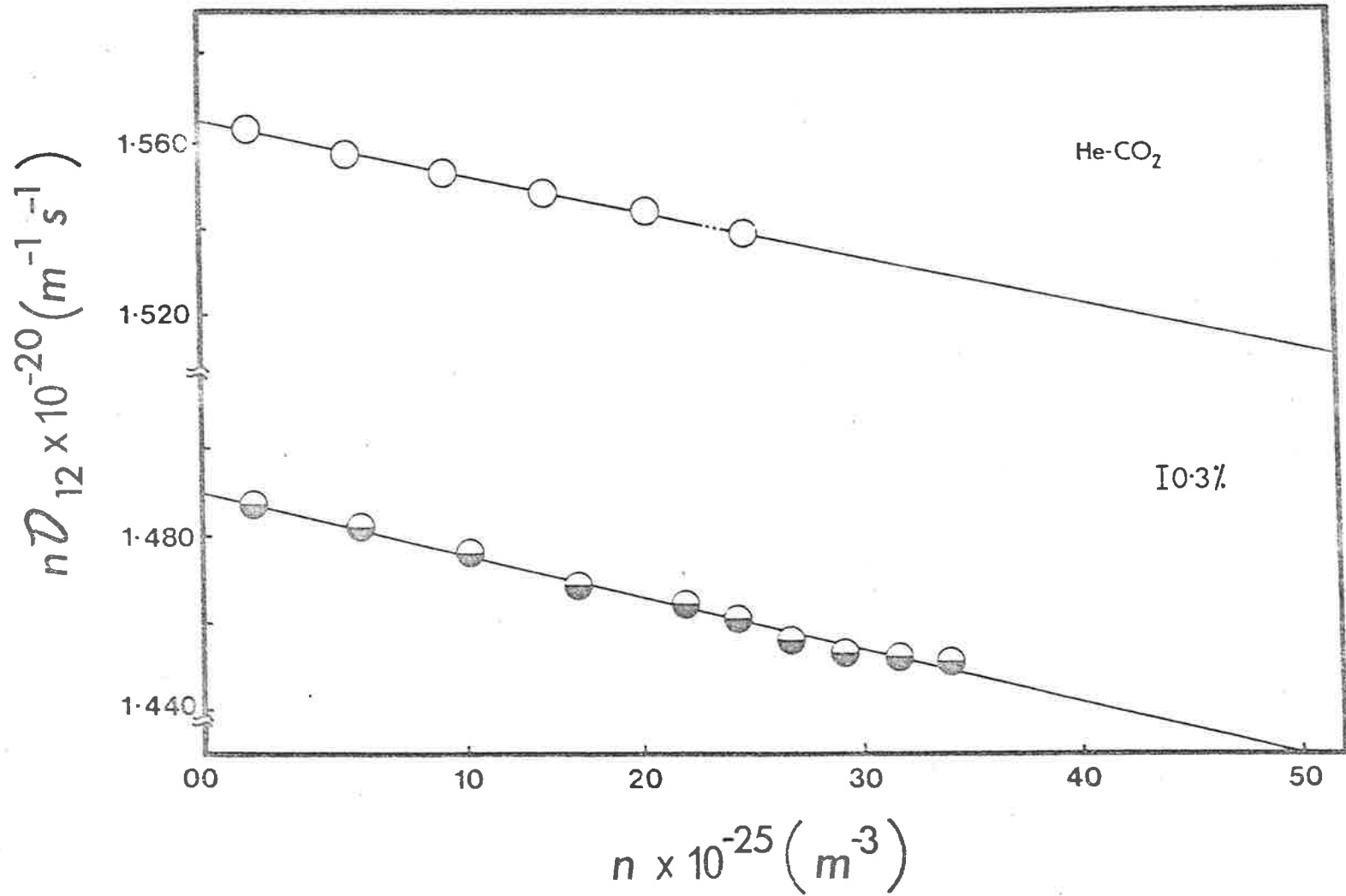


Figure 6.4: Density Dependence of the Diffusion Coefficient (n vs. nD_{12}) for the system He - CO₂.

● - 300.00K

○ - 323.15K

6.3 Comparison with Enskog-Thorne Theory

A comparison has been made between the experimental B_D^T values and the corresponding values calculated from the Enskog theory⁹. Enskog indicated that the theory of rigid spheres can be extended to study the real nature of fluids and was extensively used by many workers¹⁰⁻¹³ to predict the transport properties (viscosities and thermal conductivities) of gases at high pressure.

Equation of state (2.35) for rigid spheres may be written as:

$$\frac{p\tilde{V}}{RT} = 1 + \frac{b_0}{\tilde{V}} Y \quad \dots \quad 6.5$$

where

$$b_0 = \frac{2}{3} \pi N \sigma^3 .$$

In the derivation of the theory, Enskog replaced the external pressure with the sum of the external pressure, p , and the internal pressure $(\partial\tilde{U}/\partial\tilde{V})_T$. This sum is known as the thermal pressure which is thermodynamically equal to $T(\partial p/\partial T)_{\tilde{V}}$. For gases composed of rigid spherical molecules, the internal pressure is zero, thus leaving the external pressure equal to the thermal pressure which can be written as^{14,15}

$$T\left(\frac{\partial p}{\partial T}\right)_{\tilde{V}} = \frac{RT}{\tilde{V}} \left(1 + \frac{b_0}{\tilde{V}} Y\right) \quad \dots \quad 6.6$$

$$\frac{\tilde{V}}{R}\left(\frac{\partial p}{\partial T}\right)_{\tilde{V}} = 1 + \frac{b_0}{\tilde{V}} Y \quad \dots \quad 6.7$$

For real gases the right hand side in equation 6.7 can be calculated using the experimental compressibility data

$$\frac{\tilde{V} \left(\frac{\partial p}{\partial T} \right)_{\tilde{V}}}{R} = 1 + \frac{1}{\tilde{V}} \left(B + T \frac{\partial B}{\partial T} \right) + \frac{1}{\tilde{V}^2} \left(C + T \frac{\partial C}{\partial T} \right) + \dots \quad \dots \quad 6.8$$

From equations 6.7 and 6.8

$$\frac{b_0 Y}{\tilde{V}} = \frac{1}{\tilde{V}} \left(B + T \frac{\partial B}{\partial T} \right) + \frac{1}{\tilde{V}^2} \left(C + T \frac{\partial C}{\partial T} \right) + \dots \quad \dots \quad 6.9$$

As the transport coefficients must approach the dilute gas values in the low density limits, the relation can be written as¹⁴

$$b_0 = B_{ii} + T \frac{\partial B_{ii}}{\partial T} \quad \dots \quad 6.10$$

Thus the values of the effective rigid sphere diameters at each temperature were calculated from the relation 6.11 by using the smoothed experimental data^{6, 7}

$$\sigma_{ii}^{EFF} = (3b_0 / 2\pi, N_0)^{1/3} \quad \dots \quad 6.11$$

and are listed in Table 6.3.

In equation 2.38 Thorne's⁹ contribution is only the factor Y_{12} , whereas the first term of the same equation contributes toward the activity factor¹⁶ which tends to unity as the molefraction of one component of the mixture tends to zero and are represented by B_D^T and B_D^a respectively. Then equation 6.3 may be written as

$$nD_{12} = (nD_{12})_0 [1 + (B_D^a + B_D^T)n] \quad \dots \quad 6.12$$

$$\text{where } B_D^T = -\frac{1}{6}\pi \left[x_1 \sigma_{11}^3 \left[\frac{\sigma_{11} + 4\sigma_{22}}{\sigma_{11} + \sigma_{22}} \right] + x_2 \sigma_{22}^3 \left[\frac{4\sigma_{11} + \sigma_{22}}{\sigma_{11} + \sigma_{22}} \right] \right] \quad \dots \quad 6.13$$

$$B_D^a = -4x_1 x_2 B^E kT \quad \dots \quad 6.14$$

By comparing equations 6.4 and 6.12

$$B_D = B_D^a + B_D^T \quad \dots \quad 6.15$$

The experimental B^E data was used to calculate the activity factor B_D^a . The experimental values for B_{ii} and B^E for each temperature are also given in Table 6.3.

B_D and B_D^a were obtained experimentally from diffusion and thermodynamic measurements respectively and $(B_D^T)_{exp}$ was obtained by difference for comparison with the corresponding value calculated by means of equation 6.13. The calculated values for $(B_D^a)_{exp}$, $(B_D^T)_{exp}$ and $(B_D^T)_{calc}$ at each temperature are given at the bottom of Table 6.2 which shows:

- (i) that the B_D^T values predicted by the Thorne's equation are approximately 100% larger than the experimental values. A similar conclusion was drawn when the experimental data^{1,2} was analysed for B_D^T values in the same way¹⁷. These calculations indicate that in the systems containing helium, the non-ideality factor B_D^a is much greater than the corresponding B_D^T factor which gives the disagreement between $(B_D^T)_{exp}$ and B_D .
- (ii) that there is not any significant temperature dependence of $(B_D^T)_{exp}$ as found over the temperature range available (300 - 323K) to the present cell. This does not mean that $(B_D^T)_{exp}$ is independent of temperature, but measurements over a large temperature range may be necessary to show any significant variation.

REFERENCES

1. Staker, G.R. and Dunlop, P.J., *Chem. Phys. Letters* 42 (1976) 419.
2. Bell, T.N., Shankland, I.R. and Dunlop, P.J.,
Chem. Phys. Letters 45 (1977) 445.
3. Kirkwood, J.G., Baldwin, R.L., Dunlop, P.J., Kegeles, G.
and Gosting, L.J., *J. Chem. Phys.* 33 (1960)
1505.
4. Boots, H.M.J. and Deutch, J.M., *Physica* 94A (1978) 99.
5. Staker, G.R., Dunlop, P.J., Harris, K.R. and Bell, T.N.,
Chem. Phys. Letters 32 (1975) 561.
6. Dymond, J.H. and Smith, E.B., *The virial coefficients
of gases* (Clarendon Press, Oxford, 1969).
7. Brewer, J., *Determination of Mixed Virial Coefficients*,
Report No. MRL-2915-C, Air Force Office of Scientific
Research, No. 67-2795 (1967).
8. Bennett, D.E. and Curtiss, C.F., *J. Chem. Phys.* 51
(1969) 2811.
9. Chapman, S. and Cowling, T.G., *The mathematical theory
of non-uniform gases* (Cambridge University Press,
London, 1970).
10. Sengers, J.V., *Int. J. Heat Mass Transfer* 8 (1965)
1103.

11. Hanley, H.J.M., McCarty, R.D. and Cohen, E.G.D.,
Physica 60 (1972) 322.
12. Ely, J.F. and McQuarrie, D.A., *J. Chem. Phys.* 60
(1974) 4105.
13. Di Pippo, R., Dorfman, J.R., Kestin, J., Khalifa, H.E.,
and Mason, E.A., *Physica* 86A (1977) 205.
14. Hirschfelder, J.O., Curtiss, C.F. and Bird, R.B.,
Molecular theory of gases and liquids (4th
printing) Wiley (1967).
15. Michels, A. and Gibson, R.O., *Proc. Roy. Soc.* A134
(1931) 288.
16. Tham, M.K. and Gubbins, K.E., *J. Chem. Phys.* 55
(1971) 268.
17. Arora, P.S. and Dunlop, P.J., *J. Chem. Phys.* 71
(1979) 2430.

APPENDIX 1

The quantities P's and Q's defined in equation 2.7 can be obtained both for a Chapman-Cowling and a Kihara approximation by the following methods.

According to Kihara's scheme:

$$P_1 = \frac{2M_1^2}{M_2(M_1+M_2)} \left(\frac{2M_2}{M_1+M_2} \right)^{1/2} \left[\frac{\Omega_{11}^{(2,2)*}}{\Omega_{12}^{(1,1)*}} \right] \left(\frac{\sigma_{11}}{\sigma_{12}} \right)^2, \quad \dots \quad \text{Al.1}$$

$$P_{12} = 15 \left(\frac{M_1 - M_2}{M_1 + M_2} \right)^2 + \frac{8M_1 M_2 A_{12}^*}{(M_1 + M_2)^2}, \quad \dots \quad \text{Al.2}$$

$$Q'_1 = \frac{2}{M_2(M_1+M_2)} \left(\frac{2M_2}{M_1+M_2} \right)^{1/2} \left[\frac{\Omega_{11}^{(2,2)*}}{\Omega_{12}^{(1,1)*}} \right] \left(\frac{\sigma_{11}}{\sigma_{12}} \right)^2 \\ \times \left[M_1^2 + 3M_2^2 + \frac{8}{5} M_1 M_2 A_{12}^* \right], \quad \dots \quad \text{Al.3}$$

$$Q'_{12} = 15 \left(\frac{M_1 - M_2}{M_1 + M_2} \right)^2 + \frac{32M_1 M_2 A_{12}^*}{(M_1 + M_2)^2} + \frac{8(M_1 + M_2)}{5(M_1 M_2)^{1/2}} \\ \times \left[\frac{\Omega_{11}^{(2,2)*}}{\Omega_{12}^{(1,1)*}} \right] \left[\frac{\Omega_{22}^{(2,2)*}}{\Omega_{12}^{(1,1)*}} \right] \left(\frac{\sigma_{11}}{\sigma_{12}} \right)^2 \left(\frac{\sigma_{22}}{\sigma_{12}} \right)^2, \quad \dots \quad \text{Al.4}$$

where all symbols have their usual significance. Expressions for P_2 and Q_2 (*heavy components*) can be generated from those for P_1 and Q_1 by an interchange of subscripts.

Chapman-Cowling gave the similar expressions as Kihara for P's, whereas they differ slightly in the calculations of Q's. The equations are given as

$$Q_1 = \frac{2}{M_2 (M_1 + M_2)} \left(\frac{2M_2}{M_1 + M_2} \right)^{1/2} \left[\frac{\Omega_{11}^{(2,2)*}}{\Omega_{12}^{(1,1)*}} \right] \left(\frac{\sigma_{11}}{\sigma_{12}} \right)^2$$

$$\times \left[\left(\frac{5}{2} - \frac{6}{5} B_{12}^* \right) M_1^2 + 3M_2^2 + \frac{8}{5} M_1 M_2 A_{12}^* \right], \quad \dots \quad A1.5$$

$$Q_{12} = 15 \left(\frac{M_1 - M_2}{M_1 + M_2} \right)^2 \left(\frac{5}{2} - \frac{6}{5} B_{12}^* \right) + \frac{4M_1 M_2 A_{12}^*}{(M_1 + M_2)^2}$$

$$\times \left(11 - \frac{12}{5} B_{12}^* \right) + \frac{8(M_1 + M_2)}{5(M_1 M_2)^{1/2}} \left[\frac{\Omega_{11}^{(2,2)*}}{\Omega_{12}^{(1,1)*}} \right] \dots \quad A1.6$$

$$\times \left[\frac{\Omega_{22}^{(2,2)*}}{\Omega_{12}^{(1,1)*}} \right] \left(\frac{\sigma_{11}}{\sigma_{12}} \right)^2 \left(\frac{\sigma_{22}}{\sigma_{12}} \right)^2.$$

It has been noticed that the expressions for Kihara Q's can be obtained from the Chapman-Cowling Q's by putting B_{12}^* equal to 5/4 (Maxwellian model value).

APPENDIX 2

Guggenheim¹ gave an equation to calculate the activity, a_1 , of the component 1 for a non-ideal binary gas mixture as:

$$\ln a_1 = \ln a_1^0 + \ln x_1 + \ln(P/p^0) + (B'_{11} + 2x_2^2 E')P, \quad \dots \text{A2.1}$$

where a_1^0 is the absolute activity of the pure species 1 at temperature T and standard pressure p^0 . On differentiating equation A2.1 we get

$$\left(\frac{\partial \ln a_1}{\partial \ln x_1}\right)_{T,P} = 1 - 4x_1 x_2 B^E P, \quad \dots \text{A2.2}$$

where B^E is the excess second pressure virial coefficient and is given by:

$$B^E = B_{12} - (B_{11} + B_{22})/2. \quad \dots \text{A2.3}$$

The second virial coefficient for the rigid sphere can be expressed as:

$$B_{12} = 2\pi \sigma_{12}^3 / 3kT, \quad \dots \text{A2.4}$$

where all the symbols have their usual significance.

Substituting the values of virial coefficients A2.4 in equation A2.3

$$B^E = \frac{2\pi}{3kT} (\sigma_{12}^3 - \frac{1}{2}(\sigma_{11}^3 + \sigma_{22}^3)) . \quad \dots \text{A2.5}$$

Since for rigid spheres

$$\sigma_{12} = \frac{1}{2}(\sigma_{11} + \sigma_{22}) , \quad \dots \text{ A2.6}$$

equation A2.5 can be written as

$$B^E = \frac{2\pi}{3kT} [(\frac{1}{2}(\sigma_{11} + \sigma_{22}))^3 - \frac{1}{2}(\sigma_{11}^3 + \sigma_{22}^3)] , \quad \dots \text{ A2.7}$$

$$B^E = \frac{2\pi}{3kT} [\frac{1}{8}(\sigma_{11}^3 + \sigma_{22}^3 + 3\sigma_{11}^2\sigma_{22} + 3\sigma_{11}\sigma_{22}^2) - \frac{1}{2}\sigma_{11}^3 - \frac{1}{2}\sigma_{22}^3] , \quad \dots \text{ A2.8}$$

$$B^E = -\frac{\pi}{4kT} (\sigma_{11} - \sigma_{22})^2 (\sigma_{11} + \sigma_{22}) . \quad \dots \text{ A2.9}$$

As $kT = P/n$ equation A2.9 can be changed to

$$B^E = -\frac{\pi n}{4P} (\sigma_{11} - \sigma_{22})^2 (\sigma_{11} + \sigma_{22}) . \quad \dots \text{ A2.10}$$

Substituting the value of B^E from equation A2.10 in A2.2

we get

$$\left(\frac{\partial \ln a_1}{\partial \ln x_1}\right)_{T,P} = 1 + \pi n x_1 x_2 (\sigma_{11} - \sigma_{22})^2 (\sigma_{11} + \sigma_{22}) \dots \text{ A2.11}$$

which is the required equation used in Section 2.3.

I. Guggenheim, *Thermodynamics*, 2nd ed., Nth. Holland Pub. Co. (1950).

APPENDIX 3

The experimental results obtained using Loschmidt cell, A_3 , and small two bulb cell (STBC), A_2 , for the study of the temperature dependence of diffusion to calculate potential parameters (see Chapter 5A) are given here. The symbols used in this Appendix are defined as:

- X_2 : is the molefraction of the heavy component;
 $P\mathcal{D}_{12}$: is the numerical value of the diffusion coefficient at one atmosphere pressure.

Table A3.1:

The Temperature Dependence of the Diffusion Coefficient for the Systems

He-Ne*		He-Ar*		He-Kr#	
at 300K and at molefraction (x_2)					
$x_2 = 0.15$		0.15		0.10	
T (K)	(PD_{12}) (atm.cm. ² s ⁻¹)	T (K)	(PD_{12}) (atm.cm. ² s ⁻¹)	T (K)	(PD_{12}) (atm.cm. ² s ⁻¹)
277.00	0.9660	277.00	0.6491	276.89	0.5600
281.00	0.9890	281.00	0.6642	281.01	0.5743
284.90	1.0118	284.90	0.6797	285.07	0.5883
288.85	1.0353	288.85	0.6962	289.23	0.6028
293.05	1.0607	293.05	0.7126	293.20	0.6162
297.06	1.0820	293.30	0.7141	297.12	0.6306
300.00	1.1050	295.15	0.7217	300.01	0.6405
303.21	1.1231	300.00	0.7420	303.51	0.6532
305.17	1.1338	301.32	0.7480	307.11	0.6662
307.13	1.1488	303.21	0.7560	311.11	0.6812
309.13	1.1598	305.17	0.7637	315.22	0.6958
311.13	1.1716	307.13	0.7720	319.15	0.7108
313.11	1.1856	311.13	0.7886	323.19	0.7248
315.29	1.1976	313.11	0.7974		
317.02	1.2106	315.29	0.8065		
319.07	1.2226	317.02	0.8147		
321.05	1.2360	319.07	0.8239		
323.14	1.2493	321.05	0.8328		
		323.14	0.8401		

* Experiments were performed in Loschmidt type cell (A_3).

Experiments were performed in STBC (A_2).

Continued

Table A3.1: continued

The Temperature Dependence of the Diffusion Coefficient for the Systems

He-Xe#		Ne-Ar*		Ne-Kr#	
at 300K and at molefraction (x_2)					
$x_2 = 0.10$		0.15		0.15	
T	($P\mathcal{D}_{12}$)	T	($P\mathcal{D}_{12}$)	T	($P\mathcal{D}_{12}$)
(K)	(atm.cm. ² s ⁻¹)	(K)	(atm.cm. ² s ⁻¹)	(K)	(atm.cm. ² s ⁻¹)
277.15	0.4790	277.00	0.2822	276.15	0.2283
281.47	0.4921	281.00	0.1892	280.15	0.2340
285.05	0.5024	284.90	0.2965	283.95	0.2398
289.02	0.5136	285.32	0.2974	287.94	0.2454
293.20	0.5263	287.30	0.3006	291.88	0.2514
299.92	0.5473	289.30	0.3044	295.96	0.2569
307.20	0.5695	291.31	0.3080	299.93	0.2632
307.31	0.5700	293.05	0.3110	303.28	0.2686
311.22	0.5824	293.30	0.3112	307.25	0.2746
315.18	0.5944	295.15	0.3151	311.28	0.2810
319.21	0.6084	297.14	0.3190	314.98	0.2865
323.12	0.6202	300.00	0.3237	318.90	0.2922
		301.32	0.3267	323.17	0.2998
		303.21	0.3300		
		305.17	0.3338		
		307.13	0.3373		
		309.13	0.3411		
		311.13	0.3449		
		313.11	0.3486		
		315.29	0.3526		
		317.02	0.3561		
		319.07	0.3602		
		321.05	0.3639		
		323.14	0.3682		

* Experiments were performed in Loschmidt type cell (A_3).

Experiments were performed in STBC (A_2).

Continued

Table A3.1: continued

The Temperature Dependence of Diffusion Coefficient for the Systems

Ne-Xe#		Ar-Kr#		Ar-Xe#	
at 300K and at molefraction (x_2)					
$x_2 = 0.08$			0.15		0.15
T	(PD_{12})	T	(PD_{12})	T	(PD_{12})
(K)	($\text{atm.cm.}^2\text{s}^{-1}$)	(K)	($\text{atm.cm.}^2\text{s}^{-1}$)	(K)	($\text{atm.cm.}^2\text{s}^{-1}$)
275.77	0.1914	276.98	0.1210	276.15	0.0976
277.18	0.1932	280.27	0.1239	280.15	0.1003
281.17	0.1980	287.93	0.1300	283.94	0.1031
285.02	0.2030	292.05	0.1336	287.94	0.1058
288.99	0.2078	296.23	0.1372	291.87	0.1085
293.11	0.2130	299.99	0.1404	296.05	0.1112
297.13	0.2186	303.99	0.1438	300.00	0.1140
300.11	0.2217	307.10	0.1467	303.29	0.1164
301.21	0.2234	311.10	0.1502	307.28	0.1195
305.16	0.2284	314.93	0.1539	311.28	0.1223
309.18	0.2337	319.00	0.1574	314.98	0.1253
313.20	0.2389	323.50	0.1616	318.90	0.1281
317.16	0.2438			323.20	0.1310
320.96	0.2490				
325.02	0.2544				

Experiments were performed in STBC (A_2).

Continued

Table A3.1: continued

The Temperature Dependence of Diffusion Coefficient for the Systems

He-N ₂ #		He-O ₂ #		He-CO ₂ #		CH ₄ -CF ₄ #	
at 300K and at molefraction (x ₂)							
x ₂ = 0.20		0.15		0.15		0.15	
T	P \mathcal{D}_{12}	T	P \mathcal{D}_{12}	T	P \mathcal{D}_{12}	T	P \mathcal{D}_{12}
(K)	(atm.cm. ² s ⁻¹)	(K)	(atm.cm. ² s ⁻¹)	(K)	(atm.cm. ² s ⁻¹)	(K)	(atm.cm. ² s ⁻¹)
277.18	0.6256	277.20	0.6567	277.37	0.5340	276.28	0.1253
281.21	0.6412	281.22	0.6731	281.31	0.5465	278.32	0.1270
285.26	0.6558	285.15	0.6890	285.15	0.5599	280.26	0.1285
288.95	0.6707	289.23	0.7055	289.28	0.5724	284.23	0.1321
293.11	0.6865	293.29	0.7221	293.17	0.5851	287.93	0.1352
297.11	0.7032	300.00	0.7523	297.17	0.5986	292.06	0.1388
299.91	0.7144	303.19	0.7667	301.14	0.6116	296.23	0.1425
303.19	0.7269	307.22	0.7823	304.87	0.6255	299.99	0.1457
307.19	0.7430	311.18	0.7991	309.10	0.6395	300.00	0.1458
311.16	0.7588	315.17	0.8177	313.40	0.6548	303.97	0.1493
315.33	0.7762	319.20	0.8336	317.10	0.6665	307.10	0.1522
319.43	0.7932	323.22	0.8506	321.08	0.6812	311.14	0.1558
323.25	0.8083			323.05	0.6875	314.93	0.1593
						319.00	0.1631
						323.20	0.1669

Experiments were performed in STBC (A₂).

Continued

Table A3.1: continued
 The Temperature Dependence of Diffusion Coefficient for the Systems

Ar-N ₂ *		Ar-O ₂ #		Ar-CO#		Kr-CH ₄ #	
at 300K and at molefraction (x ₂)							
x ₂ = 0.50		0.50		0.35		0.15	
T	PD ₁₂	T	PD ₁₂	T	PD ₁₂	T	PD ₁₂
(K)	(atm.cm. ² s ⁻¹)	(K)	(atm.cm. ² s ⁻¹)	(K)	(atm.cm. ² s ⁻¹)	(K)	(atm.cm. ² s ⁻¹)
277.00	0.1762	277.02	0.1536	276.15	0.1787	277.20	0.1764
279.09	0.1787	280.13	0.1571	280.15	0.1833	281.22	0.1810
281.00	0.1809	284.23	0.1614	283.90	0.1880	285.15	0.1857
284.90	0.1857	287.93	0.1654	287.94	0.1928	289.23	0.1907
288.85	0.1903	292.05	0.1699	291.87	0.1975	293.29	0.1954
293.05	0.1950	296.23	0.1745	297.03	0.2036	299.96	0.2039
297.04	0.1998	299.99	0.1787	299.95	0.2070	303.19	0.2078
300.00	0.2037	303.93	0.1830	303.29	0.2115	307.22	0.2127
301.15	0.2054	307.10	0.1866	307.28	0.2167	311.18	0.2177
303.15	0.2076	311.12	0.1913	311.28	0.2215	315.17	0.2228
305.15	0.2103	314.93	0.1956	314.98	0.2265	319.32	0.2282
307.13	0.2126	319.00	0.2002	318.90	0.2312	323.16	0.2330
309.13	0.2149	323.20	0.2053	323.20	0.2369		
311.13	0.2174						
313.26	0.2200						
315.16	0.2224						
317.16	0.2248						
319.12	0.2272						
321.12	0.2300						
323.14	0.2325						

* Experiments were performed in Loschmidt type cell (A₃).
 # Experiments were performed in STBC (A₂).

PUBLICATIONS FROM THE THESIS

P.S. Arora, I.R. Shankland, T.N. Bell, M.A. Yabsley and P.J. Dunlop, "Use of precise binary diffusion coefficients to calibrate two-bulb cells instead of using the standard end correction for the connecting tube," *Rev. Sci. Instrum.*, 48, 1977, 673.

P.S. Arora, P.J. Carson and P.J. Dunlop, "Determination of potential parameters for the systems Ne-Ar and Ar-Kr from the temperature dependence of their binary diffusion coefficients." *Chemical Physics Letters*, 54, 1978, 117.

P.S. Arora, H.L. Robjohns, I.R. Shankland and P.J. Dunlop, "Use of binary diffusion and second virial coefficients to predict viscosities of gaseous systems." *Chemical Physics Letters*, 59, 1978, 478.

P.S. Arora, J.M. Symons, M.L. Martin and P.J. Dunlop, "Use of the (m,6,8) potential to predict thermal diffusion factors for the systems He-Ne, He-Ar, Ne-Ar, He-N₂, and He-CO₂ at 306 K." *Chemical Physics Letters*, 62, 1979, 396.

P.S. Arora, H.L. Robjohns and P.J. Dunlop, "Use of accurate diffusion and second virial coefficients to determine (m,6,8) potential parameters for nine binary noble gas systems." *Physica*, 95A, 1979, 561.

P.S. Arora and P.J. Dunlop, "The pressure dependence of the binary diffusion coefficients of the systems He-Ar, He-N₂, He-O₂ and He-CO₂ at 300 and 323 K: Tests of Thorne's Equation." *J. Chem Phys.*, 71, 1979, 2430.